Design and Synthesis of Heterocyclic Compounds for Neuroprotective Enzyme Interactions

Louis H.A. Prins

B.Pharm., M.Sc. (Pharmaceutical Chemistry)

Thesis submitted in fulfilment of the requirements for the degree

Philosophiae Doctor

in Pharmaceutical Chemistry

at the School of Pharmacy of the North-West University

(Potchefstroom Campus)

Supervisor: Prof. S.F. Malan

Co-Supervisor: Prof. J.P. Petzer

Potchefstroom

2010

Dedicated to my wife, Hester Prins.

ABSTRACT

Neurodegenerative diseases are thought to be multifactorial in nature and therefore current research focus has shifted from a 'one-drug-one-target' approach to that of multi-target directed ligands (MTDLs). These ligands are designed to address more than one etiological target, thereby increasing patient compliance and decreasing side-effects. Monoamine oxidase (MAO) and nitric oxide synthase (NOS) are enzymes that have long been associated with neurodegenerative diseases. MAO-B is responsible for the metabolism of biogenic amines, including dopamine. During this process hydrogen peroxide (H_2O_2) is formed leading to the production of highly reactive hydroxyl radicals ($^{\bullet}OH$), in the presence of free iron cations (Fe^{2+}, Fe^{3+}). NOS is responsible for the oxidation of *L*-arginine to *L*-citrulline and NO. Since NO is a free radical, an overproduction thereof by neuronal NOS (nNOS) may cause oxidative damage to neuronal cells in the substantia nigra, linking it to the development of Parkinson's disease (PD). The selective inhibition of MAO-B and nNOS is therefore hypothesised to be advantageous for the treatment and prevention of neurodegeneration. The aim of this study was therefore to synthesise a series of selective MAO-B inhibitors and to determine if they also exhibit NOS inhibitory activity.

Three series of compounds were synthesised comprising pteridine-2,4-diones, benzofuranes and indoles. The pteridine-2,4-diones were obtained by reacting 1,3-dimethyl-5,6-diaminouracil with the appropriate aldehyde to yield the pyrimidines, which were cyclicised by the addition of triethyl orthoformate to obtain the final products. For the benzofuranes activation chemistry using dicyclohexylcarbodiimide (DCC) was applied to conjugate the appropriate benzoic or cinnamic acid with 5-hydroxy-3H-benzofuran-2-one, producing the final products. The indole derivatives were synthesised by conjugating 5-amino-2-methylindole to the appropriate benzoic or cinnamic acid in the presence of either *N*-(3-dimethylaminopropyl)-*N*′-ethylcarbodiimide hydrochloride (EDC.HCl) or DCC.

The MAO-B and NOS inhibitory activity of the pteridine-2,4-diones were determined with *in vitro* spectrophotometric assays. The benzofuranes and indoles, on the other hand, were evaluated for their ability to inhibit MAO-A and –B by employing a spectrofluorometric assay method. In addition to this, selected benzofuranes and indoles were subjected to reversibility studies to determine their modes of MAO inhibition.

Results for the pteridine-2,4-diones indicated that compounds **9d** and **10d** are potent MAO-B inhibitors, exhibiting IC_{50} values of 0.602 µM and 0.314 µM respectively. However, none of the pteridine-2,4-diones were found to be significant NOS inhibitors with compound **10a** presenting with an IC_{50} value of 443.3 µM, which is approximately 23 fold less potent than aminoguanidine. The most potent MAO-B inhibitor amongst the benzofuranes was compound **8d** with a K_i value of 0.19 µM and a selectivity index of 5. Indole derivative **6g** was found to be the most potent and selective MAO-B inhibitor, not only within the indole series, but also within the entire study. It exhibited a K_i value of 0.03 µM and a selectivity index of 99. Furthermore, time dependence MAO-B inhibition studies revealed that **6g** exhibits a reversible mode of action.

The pteridine-2,4-dione and indole derivatives synthesised in this study therefore hold promise as potent, MAO-B selective inhibitors and it is recommended that these scaffolds be investigated in future studies.

UITTREKSEL

Daar is onlangs aangedui dat die oorsaak van neurodegeneratiewe siektes multifaktorieel van aard is en navorsingsfokus het daarom verskuif vanaf ‘n ‘een-geneesmiddel-een-teiken’-benadering na dié van multi-teiken-gerigte ligande (MTDLs). Hierdie ligande word ontwerp om meer as een etiologiese aspek te teiken wat pasiëntmeewerking verbeter en terselfdertyd newe-effekte verminder. Monoamienoksidase (MAO) en stikstofoksiedsintase (NOS) is ensieme wat ‘n geruime tyd reeds met neurodegeneratiewe siektes geassosieer word. MAO-B is verantwoordelik vir die metabolisme van endogene amiene wat dopamien insluit. Gedurende hierdie proses word waterstofperoksied (H_2O_2) gevorm wat in die teenwoordigheid van vry ysterkatione (Fe^{2+}, Fe^{3+}) tot die produksie van hoogs reaktiewe hidroksielradikale ($^{\bullet}OH$) lei. NOS is verantwoordelik vir die oksidasie van *L*-arginien na *L*-sitrullien en stikstofoksied (NO). Aangesien NO ‘n vryradikaal is, kan ‘n oormatige produksie daarvan deur neuronale NOS (nNOS) oksidatiewe skade aan neuronale selle in die substansia nigra aanrig. Die vorming van NO kan daarom in direkte verband met die ontwikkeling van Parkinson se siekte (PD) gebring word. Dit word derhalwe gepostuleer dat die selektiewe inhibisie van MAO-B en nNOS voordelig kan wees vir die behandeling en voorkoming van neurodegenerasie. Die hoofdoel van hierdie studie was dus om ‘n reeks selektiewe MAO-B inhibeerders te sintetiseer en te bepaal of dit NOS inhibisie ook toon.

Drie reekse verbindings is gesintetiseer wat pteridien-2,4-dione, bensofurane en indole insluit. Die pteridien-2,4-dione is gesintetiseer deur 1,3-dimetiel-5,6-diaminourasil telkens met die toepaslike aldehied te reageer om eers die pirimidiene te verkry, waarna triëtielortoformaat bygevoeg is om siklisering van die pirimidiene te veroorsaak en die finale produkte te lewer. In die geval van die bensofurane is aktiveringschemie in die vorm van disikloheksielkarbodiimied (DCC) gebruik om die toepaslike bensoë- of kaneelsuur met 5-hidroksie-3H-bensofuraan-2-oon te konjugeer ten einde die finale produkte te verkry. Die indoolderivate is gesintetiseer deur 5-amino-2-metielindool te konjugeer met die toepaslike bensoë- of kaneelsuur in die teenwoordigheid van óf *N*-(3-dimetielaminopropiel)-*N*′-etielkarbodiimied hidrochloried (EDC.HCl) óf DCC.

Die MAO-B en NOS inhiberende aktiwiteit van die pteridien-2,4-dione is bepaal deur middel van *in vitro* spektrofotometriese metodes. Die vermoë van die bensofurane en indole om MAO-A en –B te inhibeer, is bepaal deur middel van ‘n spektrofluorometriese metode. Afgesien van bogenoemde evaluasies is ‘n aantal geselekteerde bensofurane en indole onderwerp aan omkeerbaarheidstudies ten einde die aard van dié verbindings se MAO-inhibisie te bepaal.

Resultate vir die pteridien-2,4-dione het aangedui dat verbindings **9d** en **10d** potente MAO-B inhibeerders is, met IC_{50}-waardes van onderskeidelik 0.602 µM en 0.314 µM. Geen van die pteridien-2,4-dione toon egter potensiaal as NOS-inhibeerder nie. Verbinding **10a** het byvoorbeeld ‘n IC_{50}-waarde van 443.3 µM gehad wat ongeveer 23 keer minder potent is as die bekende NOS-inhibeerder, aminoguanidien. Onder die bensofurane is verbinding **8d** aangedui as die mees potente MAO-B-inhibeerder met ‘n K_i-waarde van 0.19 µM en ‘n selektiwiteitsindeks van 5. Indool **6g** is aangedui as die mees potente en mees selektiewe MAO-B-inhibeerder, nie net in die indoolreeks nie, maar ook in die studie in sy geheel. Dit het ‘n K_i-waarde van 0.03 µM en ‘n selektiwiteitsindeks van 99 getoon. Verdere tydsafhanklike MAO-B-inhibisiestudies het aangedui dat **6g** oor ‘n omkeerbare werkingsmeganisme beskik.

Die pteridien-2,4-dioon- en indoolderivate wat tydens hierdie studie gesintetiseer is, is dus belowend as potente, MAO-B-selektiewe inhibeerders en dit word aanbeveel dat hierdie verbindings in die toekoms volledig bestudeer behoort te word.

ACKNOWLEDGEMENTS

I would like to thank the following people and institutions:

- Professors Sarel Malan and Jacques Petzer for their continued support, guidance and understanding throughout the entire study.
- Prof. Jan du Preez for the use of the technical facilities at the Analytical Technology Laboratory.
- Dr. Johan Jordaan and Mr. André Joubert for the recording of the MS and NMR spectra.
- The National Research Foundation and the North-West University for financial assistance.
- Prof. Kobus Bergh and the Department of Pharmaceutical Chemistry at North-West University for their support.
- Ms. Anriëtte Pretorius for her willingness to help and always sharing a friendly word when times were tough.
- My friends Dennis, Jacques, Nellie, Gisella, Ingrid, Marli, Claudine and Theunis for encouragement and motivation.
- My parents, Hennie and Annelie Prins, for their unconditional love and support throughout my life. Words can not describe how grateful I am for this!
- My loving wife, Hester, for her patience, understanding and encouragement - I love you dearly!

TABLE OF CONTENTS

FIGURES, TABLES & SCHEMES

Article 1:

Article 2:

ABBREVIATIONS

$^{\bullet}OH$	-	Hydroxyl radical
Ach	-	Acetylcholine
AChE	-	Acetylcholinesterase
ALS	-	Amyotrophic lateral sclerosis
ATP	-	Adenosine triphosphate
Aβ	-	Amyloid-β
BuChE	-	Butyrylcholinesterase
CaM	-	Calmodulin
CNS	-	Central nervous system
COMT	-	Catechol-*O*-methyltransferase
DCC	-	Dicyclohexylcarbodiimide
DHLA	-	Dihydrolipoic acid
EDC.HCl	-	*N*-(3-Dimethylaminopropyl)-*N*′-ethylcarbodiimide hydrochloride
EDTA	-	Ethylenediaminetetra-acetic acid
eNOS	-	Endothelial NOS
ER	-	Endoplasmic reticulum
FAD	-	Flavin adenine dinucleotide
Fe^{2+}	-	Ferrous iron cation
Fe^{3+}	-	Ferric iron cation
FMN	-	Flavin mononucleotide
GEM	-	Ginkgo evaluation of memory study
GSH	-	Glutathione
H_2O_2	-	Hydrogen peroxide
H_4B	-	Tetrahydrobiopterin
Hb	-	Haemoglobin
HD	-	Huntington's disease
HEPES	-	4-(2-Hydroxyethyl)piperazine-1-ethanesulfonic acid
iNOS	-	Inducible NOS

LA	-	Lipoic acid
MAO	-	Monoamine oxidase
MMTP	-	1-Methyl-4-(1-methylpyrrol-2-yl)-1,2,3,6-tetrahydropyridine
MPTP	-	1-Methyl-4-phenyl-1,2,3,6-tetrahydropyridine
MTDLs	-	Multi-target-directed ligands
MTP	-	Mitochondrial transition pore
NMDA	-	N-Methyl-D-aspartate
nNOS	-	Neuronal NOS
NO	-	Nitric oxide
NOS	-	Nitric oxide synthase
NSAIDs	-	Non-steroidal anti-inflammatory drugs
$O_2^{\bullet-}$	-	Superoxide radical
$ONOO^-$	-	Peroxynitrate
PAOs	-	Polyamine oxidases
PD	-	Parkinson's disease
PMSF	-	Phenylmethylsulfonyl fluoride
ROS	-	Reactive oxygen species
SEM	-	Standard error of the mean
SI	-	Selectivity index
TPQ	-	Topa-quinone

CHAPTER 1
INTRODUCTION & RATIONALE

Neuropsychiatric disorders such as Parkinson's and Alzheimer's diseases, are increasingly affecting the lives of a growing number of people worldwide. These debilitating conditions lead to a general decrease in quality of life as well as burdening individuals and/or governments with an economical liability. At this stage Alzheimer's disease alone affects 4.5 million Americans and medical as well as institutional care for affected people amounts to more than US$100 billion per year (Kabanov *et al.*, 2007:1054). Parkinson's disease has a mean age onset of 55 with the incidence increasing markedly with age, from 20/100,000 overall to 120/100,000 at age 70 (Dauer *et al.*, 2003:889).

The pressing need for therapeutics to effectively prevent and treat these conditions are therefore of utmost importance.

1.1 Neurodegenerative and Neuropsychiatric Diseases

1.1.1 *Parkinson's Disease*

Parkinson's disease (PD) is a condition associated with the degeneration of dopamine containing nigro-striatal neurons in the substantia nigra pars compacta situated at the base of the midbrain in the thalamus. Through its actions on dopamine receptors D_1 – D_5, dopamine (**1**, fig. 1) reduces the influence of the indirect pathway, and increases the actions of the direct pathway within the basal ganglia. This phasic dopaminergic activation seems to be crucial with respect to a lasting internal encoding of motor skills.

Symptomatically PD presents as a loss of control over motor function, bradykinesia (slowness of movement), rigidity (stiffness) of patients' limbs, hypokinesia (reduction in movement amplitude), akinesia (absence of normal unconscious movements) and other extrapyramidal effects. The quality of life may be significantly impaired by bradykinesia as it takes much longer to perform everyday tasks such as dressing and eating (Dauer *et al.*, 2003:889). Additional neurotransmitter systems are also involved in PD and

therefore noradrenergic, serotoninergic, and cholinergic neurons are also lost with time. This results in several nonmotor symptoms including cognitive decline, sleep abnormalities and depression, which normally present in the later stages of the disease (Cavalli *et al.*, 2008:347).

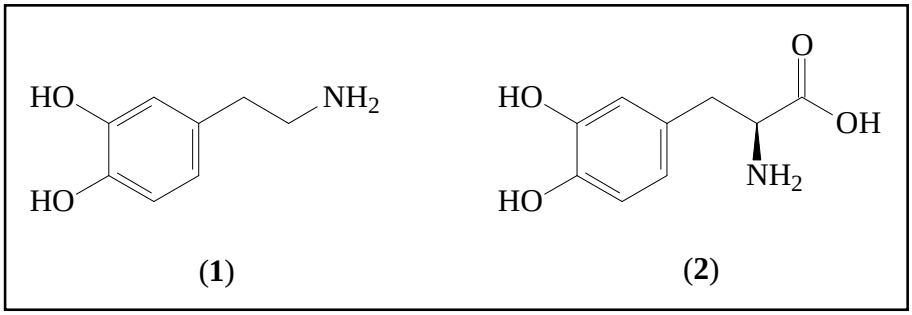

Figure 1: Chemical structures of dopamine (1) and L-dopa (2).

Current PD therapies are principally based on the exogenous replacement of dopamine within the striatum (fig. 2), which substantially improves disease symptoms but without halting the neurodegenerative process. Compound classes that hold a prominent position in current PD treatment are *L*-dopa (**2**), dopamine receptor agonists and multiple medication therapies of *L*-dopa with dopamine modifying drugs, such as: (a) peripheral dopa decarboxylase inhibitors, (b) catechol-*O*-methyltransferase (COMT) inhibitors and (c) monoamine oxidase B (MAO-B) selective inhibitors (Cavalli *et al.*, 2008:347). Although *L*-dopa treatment has dramatically improved the quality of life for PD patients, population-based surveys suggest that these patients continue to display decreased longevity when compared to the general population (Levy *et al.*, 2002:1708, Morgante *et al.*, 2000:507), and that they also present with substantial side-effects at the high doses required for *L*-dopa's therapeutic action (Singh *et al.*, 2007:29).

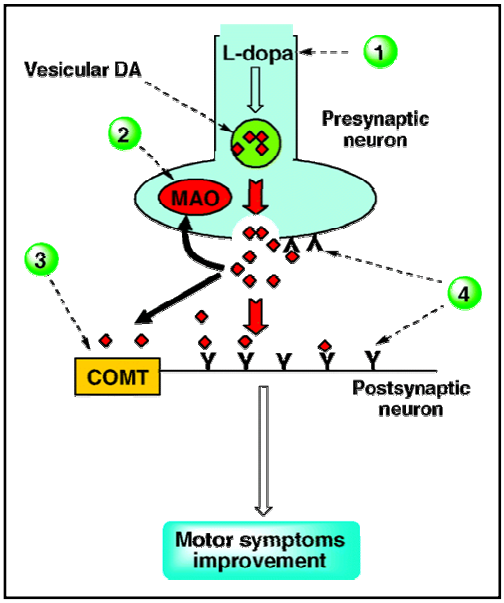

Figure 2: Points of action for currently available anti-PD drugs (Cavalli *et al.*, 2008:347). (**1** = $_L$-Dopa; **2** = MAO inhibitors; **3** = COMT inhibitors; **4** = Dopamine receptor agonists)

The propargylamines are a class of compounds that irreversibly inhibit both MAO-A and –B as well as displaying an array of attributes associated with anti-PD activity:

Selegiline/(*R*)-deprenyl (**3**, fig. 3) is the first MAO-B selective inhibitor used for the treatment of PD (Knoll *et al.*, 1972:393) and has since been indicated to be neuroprotective (Heikkila *et al.*, 1984:467, Yu *et al.*, 1994:697). This neuroprotection could be as a result of its ability to inhibit peroxide formation from the oxidative metabolism of dopamine (Olanow, 1992:S2). Studies performed by Wu *et al.* (1993:241) indicated that (*R*)-deprenyl, at doses that do not inhibit MAO-B, limited free radical formation and prevented nigral damage. These observations suggested that (*R*)-deprenyl may be neuroprotective through mechanisms independent of MAO-B inhibition.

In 1978 it was found that an *N*-demethylated aminoindan propargylamine derivative named AGN 1135 is a potent and selective inhibitor of MAO-B (Finberg *et al.*, 1981:65). This compound is different from (*R*)-deprenyl in that it is not an amphetamine derivative and therefore does not present with any sympathomimetic side-effects. AGN 1135 occurrs as a mixture of two isomers and the *R*(+) enantiomer, now called rasagiline (**4**), is

nearly three orders of magnitude more potent than the *S*(-) enantiomer in inhibiting MAO-B (Youdim *et al.*, 2001:500). When rasagiline was administered systemically together with $_L$-dopa to subhuman primates, increased striatal dopamine levels were detected in microdialysate (Finberg *et al.*, 1998:279), indicating that this new compound had the appropriate activities to alleviate the symptoms of PD. Cavalli *et al.* (2008:347) indicated that rasagiline specifically activated enzymes playing a key role in cellular events including mitochondrial viability, modulation of apoptotic processes and neuronal plasticity.

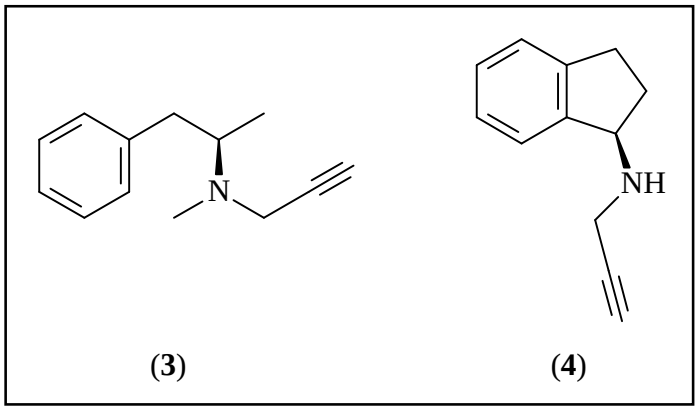

Figure 3: Chemical structures of selegiline/(*R*)-deprenyl (**3**) and rasagiline (**4**).

1.1.2 *Alzheimer's Disease*

Alzheimer's disease (AD) is the fourth leading cause of death in the Western world and the most common cause of acquired dementia in the elderly population. As longevity increases the number of people affected by this disease gradually increases. It is expected that the number of AD sufferers will triple by 2050 (Mount *et al.*, 2006:780). Pathological characteristics definitive of the disease include amyloid-β (Aβ) deposits in senile plaques and neurofibrillary tangles, which mainly consist of paired helical filaments of abnormally phosphorylated τ protein. With disease progression cholinergic neurons and synapses of the basal forebrain are selectively lost, accounting for development of cognitive impairments. The pathophysiological basis of AD, however, remains to be elucidated.

Deficits in learning, memory, language and visuospatial skills are symptoms commonly associated with AD and are as a result of neuropathological changes in the cerebral cortex

and limbic system (Corey-Bloom, 2002:51). Apart from the decline observed in cognitive ability, some AD patients also present with behavioural and psychological symptoms of dementia. These include noncognitive disturbances such as anxiety, depression, psychosis, aggression, eating disorders and inappropriate social or sexual behaviour (Rainer *et al.*, 2004:49).

In 1993 tacrine (**5**, fig. 4), an acetylcholinesterase (AChE) inhibitor, was the first drug to be approved for the treatment of AD. Nowadays this compound is rarely used because of its hepatotoxicity. Donepezil (**6**), rivastigmine (**7**) and galantamine (**8**) reached the market a few years later and became the standard for AD therapy, and was only later complemented by memantine (**9**), which is a noncompetitive *N*-methyl-*D*-aspartate (NMDA) receptor antagonist (Cavalli *et al.*, 2008:347).

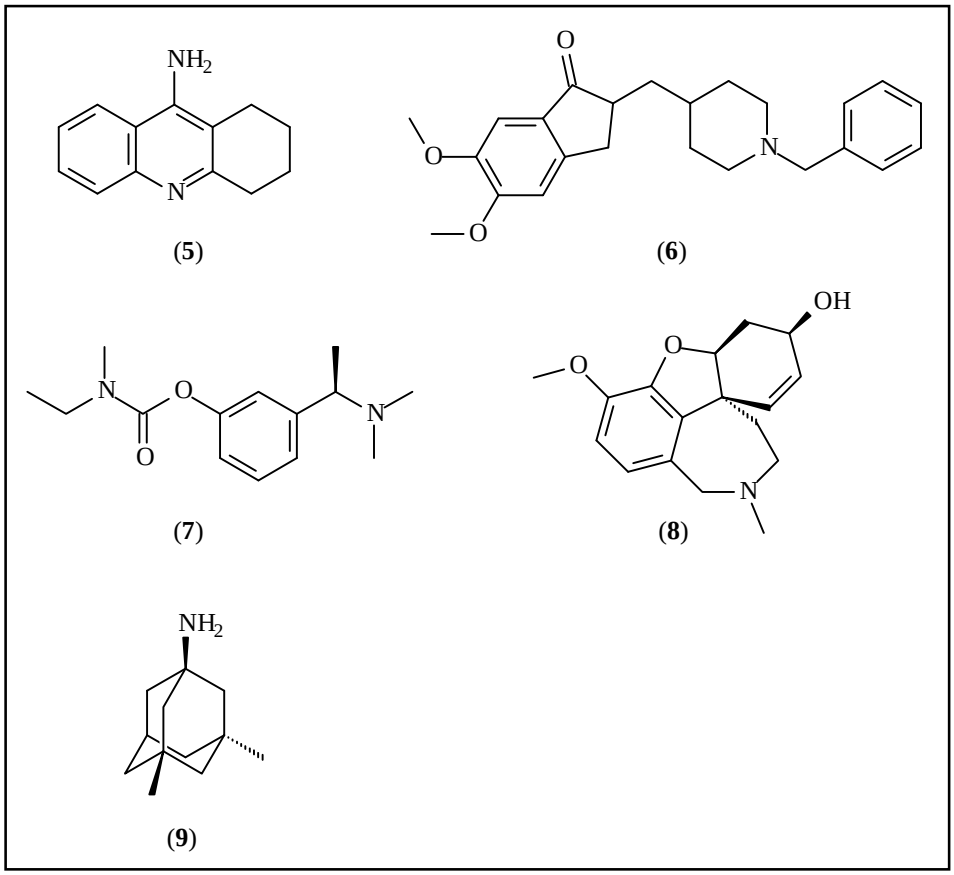

Figure 4: Chemical structures of tacrine (**5**), donepezil (**6**), rivastigmine (**7**), galantamine (**8**) and memantine (**9**).

Ginkgo biloba, used for centuries by the Chinese to treat a variety of health disorders, has recently emerged as a possible treatment for AD. Ernst *et al.* (2005:388) indicated that this herbal medicine has potential for the symptomatic treatment of vascular dementia and AD. Another study indicated that chronic *Ginkgo biloba* treatment could block the age-dependent decline in spatial cognition without altering Aβ levels or suppressing protein oxidation (Stackman *et al.*, 2003:510) and it has even been suggested that the debilitating neurodegenerative declines of AD can be prevented by using *Ginkgo biloba* prophylactic (Oomah, 2004:44). Egb 761, a standardised extract of *Ginkgo biloba*, is currently the focus of two separate phase III clinical trials namely the GEM study (Ginkgo Evaluation of Memory Study) in the United States and the GuidAge study in France. Both of these have more than 3,000 individuals over the age of 70. Egb 761 is known to have anti-oxidant activity and could prevent the oxidative damage induced by Aβ. There is however data suggesting that its activity may not be limited to anti-oxidant properties, but that Egb 761 could display multifunctional activity such as beneficial effects on Aβ-induced toxicity and the anti-amyloidogenic pathway as well as a procholinergic, cholesterol lowering and anti-inflammatory effect (Ramassamy *et al.*, 2007:253).

Other drugs that have been evaluated for AD treatment include estrogens and non-steroidal anti-inflammatory drugs (NSAIDs) such as naproxen and rofecoxib. The NSAIDs which were evaluated produced unwanted cardiovascular side-effects with only slight benefits (Aisen *et al.*, 2003:2819) whereas the risk of dementia was even higher with estrogen (Craig *et al.*, 2005:190). Tramiprosate (3-amino-1-propanesulfonic acid) is an amyloid-binding drug that is effective in reducing polymerisation *in vitro* and plaque deposition in animals. This compound has now reached phase III clinical trials (Aisen, 2005:989).

1.2 The Multifactorial Nature of Neurodegenerative Diseases

It has become increasingly evident that neurodegenerative diseases are not the result of a single cause but that the processes involved are of a multifactorial nature. It is hypothesised that genetic, environmental and endogenous factors may be involved in neurodegenerative diseases such as AD, PD, Huntington's disease (HD) and amyotrophic

lateral sclerosis (ALS). A series of general pathways have been identified in different pathogenic cascades that may be common to these disorders. These include protein misfolding and aggregation, oxidative stress and free radical formation, metal dyshomeostasis, mitochondrial dysfunction and phosphorylation impairment. All of the above seem to occur simultaneously (fig. 5), leading to the demise of key neuronal cells (Jellinger, 2003:101).

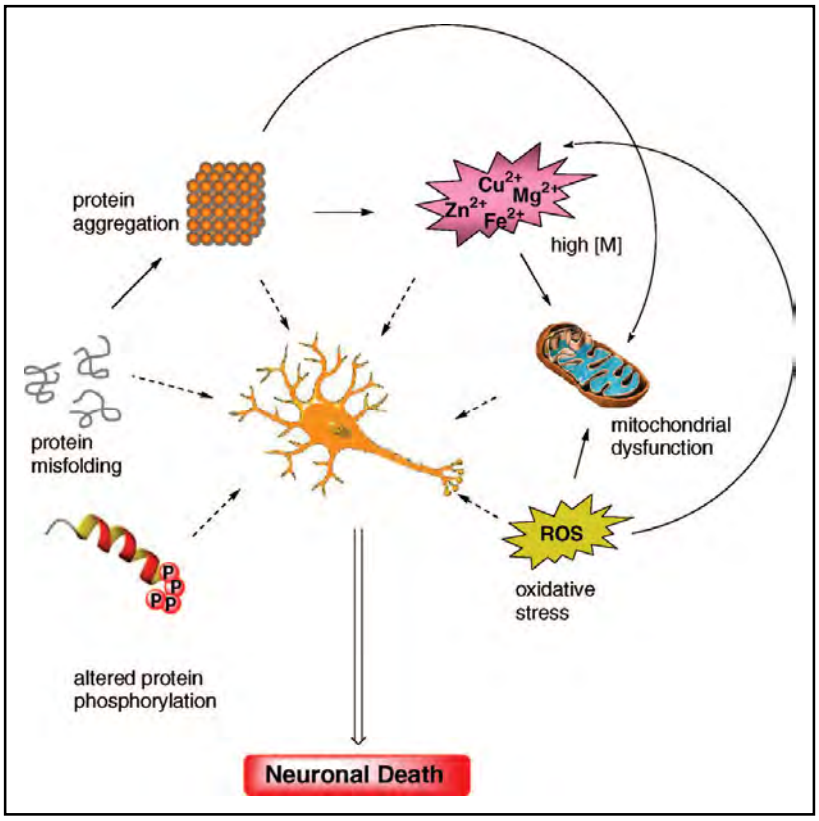

Figure 5: Schematic representation of the multifactorial events leading to neurodegeneration (Jellinger, 2003:101).

1.2.1 *Protein Misfolding*

Protein misfolding followed by self-association and ensuing deposition of the aggregated proteins has been observed in the brain tissues of patients suffering from neurological disease (Gaggelli *et al.*, 2006:1995). The biophysical behaviour of these proteins, leading to their misfolding, aggregation, and deposition, has incited scientists to group these kinds of neurological disorders under the common name of "conformational diseases"

(Carrell *et al.*, 1997:134). As it is well known that amyloid oligomers such as Aβ and α-synuclein are able to permeate both cell and mitochondrial membranes (Caughey *et al.*, 2003:267), it is hypothesised that they are responsible for calcium dysregulation, membrane depolarisation and impairment of mitochondrial functions that have been identified as a further characteristic feature of most neurodegenerative diseases (Lin *et al.*, 2006:787).

1.2.2 *Oxidative Stress*

The role of reactive oxygen species (ROS) in neurodegeneration has been the topic of heated debate (Andersen, 2004:S18). Currently it is thought that imbalance of intracellular oxidation state is likely to be one of the major factors causing neurodegenerative diseases. Neuronal tissue is particularly sensitive to oxidative stress and imbalance in pro-oxidant versus antioxidant homeostasis in the central nervous system (CNS) leads to the production of several potentially toxic ROS. These include both the radical and non-radical species that participate in the initiation and/or propagation of radical chain reactions. In AD, PD, HD and ALS oxidative damage is found in every class of biological molecules within neurons, from lipids to DNA and proteins (Contestabile, 2001:553). However, several clinical studies have indicated only modest success may be achieved when treating neurodegeneration with antioxidants. This suggests that the administration of one or a few antioxidants is too simplistic (Wang *et al.*, 2006:3521).

1.2.3 *Metal Abnormalities*

A direct cause and effect relationship between metal abnormalities and increased oxidative damage has been hypothesised for the abovementioned neurodegenerative diseases. Alterations in the homeostasis of transition metals, essential in many biological reactions, result in increased free radical production that is catalysed by iron, copper, and other trace redox active metals (Doraiswamy *et al.*, 2004:431, Gaggelli *et al.*, 2006:1995). In all cases, metal-mediated oxidative stress is also linked to mitochondrial dysfunction (Lin *et al.*, 2006:787). As discussed below mitochondrial dysfunction may result in the generation of ROS which may in turn react with free metals to produce highly destructive radical species.

1.2.4 *Mitochondrial Dysfunction*

With aging the efficiency of mitochondrial electron transport gradually decreases and the production of hydrogen peroxide (H_2O_2) and superoxide radical ($O_2^{\bullet-}$) increases as a result thereof (Beal, 1995:357, Hagen *et al.*, 1997:3064). These events may lead to the production of additional highly reactive oxidants such as hydroxyl radicals ($^{\bullet}OH$) and peroxynitrate ($ONOO^-$) as well as causing damage to essential cellular proteins, lipids and DNA. Mitochondrial membrane depolarisation and increased susceptibility to both excitotoxicity and apoptosis may also occur (Beckman, 1996:836, Wei *et al.*, 1996:24). Another mitochondrial related factor, which may be involved in the neurodegenerative process, is the mitochondrial transition pore (MTP). The MTP is a non-selective, high conductance channel spanning the inner and outer mitochondrial membranes (Beutner *et al.*, 1996:189, Zoratti *et al.*, 1995:139) and has been shown to be involved in oxidant-induced mitochondrial large-amplitude swelling (Chernyak *et al.*, 1996:623), Ca^{2+} release (Packer *et al.*, 1996:267) and cell death (Marchetti *et al.*, 1996:1155). In its open conformation, the MTP allows efflux of essential metabolic substrates and anti-oxidants such as NADH, adenosine triphosphate (ATP) and glutathione (GSH) (Zoratti *et al.*, 1995:139). GSH depletion may be critical in causing loss of mitochondrial viability, as it is required for the reduction of H_2O_2 and other ROS (Jain *et al.*, 1991:1913). The release of mitochondrial stores of Ca^{2+} is also associated with opening of the pore, which may then activate cellular proteases involved in the apoptotic pathway (Khan *et al.*, 1996:503). A cytochrome c/MTP-dependent pathway has also been proposed as a possible cause of neuronal cell death wherein MTP opening leads to a loss of mitochondrial membrane potential and the subsequent release of pro-apoptotic factors such as apoptosis inducing factor and cytochrome c (Cassarino *et al.*, 1999:1). Apart from the mitochondria, the endoplasmic reticulum (ER) has also gained interest as an important apoptotic checkpoint. It has been shown, for instance, that AD apoptosis induced by misfolded proteins involves impairment of the ER (Danial *et al.*, 2004:205).

1.2.5 *Protein Phosphorylation State*

A recently identified mechanism shared by neurodegenerative diseases involves the alteration of the phosphorylation state of some key proteins involved in the pathogenic

cascades. Besides the well-recognised hyperphosphorylated state of τ protein in the neurofibrillary tangles observed in AD brain (Kaihong *et al.*, 2006:449), specific altered patterns of kinase and phosphatase activities are associated with alteration in the phosphorylation state of disease-specific proteins in PD (Saito *et al.*, 2003:644), ALS (Strong *et al.*, 2005:649) and HD (Liévens *et al.*, 2002:638).

1.2.6 *Exogenous Agents*

Since the discovery that 1-methyl-4-phenyl-1,2,3,6-tetrahydropyridine (MPTP) can cause Parkinsonism in both humans and animals it has been hypothesised that exposure to some exogenous agent may cause PD (Tanner *et al.*, 1990:17). It is well known that substances such as carbon monoxide, cyanide, manganese, carbon disulfide and organophosphates can cause a Parkinsonian syndrome. Various risk factors have also been identified for the development of PD, including rural living, drinking well water and exposure to insecticides and industrial pollutants. All of these strongly suggest an environmental causation (Koller *et al.*, 1990:1218).

1.2.7 *Excitotoxicity*

It is well known that excessive excitation may be harmful to cells causing neuronal death. Various indirect evidence have suggested that glutamate-mediated excitotoxicity may play a role in the pathogenesis of PD (Greenamyre *et al.*, 1991:977) and therefore glutamate antagonists may be neuroprotective.

1.2.8 *Immunologic Mechanism*

It is hypothesised that neurodegenerative disorders such as PD may be caused, at least in part, by an immunologic mechanism, although this idea has not received much acceptance. Antibodies to dopaminergic neurons have been found in the cerebrospinal fluid of patients suffering from PD, although it is possible that this is a reaction rather than a cause of the disease (Carvey *et al.*, 1991:53).

1.2.9 *Infectious Agents*

An array of different infectious agents has been reported to cause Parkinsonian symptoms as part of an encephalitic process. However, as of yet no definitive evidence has been found that implicates an infectious agent in the pathogenesis of PD or AD.

From the above discussions it is evident that the precise pathophysiology of neurodegeneration is still shrouded in uncertainty, but that it might involve a complex combination of mechanisms that might not be adequately addressed by following the one-molecule, one-target paradigm. The resulting need is for an approach where multi-target-directed ligands (MTDLs) are employed to address these neurodegenerative mechanisms and provide real disease-modifying drug candidates for these diseases. Since the majority of these neurodegenerative mechanisms are shared by many neuronal disorders, MTDLs may also be of potential use as medications for more than one illness (Cavalli *et al.*, 2008:347).

1.3 Multifunctional Drugs for Neurodegenerative Disease Treatment

1.3.1 *Introduction*

Keeping the above discussion in mind, it is not surprising that the current design paradigm of 'one-drug-one-target' may not be the most optimal approach to develop effective treatment regimens for neuropsychiatric diseases such as AD and PD. More and more scientists are becoming convinced that a strategy aimed at targeting multiple disease etiologies simultaneously can be more beneficial than the currently accepted 'silver bullet' approach for the treatment of various diseases (Morphy *et al.*, 2005:6523, Youdim *et al.*, 2005:519). A polypharmaceutical approach has been used as a means of multiple targeting in the clinical setting, wherein several drugs that act independently on different etiological targets of a disease are combined. However, this strategy of combining several drug molecules raises several challenges. A combined or even multiplied toxicity and side-effect profile may be experienced, while it is very likely that unforeseen drug-drug interactions may occur (Smid *et al.*, 2005:6855). Research has therefore focused on the design of single drug molecules that act on two or more specific etiological targets of a particular disease. The advantages associated with this strategy includes a lower likelihood of encountering unwanted side-effects and the possibility to 'design out' any side-effects when only using one ligand, as opposed to using two or more ligands (Van der Schyf *et al.*, 2006:1033). For the treatment of neurodegenerative diseases, single molecular entities may be designed that combine two or more of the following properties:

- Cholinesterase inhibition.
- Activation/inhibition of acetylcholine (ACh) receptor or α-adrenoceptor subtypes.
- Anti-inflammatory activity.
- MAO inhibition.
- COMT inhibition.
- Nitric oxide synthase (NOS) inhibition.
- Anti-apoptotic activity.
- Activation of mitochondrial-dependent cell-survival genes and proteins.
- Neuroprotection.

These MTDLs, being able to simultaneously modulate different molecular targets responsible for a multifactorial disease, are likely to provide greater symptomatic efficacy and better utility as potential neuroprotective, disease-modifying drugs (Youdim *et al.*, 2005:27).

1.3.2 *MTDLs as PD Therapy*

As previously discussed PD has a complex etiology not yet fully understood. Multiple-medication therapy where drugs with different therapeutic mechanisms are combined are currently applied for the treatment of PD (Roach, 2004:1972). For example, the combination of $_L$-dopa with either a MAO-B or COMT inhibitor allows for the decrease in the dose of $_L$-dopa required. A similar result can also be achieved by co-administering a dopaminergic receptor agonist (for example bromocriptine) and $_L$-dopa. It is therefore apparent that in PD too, MTDL design and discovery emerge as a possible alternative strategy to multiple-medication therapy.

Youdim *et al.* (2005:27) designed a series of compounds (**10**-**12**, fig. 6), which incorporates the iron-chelating (VK-28) and antioxidant features with MAO-B inhibitory activity (rasagiline). The rationale for this design strategy was related to the observation that iron concentrations are significantly elevated at the neurodegenerative neuronal site (Mattson, 2004:37) and that iron chelators result in a neuroprotective action in animal models of PD (Kaur *et al.*, 2003:899). A link between elevated iron concentrations and

the involvement of MAO in oxidative neuronal stress as well as ROS production has also been advanced (Shoham *et al.*, 2000:743). It is well known that MAO is one of the major enzymes able to generate H_2O_2 as a result of its ability to oxidatively deaminate monoamines, especially dopamine, in the substantia nigra pars compacta and striatum. According to the Fenton reaction, either ferrous (Fe^{2+}) or ferric (Fe^{3+}) free cations can interact with H_2O_2 to generate $^{\bullet}OH$ radicals. By chelating iron and decreasing H_2O_2 production by means of a MAO inhibitor, the Fenton reaction and $^{\bullet}OH$ radical formation is dramatically reduced (Cavalli *et al.*, 2008:347).

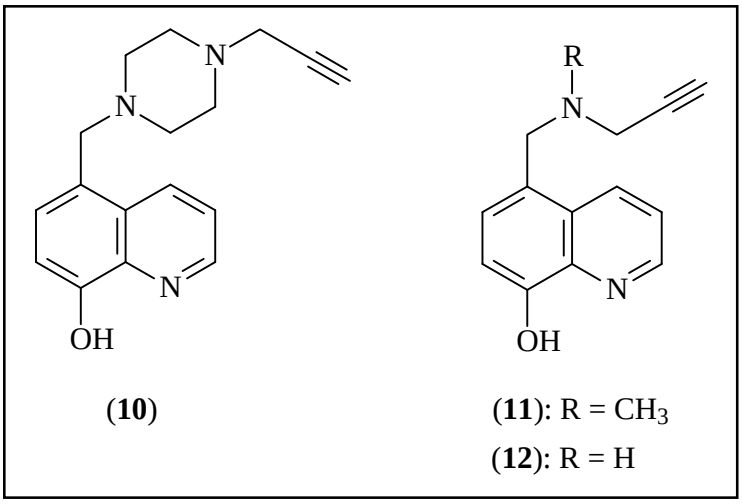

(**10**) (**11**): R = CH_3
(**12**): R = H

Figure 6: Bifunctional derivatives incorporating the pharmacophoric groups of VK-28 (iron chelator) and rasagiline (MAO-B inhibitor) (Youdim *et al.*, 2005:27).

The observation that caffeine consumption is associated with a reduced risk of developing PD (Ross *et al.*, 2000:2674) has prompted the development of a second class of potential MTDLs for PD treatment combining MAO inhibition and adenosine A_{2A} receptor antagonism (**13**, fig. 7). The MAO-B inhibiting properties of the well described and characterised A_{2A} receptor antagonist (*E*)-8-(3-chlorostyryl)-caffeine (CSC), was evaluated *in vitro*. CSC was found to inhibit MAO-B with an enzyme-inhibitor dissociation constant (K_i value) of approximately 100 nM (Chen *et al.*, 2002:36040). Within the same study it was also shown that CSC inhibits the MAO-B catalysed oxidation of MPTP. The two biological profiles, MAO-B inhibition and adenosine A_{2A} receptor antagonism are thought to be unrelated, acting on two parallel biochemical

pathways. Following the abovementioned observations a series of CSC derivatives were prepared and evaluated against both biological targets (Petzer *et al.*, 2003:1299, Vlok *et al.*, 2006:3512) and the structural requirements of A_{2A} receptor antagonists to act as MAO-B inhibitors were defined.

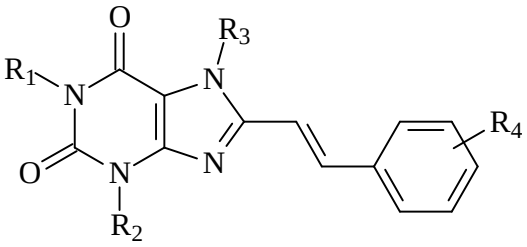

(**13**): $R_{1\text{-}2}$ = CH_3/CH_2CH_3, R_3 = CH_3/H,

R_4 = 3-Cl/-F/-CF_3/-CH_3/-NO_2 or 4-Cl/-F/-CF_3/-CH_3 or 3,4-di-OCH_3/-OCH_2O

Figure 7: CSC derivatives (**13**) evaluated for A_{2A} receptor antagonism and MAO-B inhibition (Petzer *et al.*, 2003:1299, Vlok *et al.*, 2006:3512).

Low molecular weight free radical scavengers including GSH, vitamin E, carnosine and ascorbic acid have limited antioxidant activity because of their low efficiency in permeating the blood-brain barrier and/or affecting iron accumulation. Lipoic acid (LA) (**14**, fig. 8), a metabolic antioxidant, on the other hand readily crosses the blood-brain barrier, accumulates in neuronal cell types (Packer *et al.*, 1997:359) and is reduced by mitochondrial dehydrogenases to dihydrolipoic acid (DHLA), which lowers the redox activities of the free iron cations (Suh *et al.*, 2004:57). LA intrinsically chelates metal ions and can therefore also contribute to lowering iron accumulation in aging brains. Taking these attributes of LA into account, a series of prodrugs (**15**–**18**, fig. 9) were synthesised incorporating dopamine, *L*-dopa and LA (DiStefano *et al.*, 2006:1486), all of which were shown to pass unhydrolysed through the stomach and to release dopamine, *L*-dopa and LA into human plasma after enzymatic hydrolysis. This prodrug displayed antioxidant activities when compared to *L*-dopa, highlighting their potential in brain diseases where there is an involvement of dopamine concentration and free radical damage.

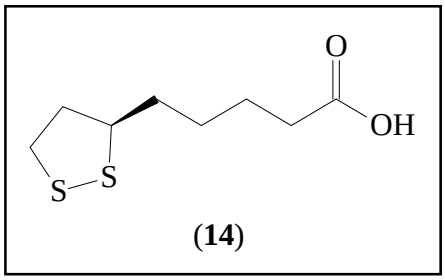

(**14**)

Figure 8: Chemical structure of lipoic acid (LA).

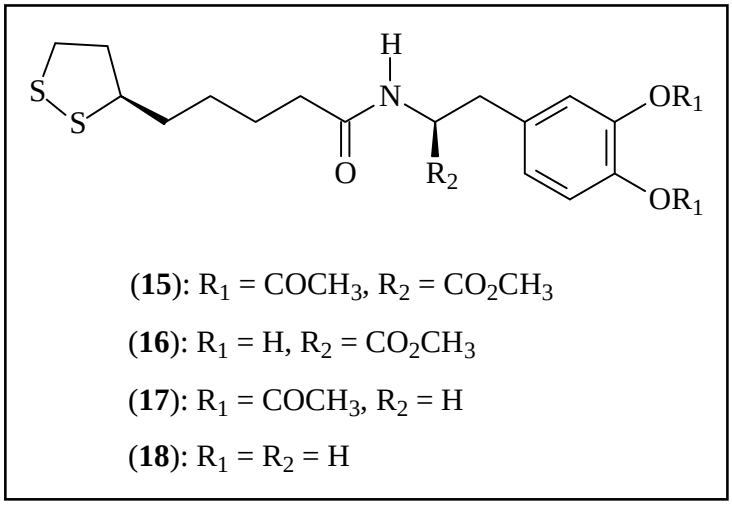

(**15**): $R_1 = COCH_3$, $R_2 = CO_2CH_3$

(**16**): $R_1 = H$, $R_2 = CO_2CH_3$

(**17**): $R_1 = COCH_3$, $R_2 = H$

(**18**): $R_1 = R_2 = H$

Figure 9: Compounds incorporating the structural features of dopamine or $_L$-dopa and lipoic acid (LA) (DiStefano *et al.*, 2006:1486).

Sarizotan (**19**, fig. 10) is a chromane derivative that has recently been developed as a MTDL for the treatment of PD and exhibits dual serotoninergic 5-HT_{1A} receptor agonism as well as dopaminergic receptor antagonism/partial agonism (McIntyre *et al.*, 2006:314). The rationale for its design lies in the observation that serotoninergic 5-HT_{1A} receptor agonists are able to reduce some relevant side-effects associated with $_L$-dopa therapy such as wearing-off and $_L$-dopa-induced dyskinesia (Nicholson *et al.*, 2002:1). Sarizotan exhibited high affinity for human dopaminergic D_2 – D_4 and serotoninergic 5-HT_{1A} receptors, with IC_{50} (concentration of the compound that inhibits 50% of the activity) values less than 6 nM. In clinical trials it was shown that sarizotan could improve dopamine-induced motor complications by reducing striatal serotoninergic nerve impulse activity without altering $_L$-dopa efficacy. This novel compound therefore emerges as a

bifunctional drug for the treatment of dyskinesias associated with *L*-dopa treatment in PD (McIntyre *et al.*, 2006:314).

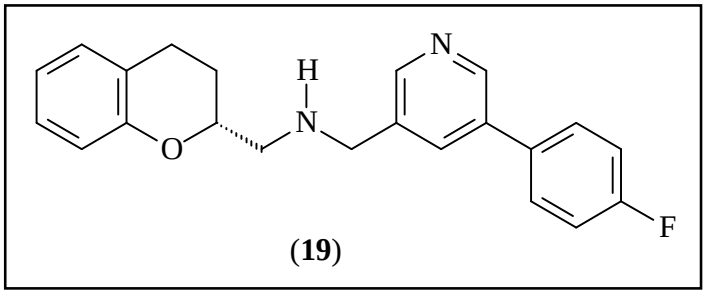

(**19**)

Figure 10: Chemical structure of sarizotan, exhibiting both serotoninergic 5-HT_{1A} receptor agonism as well as dopaminergic D_2 receptor antagonism/partial agonism (McIntyre *et al.*, 2006:314).

1.3.3 *MTDLs as AD Therapy*

During the past decade a great deal of insight has been gained into the complex nature of the multiple etiology contributing to the development of AD. This has left the scientific community with the notion that multiple-medication therapy or multiple-compound medication might result in a more effective treatment strategy for this disease (Schmitt *et al.*, 2004:827). By employing these strategies the multiple pathological processes involved in AD can be targeted simultaneously, which may offer additional benefits with respect to single-drug treatments. It is therefore possible that targeting multiple brain substrates might develop additive or synergistic positive mnemonic effects (Youdim *et al.*, 2005:27). Multiple-medication therapy has already achieved great success in the treatment of similarly complex diseases such as cancer, HIV and hypertension, where it achieves maximum efficacy by addressing several targets concurrently, exploiting synergy and minimising individual toxicity (Cavalli *et al.*, 2008:347).

In view of the therapeutic potential of multiple-medication therapy MTDLs should be the next step toward the design of drugs that effectively target the multiple etiology of AD, possibly resulting in disease cessation.

When designing MTDLs the approach is usually to combine the pharmacophores of different drugs in order to obtain hybrid molecules that produce specific pharmacological responses slowing or stopping the neurodegenerative process. The idea is that each

pharmacophore of the new drug should retain the ability to interact with its specific site(s) on the target. An approach applied very often when designing MTDLs for AD has been to structurally modify an AChE inhibitor to provide it with biological properties useful for AD treatment (Cavalli *et al.*, 2008:347).

Research efforts with regards to AD treatment have been focused on the development of so-called "dual binding site" AChE inhibitors. These compounds might alleviate cognitive deficit by restoring cholinergic activity through simultaneous interaction with both AChE catalytic and peripheral sites. More importantly, they might have the ability to address the disease mechanisms by reducing Aβ aggregation (Cavalli *et al.*, 2008:347). Caproctamine (**20**, fig. 11) is an example of one of the first successfully designed AChE inhibitors endowed with additional pharmacological effects beneficial in AD. The observation that the tetraamine, disulfide benextramine (**21**), showed muscarinic M_2 receptor antagonism as well as reversibly inhibiting AChE, served as the starting point for this study. Structural modifications of the tetraamine backbone of **21** led to **20**, which emerged with suitable biological attributes for the treatment of AD. These included AChE inhibition and competitive muscarinic M_2 receptor antagonism (Melchiorre *et al.*, 1998:4186).

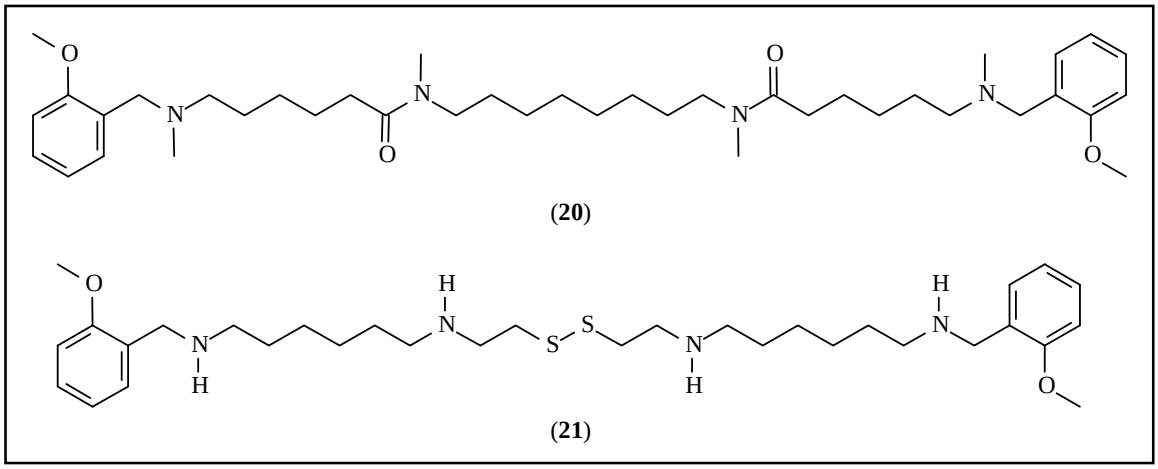

Figure 11: Chemical structures of caproctamine (**20**) and the tetraamine, disulfide benextramine (**21**) used as lead compound (Melchiorre *et al.*, 1998:4186).

AChE inhibitors specifically designed to bind both the catalytic site and peripheral anionic site of human AChE were shown to possess Aβ anti-aggregating activity. An example of such a compound is AP2238 (3-{4-[(benzyl-methyl-amino)-methyl]phenyl}-6,7-dimethoxy-2H-2-chromenone) (**22**, fig. 12). This compound was designed by combining in one molecule two moieties that are optimal for binding each enzyme site, separated by an appropriate spacer. The two moieties, a benzylamino and a coumarin (2H-2-chromenone) heterocyclic group, were selected from previously developed AChE inhibitors and the phenyl ring spacer was used as it could favourably interact with some of the numerous aromatic residues lining the AChE gorge. AP2238 was shown to have an AChE inhibitory activity comparable to donepezil and was able to counteract Aβ aggregation with a higher potency than other tested AChE inhibitors (Piazzi *et al.*, 2003:2279).

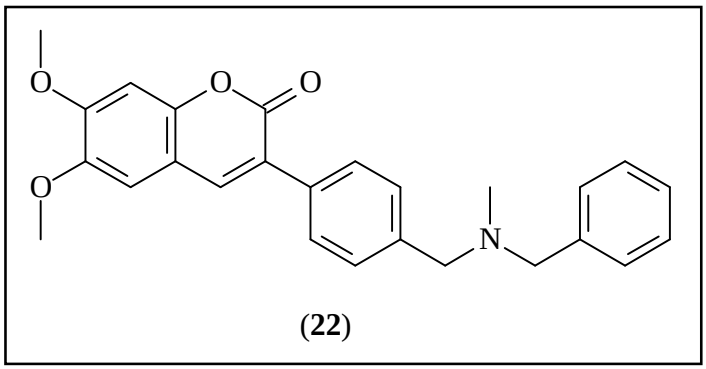

(**22**)

Figure 12: AP2238, a compound designed to simultaneously bind the AChE catalytic site and peripheral anionic site to counteract AChE-induced Aβ aggregation as well as increasing ACh content (Piazzi *et al.*, 2003:2279).

It is widely acknowledged that the cognitive decline associated with AD is related to the loss of cholinergic and glutamatergic neurons. However, behavioural change may not only be related to the severity of cholinergic loss but may also be as a result of alterations in the serotoninergic and noradrenergic systems (Cavalli *et al.*, 2008:347). The noradrenergic deficits of AD are linked to depression (Gottfries, 1990:541) whereas the serotoninergic deficits are linked to depression and psychosis (Meltzer *et al.*, 1998:407).

Keeping the above in mind, drugs that increase the activity of biogenic amines while simultaneously acting on the cholinergic system, may be a promising approach for future

AD treatment. A series of compounds incorporating a carbamate moiety and based on the pharmacophores of selegiline/(*R*)-deprenyl and rasagiline were synthesised and tested as inhibitors of MAO-B and AChE (Mandel *et al.*, 2005:379). One of these, ladostigil (TV3326) (**23**, fig. 13), was selected for further investigation. It was determined that this compound is an inhibitor of both AChE as well as butyrylcholinesterase (BuChE) and exhibits cognitive actions in animal models comparable to those of rivastigmine or galantamine, two AChE inhibitors already used for AD treatment. After chronic treatment for 1 – 8 weeks with ladostigil, both MAO isoforms were inhibited in the brain with very little inhibition of the enzyme in gut or liver. This observation therefore allowed the irreversible inhibition of all MAO activity in the brain with no cheese reaction and because it was a non-selective MAO inhibitor it increased the noradrenaline, serotonin and dopamine concentrations in rat/mice hippocampus and striatum. Ladostigil also presented with neuroprotective activity in cultures of neuronal cells and it was determined that it posessess anti-apoptotic activity identical to those of rasagiline. This compound is currently in phase II clinical trials for AD and diffuse Lewy body disease and will eventually be tested for PD as well.

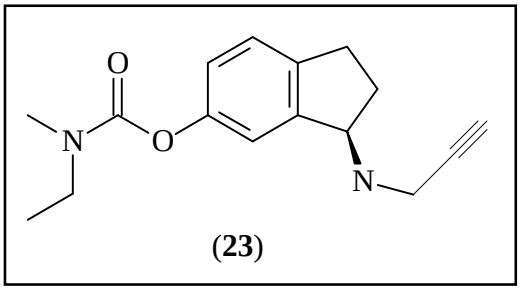

(**23**)

Figure 13: Chemical structure of ladostigil (TV3326), a dual MAO and AChE inhibitor (Mandel *et al.*, 2005:379).

Narahashi *et al.* (2004:1701) indicated that the nootropic compound nefiracetam (**24**, fig. 14) has a dual mechanism of action, both of which are thought to be beneficial for AD patients. The compound exhibits the ability to potentiate NMDA and nicotinic acetylcholine receptors in nanomolar concentrations, binding with the glycine binding site of the NMDA receptor. These attributes may be beneficial for cognition enhancement in AD patients and should be the topic of further investigation.

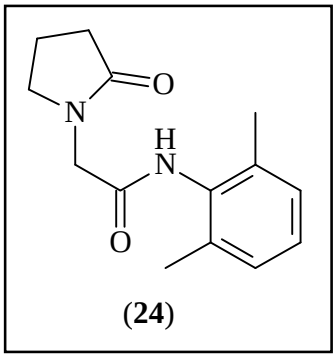

(**24**)

Figure 14: Nefiracetam, a dual mechanism drug for the possible treatment of AD (Narahashi *et al.*, 2004:1701).

Recent studies have focused on the development of AChE inhibitors with the additional benefit of having antioxidant activity, of which the following two are examples:

The structure of LA, which is an antioxidant having several protective effects in neurodegeneration (Holmquist *et al.*, 2007:154) was combined with that of tacrine, a well-established AChE inhibitor (Rosini *et al.*, 2005:360). It was hypothesised that the cyclic moiety of LA could also interact with the peripheral anionic site of the AChE enzyme, commonly associated with Aβ aggregation. By combining these two molecules into one structure cholinergic transmission was improved and Aβ aggregation as well as oxidative damage were inhibited (Bolognesi *et al.*, 2006:1269). Lipocrine (**25**, fig. 15) served as a prototype for the derivatives of this group of compounds and it was indicated that it was able to protect neuronal cells against ROS to a greater extent than the parent compound, LA.

The same strategy as above was followed to design a series of compounds incorporating tacrine and the potent antioxidant, melatonin. It has recently been reported that apart from this property melatonin has the ability to act as a neuroprotectant in AD (Cheng *et al.*, 2006:129). The most potent compound (**26**) of the synthesised series exhibited excellent potency (IC_{50} = 0.008 nM) and selectivity (1000-fold) for AChE inhibition relative to BuChE. It was also determined that **26** had an antioxidant potency 2.5-fold higher than trolox, a vitamin E analogue universally used as a reference compound for the assessment of antioxidant properties (Rodriguez-Franco *et al.*, 2006:459).

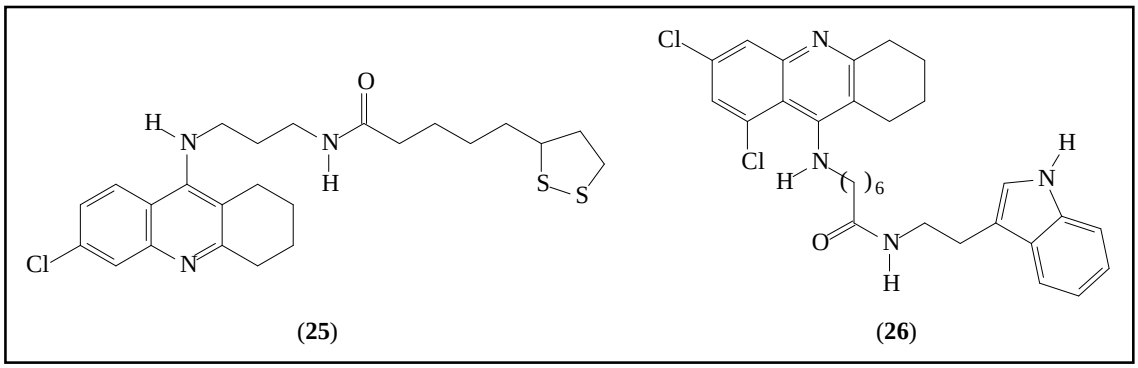

Figure 15: Compounds combining the AChE inhibiting profile of tacrine with the antioxidant activities of LA and melatonin (Bolognesi *et al.*, 2006:1269).

From the discussions above it is clear that scientific focus has shifted from a single drug target paradigm to that of a multiple drug target paradigm for the treatment of neuropsychiatric disorders such as AD and PD. When designing novel neuroprotective compounds, be it in the industry or academia, this should be kept in mind. However, the challenge is to identify additional pharmacophores that interact with other relevant therapeutic targets and that do not lose activity when combined with other structures.

1.4 Study Aim

The major MAO isoform present in the human brain is MAO-B (Saura *et al.*, 1996:755). In the substantia nigra MAO-B is located primarily in glial cells (Konradi *et al.*, 1989:383), which is an area commonly affected by PD. The expression levels of MAO-B in neuronal tissue increase approximately 4-fold with age (Fowler *et al.*, 2003:11600), resulting in increased dopamine metabolism. Higher levels of H_2O_2 are produced as a result of this, which may lead to further neurodegeneration (Kumar *et al.*, 2003:46432). Selective inhibition of MAO-B results in an increase of the dopamine concentration in the synaptic cleft of nigrostriatal neurons (Wouters *et al.*, 1997:721). Selegiline/(*R*)-deprenyl, a clinically used anti-PD drug, is a selective irreversible inhibitor of MAO-B. After treatment with (*R*)-deprenyl, it may require as long as 40 days for MAO-B activity to recover to normal levels (Fowler *et al.*, 1994:86) as *de novo* synthesis of the enzyme has to occur. There are currently fewer specific reversible MAO-B inhibitors than those available for MAO-A, and their low potency limit their therapeutic potential (Foley *et al.*, 2000:25). The need to develop MAO-B selective, reversible inhibitors with high potency is thus warranted.

Nitric oxide (NO) is a biological messenger involved in numerous fundamental functions including neurotransmission (Kiss *et al.*, 2001:211), blood pressure and blood flow regulation (Kadekaro *et al.*, 2000:450), platelet aggregation and inflammation (Bredt, 1999:577). An overproduction of NO plays an important role in a variety of disorders, such as septic shock, pain (Cheshire, 2001:795), ischaemia (Endres *et al.*, 2004:283) and several neurodegenerative diseases (Togo *et al.*, 2004:563) including PD. Three isoforms of NOS have been cloned: neuronal (nNOS), endothelial (eNOS) and inducible (iNOS) (Stuehr, 1997:339). The latter isoform is calcium independent whereas the former two are both constitutive and calcium dependent enzymes. NOS is an important drug target (Babu *et al.*, 1998:491), and in order to prevent uncontrolled NO production in disease states, isoform-selective inhibitors are required (Southan *et al.*, 1996:383). It is extremely important not to inhibit eNOS because of its crucial role in maintaining blood flow. The design and development of isoform-selective NOS inhibitors, for example specific nNOS inhibitors, are thus also merited.

For this study our primary objective is to synthesise a series of selective MAO-B enzyme inhibitors and to evaluate the possibility that they may exhibit NOS inhibitory activity as well. The biological activity profiles of these novel compounds will be assessed thoroughly by evaluating the compounds as inhibitors of MAO-A/B and NOS, respectively. Molecular modelling using Discovery Studio® (Accelrys® Software Inc., San Diego, USA) will also be applied to determine the correlation between theoretical ("docking") results and experimental inhibition data. The final findings from the study will be compiled into two articles to be submitted to peer-reviewed journals. The first article describes the MAO-B and NOS inhibitory activities of a selected series of pteridine-2,4-dione derivatives (**27**-**28**, fig. 16) while the second article describes the MAO-A and –B potencies of the indole and benzofuran derivatives (**29**-**30**, fig. 17) selected for this study.

The pteridine-2,4-dione nucleus (**31**) bear structural resemblance to caffeine and therefore it is of great interest to determine whether the pteridine-2,4-dione derivatives (**27**-**28**) possess MAO-B inhibition properties that are comparable to those of the recently described caffeine derivatives (Vlok *et al.*, 2006:3512, Van den Berg *et al.*, 2007:3692). Pteridine-2,4-dione is also structurally similar to the essential NOS cofactor,

tetrahydrobiopterin (BH_4) (**32**), and because of this structural relationship with BH_4, pteridine derivatives have been described as NOS inhibitors.

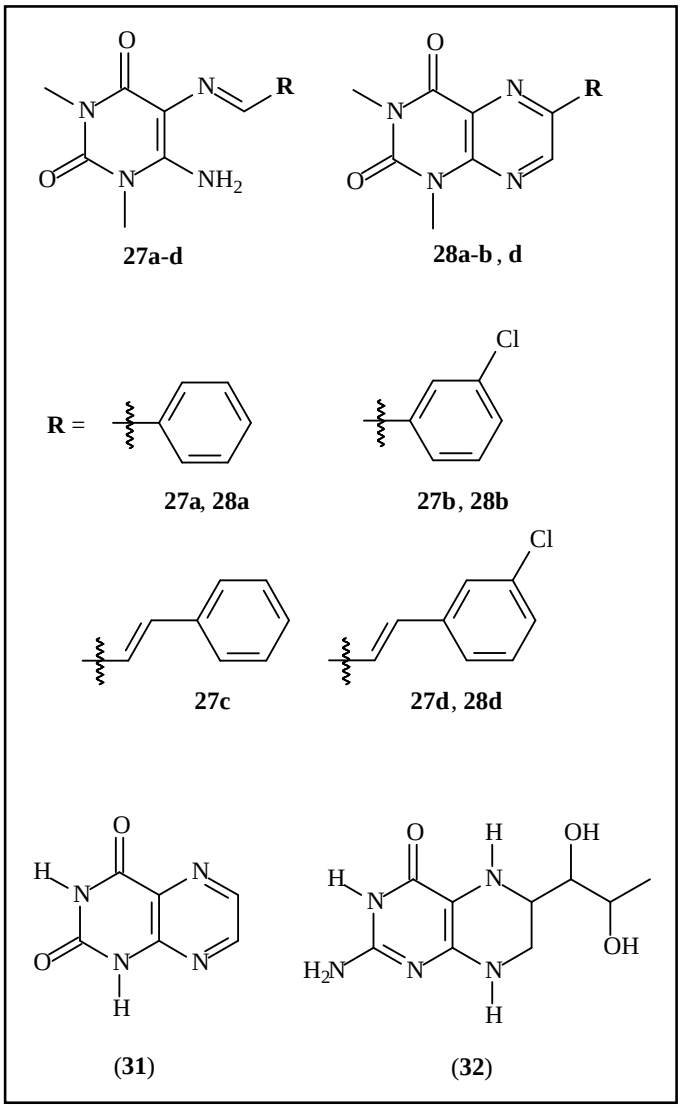

Figure 16: Structures of the selected pteridine-2,4-dione derivatives (**27-28**), the pteridine-2,4-dione nucleus (**31**) and BH_4 (**32**).

Several previous studies (Balsa *et al.*, 1990:103, Balsa *et al.*, 1991:215, Fernández García *et al.*, 1992:909) have indicated that the indole nucleus (**33**) may be useful as a scaffold for the design of MAO inhibitors. For example, a variety of indolylmethylamine derivatives have been shown to act as irreversible MAO inhibitors (Morón *et al.*, 2000:1684). In the second article a series of indole derivatives (**29a**-**h**) and structurally

related benzofuranes (**30a-d**) were synthesised and evaluated for their ability to selectively inhibit recombinant human MAO-B.

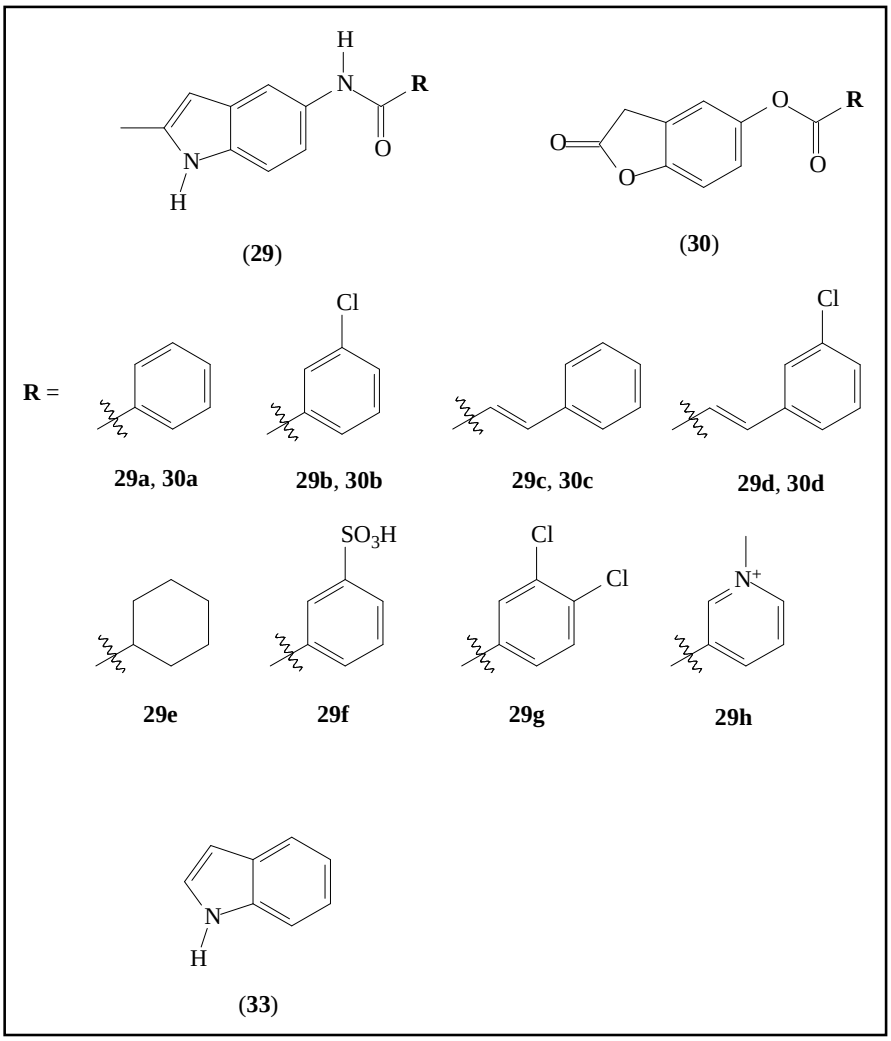

Figure 17: Structures of the selected indole (**29**) and benzofuran (**30**) derivatives, as well as the indole nucleus (**33**).

References

AISEN, P.S. 2005. The development of anti-amyloid therapy for Alzheimer's disease: From secretase modulators to polymerisation inhibitors. *CNS drugs,* 19(12):989-996.

AISEN, P.S., SCHAFER, K.A., GRUNDMAN, M., PFEIFFER, E., SANO, M., DAVIS, K.L., FARLOW, M.R., JIN, S., THOMAS, R.G. & THAL, L.J. 2003. Effects of rofecoxib or naproxen vs placebo on Alzheimer's disease progression: A randomized controlled trial. *Journal of the American medical association.,* 289(21):2819-2826.

ANDERSEN, J.K. 2004. Oxidative stress in neurodegeneration: Cause or consequence? *Nature medicine, supplement,* 10:S18-S25.

BABU, B.R. & GRIFFITH, O.W. 1998. Design of isoform-selective inhibitors of nitric oxide synthase. *Current opinion in chemical biology,* 2(4):491-500.

BALSA, D., FERNÁNDEZ-ÁLVAREZ, E., TIPTON, K.F., UNZETA, M. 1990. Inhibition of MAO by substituted tryptamine analogues. *Journal of neural transmission, supplement,* 32:103-105.

BALSA, D., FERNÁNDEZ-ÁLVAREZ, E., TIPTON, K.F., UNZETA, M. 1991. Monoamine oxidase inhibitory potencies and selectivities of 2-[N-(2-propynyl)-aminomethyl]-1-methyl indole derivatives. *Biochemical society transactions,* 19(1):215-218.

BEAL, M.F. 1995. Aging, energy, and oxidative stress in neurodegenerative diseases. *Annals of neurology,* 38(3):357-366.

BECKMAN, J.S. 1996. Oxidative damage and tyrosine nitration from peroxynitrite. *Chemical research in toxicology,* 9(5):836-844.

BEUTNER, G., RÜCK, A., RIEDE, B., WELTE, W. & BRDICZKA, D. 1996. Complexes between kinases, mitochondrial porin and adenylate translocator in rat brain resemble the permeability transition pore. *FEBS letters,* 396(2-3):189-195.

BOLOGNESI, M.L., MINARINI, A., TUMIATTI, V. & MELCHIORRE, C. 2006. Lipoic acid, a lead structure for multi-target-directed drugs for neurodegeneration. *Mini reviews in medicinal chemistry,* 6(11):1269-1274.

BREDT, D.S. 1999. Endogenous nitric oxide synthesis: Biological functions and pathophysiology. *Free radical research,* 31(6):577-596.

CARRELL, R.W. & LOMAS, D.A. 1997. Conformational disease. *Lancet,* 350(9071):134-138.

CARVEY, P.M., MCRAE, A., LINT, T.F., PTAK, L.R., LO, E.S., GOETZ, C.G. & KLAWANS, H.L. 1991. The potential use of a dopamine neuron antibody and a striatal-derived neurotrophic factor as diagnostic markers in Parkinson's disease. *Neurology, supplement 2,* 41(5):53-58.

CASSARINO, D.S. & BENNETT, J.P. 1999. An evaluation of the role of mitochondria in neurodegenerative diseases: Mitochondrial mutations and oxidative pathology, protective nuclear responses, and cell death in neurodegeneration. *Brain research reviews,* 29(1):1-25.

CAUGHEY, B. & LANSBURY P.T., Jr. 2003. Protofibrils, pores, fibrils, and neurodegeneration: Separating the responsible protein aggregates from the innocent bystanders. *Annual review of neuroscience,* 26(1):267-298.

CAVALLI, A., BOLOGNESI, M.L., MINARINI, A., ROSINI, M., TUMIATTI, V., RECANATINI, M. & MELCHIORRE, C. 2008. Multi-target-directed ligands to combat neurodegenerative diseases. *Journal of medicinal chemistry,* 51(3):347-372.

CHEN, J.-F., STEYN, S., STAAL, R., PETZER, J.P., XU, K., VAN DER SCHYF, C.J., CASTAGNOLI, K.P., SONSALLA, P.K., CASTAGNOLI, N., Jr. & SCHWARZSCHILD, M.A. 2002. 8-(3-Chlorostyryl)caffeine may attenuate MPTP neurotoxicity through dual actions of monoamine oxidase inhibition and A_{2A} receptor antagonism. *Journal of biological chemistry,* 277(39):36040-36044.

CHENG, Y., FENG, Z., ZHANG, Q.Z. & ZHANG, J.T. 2006. Beneficial effects of melatonin in experimental models of Alzheimer's disease. *Acta pharmacologica sinica,* 27(2):129-139.

CHERNYAK, B.V. & BERNARDI, P. 1996. The mitochondrial permeability transition pore is modulated by oxidative agents through both pyridine nucleotides and glutathione at two separate sites. *European journal of biochemistry,* 238(3):623-630.

CHESHIRE, D.R. 2001. Use of nitric oxide synthase inhibitors for the treatment of inflammatory disease and pain. *IDrugs,* 4(7):795-803.

CONTESTABILE, A. 2001. Oxidative stress in neurodegeneration: Mechanisms and therapeutic perspectives. *Current topics in medicinal chemistry,* 1(6):553-568.

COREY-BLOOM, J. 2002. The ABC of Alzheimer's disease: Cognitive changes and their management in Alzheimer's disease and related dementias. *International psychogeriatrics, supplement 1,* 14:51-75.

CRAIG, M.C., MAKI, P.M. & MURPHY, D.G. 2005. The women's health initiative memory study: Findings and implications for treatment. *The lancet neurology,* 4(3):190-194.

DANIAL, N.N. & KORSMEYER, S.J. 2004. Cell death: Critical control points. *Cell,* 116(2):205-219.

DAUER, W. & PRZEDBORSKI, S. 2003. Parkinson's disease: Mechanisms and models. *Neuron,* 39(6):889-909.

DISTEFANO, A., SOZIO, P., COCCO, A., IANNITELLI, A., SANTUCCI, E., COSTA, M., PECCI, L., NASUTI, C., CANTALAMESSA, F. & PINNEN, F. 2006. $_L$-dopa- and dopamine-(R)-α-lipoic acid conjugates as multifunctional codrugs with antioxidant properties. *Journal of medicinal chemistry,* 49(4):1486-1493.

DORAISWAMY, P.M. & FINEFROCK, A.E. 2004. Metals in our minds: Therapeutic implications for neurodegenerative disorders. *The lancet neurology,* 3(7):431-434.

ENDRES, M., LAUFS, U., LIAO, J.K. & MOSKOWITZ, M.A. 2004. Targeting eNOS for stroke protection. *Trends in neurosciences,* 27(5):283-289.

ERNST, E. & PITTLER, M.H. 2005. Ginkgo biloba for vascular dementia and Alzheimer's disease: Updated systematic review of double-blind, placebo-controlled, randomized trials. *Perfusion,* 18(12):388-392.

FERNÁNDEZ GARCÍA, C., MARCO, J.L., FERNÁNDEZ-ÁLVAREZ, E. 1992. Acetylenic and allenic derivatives of 2-(5-methoxy-1-methylindolyl) alkylamines: Synthesis and evaluation as selective inhibitors of the monoamine oxidases A and B. *European journal of medicinal chemistry,* 27:909-918.

FINBERG, J.P.M., TENNE, M. & YOUDIM, M.B.H. 1981. Tyramine antagonistic properties of AGN 1135, an irreversible inhibitor of monoamine oxidase type B. *British journal of pharmacology,* 73(1):65-74.

FINBERG, J.P.M., WANG, J., BANKIEWICZ, K., HARVEY-WHITE, J., KOPIN, I.J. & GOLDSTEIN, D.S. 1998. Increased striatal dopamine production from $_L$-DOPA following selective inhibition of monoamine oxidase B by R(+)-N-propargyl-1-aminoindan (rasagiline) in the monkey. *Journal of neural transmission, supplement,* 52:279-285.

FOLEY, P., GERLACH, M., YOUDIM, M.B.H. & RIEDERER, P. 2000. MAO-B inhibitors: Multiple roles in the therapy of neurodegenerative disorders? *Parkinsonism & related disorders,* 6(1):25-47.

FOWLER, J.S., LOGAN, J., WANG, G., VOLKOW, N.D., TELANG, F., ZHU, W., FRANCESCHI, D., PAPPAS, N., FERRIERI, R., SHEA, C., GARZA, V., XU, Y., SCHLYER, D., GATLEY, S.J., DING, Y., ALEXOFF, D., WARNER, D., NETUSIL, N., CARTER, P., JAYNE, M., KING, P. & VASKA, P. 2003. Low monoamine oxidase B in peripheral organs in smokers. *Proceedings of the national academy of sciences of the United States of America,* 100(20):11600-11605.

FOWLER, J.S., VOLKOW, N.D., LOGAN, J., WANG, G.J., MACGREGOR, R.R., SCHLYER, D., WOLF, A.P., PAPPAS, N., ALEXOFF, D. & SHEA, C. 1994. Slow recovery of human brain MAO B after $_L$-deprenyl (selegeline) withdrawal. *Synapse,* 18(2):86-93.

GAGGELLI, E., KOZLOWSKI, H., VALENSIN, D. & VALENSIN, G. 2006. Copper homeostasis and neurodegenerative disorders (Alzheimer's, prion, and Parkinson's diseases and amyotrophic lateral sclerosis). *Chemical reviews,* 106(6):1995-2044.

GOTTFRIES, C.G. 1990. Neurochemical aspects on aging and diseases with cognitive impairment. *Journal of neuroscience research,* 27(4):541-547.

GREENAMYRE, J.T. & O BRIEN, C. 1991. N-methyl-D-aspartate antagonists in the treatment of Parkinson s disease. *Archives of neurology,* 48(9):977-981.

HAGEN, T.M., YOWE, D.L., BARTHOLOMEW, J.C., WEHR, C.M., DO, K.L., PARK, J. & AMES, B.N. 1997. Mitochondrial decay in hepatocytes from old rats: Membrane potential declines, heterogeneity and oxidants increase. *Proceedings of the national academy of sciences of the United States of America,* 94(7):3064-3069.

HEIKKILA, R.E., MANZINO, L., CABBAT, F.S. & DUVOISIN, R.C. 1984. Protection against the dopaminergic neurotoxicity of 1-methyl-4-phenyl-1,2,3,6-tetrahydropyridine by monoamine oxidase inhibitors. *Nature,* 311(5985):467-469.

HOLMQUIST, L., STUCHBURY, G., BERBAUM, K., MUSCAT, S., YOUNG, S., HAGER, K., ENGEL, J. & MÜNCH, G. 2007. Lipoic acid as a novel treatment for Alzheimer s disease and related dementias. *Pharmacology & therapeutics,* 113(1):154-164.

JAIN, A., MÅRTENSSON, J., STOLE, E., AULD, P.A. & MEISTER, A. 1991. Glutathione deficiency leads to mitochondrial damage in brain. *Proceedings of the national academy of sciences of the United States of America,* 88(5):1913-1917.

JELLINGER, K.A. 2003. General aspects of neurodegeneration. *Journal of neural transmission, supplement,* 65:101-144.

KABANOV, A.V. & GENDELMAN, H.E. 2007. Nanomedicine in the diagnosis and therapy of neurodegenerative disorders. *Progress in polymer science,* 32(8-9):1054-1082.

KADEKARO, M. & SUMMY-LONG, J.Y. 2000. Centrally produced nitric oxide and the regulation of body fluid and blood pressure homeostases. *Clinical & experimental pharmacology & physiology,* 57(5):450-459.

KAIHONG M. & JOHNSON, G.V.W. 2006. The role of tau phosphorylation in the pathogenesis of Alzheimer s disease. *Current Alzheimer research,* 3(5):449-463.

KAUR, D., YANTIRI, F., RAJAGOPALAN, S., KUMAR, J., MO, J.Q., BOONPLUEANG, R., VISWANATH, V., JACOBS, R., YANG, L., BEAL, M.F., DIMONTE, D., VOLITASKIS, I., ELLERBY, L., CHERNY, R.A., BUSH, A.I. & ANDERSEN, J.K. 2003. Genetic or pharmacological iron chelation prevents MPTP-induced neurotoxicity in vivo: A novel therapy for Parkinson's disease. *Neuron,* 37(6):899-909.

KHAN, A.A., SOLOSKI, M.J., SHARP, A.H., SCHILLING, G., SABATINI, D.M., LI, S.H., ROSS, C.A. & SNYDER, S.H. 1996. Lymphocyte apoptosis: Mediation by increased type 3 inositol 1,4,5- trisphosphate receptor. *Science,* 273(5274):503-507.

KISS, J.P. & VIZI, E.S. 2001. Nitric oxide: A novel link between synaptic and nonsynaptic transmission. *Trends in neurosciences,* 24(4):211-215.

KNOLL, J. & MAGYAR, K. 1972. Some puzzling pharmacological effects of monoamine oxidase inhibitors. *Advances in biochemical psychopharmacology,* 5:393-408.

KOLLER, W.C., VETERE-OVERFIELD, B., GRAY, C., ALEXANDER, C., CHIN, T., DOLEZAL, J., HASSANEIN, R. & TANNER, C. 1990. Environmental risk factors in Parkinson's disease. *Neurology,* 40(8):1218-1221.

KONRADI, C., KORNHUBER, J., FROELICH, L., FRITZE, J., HEINSEN, H., BECKMANN, H., SCHULTZ, E. & RIEDERER, P. 1989. Demonstration of monoamine oxidase A and B in the human brainstem by a histochemical technique. *Neuroscience,* 33(2):383-400.

KUMAR, M.J., NICHOLLS, D.G. & ANDERSEN, J.K. 2003. Oxidative α-ketoglutarate dehydrogenase inhibition via subtle elevations in monoamine oxidase B levels results in loss of spare respiratory capacity: Implications for Parkinson's disease. *Journal of biological chemistry,* 278(47):46432-46439.

LEVY, G., TANG, M.X., LOUIS, E.D., COTE, L.J., ALFARO, B., MEJIA, H., STERN, Y. & MARDER, K. 2002. The association of incident dementia with mortality in PD. *Neurology,* 59(11):1708-1713.

LIÉVENS, J., WOODMAN, B., MAHAL, A. & BATES, G.P. 2002. Abnormal phosphorylation of synapsin I predicts a neuronal transmission impairment in the R6/2 Huntington's disease transgenic mice. *Molecular and cellular neuroscience,* 20(4):638-648.

LIN, M.T. & BEAL, M.F. 2006. Mitochondrial dysfunction and oxidative stress in neurodegenerative diseases. *Nature,* 443(7113):787-795.

LIN, M.T. & BEAL, M.F. 2006. Mitochondrial dysfunction and oxidative stress in neurodegenerative diseases. *Nature,* 443(7113):787-795.

MANDEL, S., WEINREB, O., AMIT, T. & YOUDIM, M.B.H. 2005. Mechanism of neuroprotective action of the anti-Parkinson drug rasagiline and its derivatives. *Brain research reviews,* 48(2):379-387.

MARCHETTI, P., CASTEDO, M., SUSIN, S., ZAMZAMI, N., HIRSCH, T., MACHO, A., HAEFFNER, A., HIRSCH, F., GEUSKENS, M. & KROEMER, G. 1996. Mitochondrial permeability transition is a central coordinating event of apoptosis. *The journal of experimental medicine,* 184(3):1155-1160.

MATTSON, M.P. 2004. Metal-catalyzed disruption of membrane protein and lipid signaling in the pathogenesis of neurodegenerative disorders. *Annals of the New York academy of sciences,* 1012:37-50.

MCINTYRE, J.A., CASTAÑER, J. & BAYÉS, M. 2006. Sarizotan hydrochloride. antidyskinetic drug 5-HT_{1A} receptor agonist dopamine D_2 receptor ligand. *Drugs of the future,* 31(4):314-319.

MELCHIORRE, C., ANDRISANO, V., BOLOGNESI, M.L., BUDRIESI, R., CAVALLI, A., CAVRINI, V., ROSINI, M., TUMIATTI, V. & RECANATINI, M. 1998. Acetylcholinesterase noncovalent inhibitors based on a polyamine backbone for potential use against Alzheimer's disease. *Journal of medicinal chemistry,* 41(22):4186-4189.

MELTZER, C.C., SMITH, G., DEKOSKY, S.T., POLLOCK, B.G., MATHIS, C.A., MOORE, R.Y., KUPFER, D.J. & REYNOLDS, C.F. 1998. Serotonin in aging, late-life depression, and Alzheimer's disease: The emerging role of functional imaging. *Neuropsychopharmacology,* 18(6):407-430.

MORGANTE, L., SALEMI, G., MENEGHINI, F., DI ROSA, A.E., EPIFANIO, A., GRIGOLETTO, F., RAGONESE, P., PATTI, F., REGGIO, A., DI PERRI, R. & SAVETTIERE, G. 2000. Parkinson's disease survival: A population-based study. *Archives of neurology,* 57(4):507-512.

MORÓN, J.A., CAMPILLO, M., PÉREZ, V., UNZETA, M., PARDO, L., 2000. Molecular determinants of MAO selectivity in a series of indolylmethylamine derivatives: biological activities, 3D-QSAR/CoMFA analysis, and computational simulation of ligand recognition. *Journal of medicinal chemistry,* 43(9):1684-1691.

MORPHY, R. & RANKOVIC, Z. 2005. Designed multiple ligands: An emerging drug discovery paradigm. *Journal of medicinal chemistry,* 48(21):6523-6543.

MOUNT, C. & DOWNTON, C. 2006. Alzheimer's disease: Progress or profit? *Nature medicine,* 12(7):780-784.

NARAHASHI, T., MORIGUCHI, S., ZAO, X., MARSZALEC, W. & YEH, J.Z. 2004. Mechanisms of action of cognitive enhancers on neuroreceptors. *Biological and pharmaceutical bulletin,* 27(11):1701-1706.

NICHOLSON, S.L. & BROTCHIE, J.M. 2002. 5-hydroxytryptamine (5-HT, serotonin) and Parkinson's disease – opportunities for novel therapeutics to reduce the problems of levodopa therapy. *European journal of neurology,* 9(3):1-6.

OLANOW, C.W. 1992. An introduction to the free radical hypothesis in Parkinson's disease. *Annals of neurology, supplement,* 32:S2-S9.

OOMAH, B.D. 2004. Ginkgo biloba and Alzheimer's disease. *Agro food industry hi-tech,* 15(4):44-46.

PACKER, L., TRITSCHLER, H.J. & WESSEL, K. 1997. Neuroprotection by the metabolic antioxidant α-lipoic acid. *Free radical biology and medicine,* 22(1-2):359-378.

PACKER, M.A., MIESEL, R. & MURPHY, M.P. 1996. Exposure to the Parkinsonian neurotoxin 1-methyl-4-phenylpyridinium (MPP^+) and nitric oxide simultaneously causes cyclosporin A-sensitive mitochondrial calcium efflux and depolarisation. *Biochemical pharmacology,* 51(3):267-273.

PETZER, J.P., STEYN, S., CASTAGNOLI, K.P., CHEN, J., SCHWARZSCHILD, M.A., VAN DER SCHYF, C.J. & CASTAGNOLI, N., Jr. 2003. Inhibition of monoamine oxidase B by selective adenosine A_{2A} receptor antagonists. *Bioorganic & medicinal chemistry,* 11(7):1299-1310.

PIAZZI, L., RAMPA, A., BISI, A., GOBBI, S., BELLUTI, F., CAVALLI, A., BARTOLINI, M., ANDRISANO, V., VALENTI, P. & RECANATINI, M. 2003. 3-(4-{[benzyl(methyl)amino]methyl}phenyl)-6,7-dimethoxy-2H-2-chromenone (AP2238) inhibits both acetylcholinesterase and acetylcholinesterase-induced β-amyloid aggregation: A dual function lead for Alzheimer's disease therapy. *Journal of medicinal chemistry,* 46(12):2279-2282.

RAINER, M.K., MUCKE, H.A.M., KRÜGER-RAINER, C., HAUSHOFER, M. & KASPER, S. 2004. Zotepine for behavioural and psychological symptoms in dementia: An open-label study. *CNS drugs,* 18(1):49-55.

RAMASSAMY, C., LONGPRÉ, F. & CHRISTEN, Y. 2007. Ginkgo biloba extract (EGb 761) in Alzheimer's disease: Is there any evidence? *Current Alzheimer research,* 4(3):253-262.

ROACH, E.S. 2004. Initial parkinson disease therapy: Levodopa, dopamine agonists, or both? *Archives of neurology,* 61(12):1972-1973.

RODRIGUEZ-FRANCO, M.I., FERNANDEZ-BACHILLER, M.I., PÉREZ, C., HERNANDEZ-LEDESMA, B. & BARTOLOME, B. 2006. Novel tacrine-melatonin hybrids as dual-acting drugs for Alzheimer's disease, with improved acetylcholinesterase inhibitory and antioxidant properties. *Journal of medicinal chemistry,* 49(2):459-462.

ROSINI, M., ANDRISANO, V., BARTOLINI, M., BOLOGNESI, M.L., HRELIA, P., MINARINI, A., TAROZZI, A. & MELCHIORRE, C. 2005. Rational approach to discover multipotent anti-Alzheimer drugs. *Journal of medicinal chemistry,* 48(2):360-363.

ROSS, G.W., ABBOTT, R.D., PETROVITCH, H., MORENS, D.M., GRANDINETTI, A., TUNG, K., TANNER, C.M., MASAKI, K.H., BLANCHETTE, P.L., CURB, J.D., POPPER, J.S. & WHITE, L.R. 2000. Association of coffee and caffeine intake with the risk of Parkinson's disease. *JAMA: The journal of the American medical association,* 283(20):2674-2679.

SAITO, Y., KAWASHIMA, A., RUBERU, N.N., FUJIWARA, H., KOYAMA, S., SAWABE, M., ARAI, T., NAGURA, H., YAMANOUCHI, H., HASEGAWA, M., IWATSUBO, T. & MURAYAMA, S. 2003. Accumulation of phosphorylated alpha-synuclein in aging human brain. *Journal of neuropathology and experimental neurology,* 62:644-654.

SAURA, J., BLEUEL, Z., ULRICH, J., MENDELOWITSCH, A., CHEN, K., SHIH, J.C., MALHERBE, P., DA PRADA, M. & RICHARDS, J.G. 1996. Molecular neuroanatomy of human monoamine oxidases A and B revealed by quantitative enzyme radioautography and in situ hybridization histochemistry. *Neuroscience,* 70(3):755-774.

SCHMITT, B., BERNHARDT, T., MOELLER, H., HEUSER, I. & FRÖLICH, L. 2004. Combination therapy in Alzheimer's disease: A review of current evidence. *CNS drugs,* 18(13):827-844.

SHOHAM, S. & YOUDIM, M.B.H. 2000. Iron involvement in neural damage and microgliosis in models of neurodegenerative diseases. *Cellular and molecular biology,* 46(4):743-760.

SINGH, N., PILLAY, V. & CHOONARA, Y.E. 2007. Advances in the treatment of Parkinson's disease. *Progress in neurobiology,* 81(1):29-44.

SMID, P., COOLEN, H.K.A.C., KEIZER, H.G., VAN HES, R., DE MOES, J.-P., DEN HARTOG, A.P., STORK, B., PLEKKENPOL, R.H., NIEMANN, L.C., STROOMER, C.N.J., TULP, M.T.M., VAN STUIVENBERG, H.H., MCCREARY, A.C., HESSELINK, M.B., HERREMANS, A.H.J. & KRUSE, C.G. 2005. Synthesis, structure-activity relationships, and biological properties of 1-heteroaryl-4-[ω-(1H-indol-3-yl)alkyl]piperazines, novel potential antipsychotics combining potent dopamine D_2 receptor antagonism with potent serotonin reuptake inhibition. *Journal of medicinal chemistry,* 48(22):6855-6869.

SOUTHAN, G.J. & SZABÓ, C. 1996. Selective pharmacological inhibition of distinct nitric oxide synthase isoforms. *Biochemical pharmacology,* 51(4):383-394.

STACKMAN, R.W., ECKENSTEIN, F., FREI, B., KULHANEK, D., NOWLIN, J. & QUINN, J.F. 2003. Prevention of age-related spatial memory deficits in a transgenic mouse model of Alzheimer's disease by chronic ginkgo biloba treatment. *Experimental neurology,* 184(1):510-520.

STRONG, M.J., KESAVAPANY, S. & PANT, H.C. 2005. The pathobiology of amyotrophic lateral sclerosis: A proteinopathy? *Journal of neuropathology and experimental neurology.,* 64:649-664.

STUEHR, D.J. 1997. Structure-function aspects in the nitric oxide synthases. *Annual review of pharmacology & toxicology,* 37(1):339.

SUH, J.H., ZHU, B.-Z., DE SZOEKE, E., FREI, B. & HAGEN, T.M. 2004. Dihydrolipoic acid lowers the redox activity of transition metal ions but does not remove them from the active site of enzymes. *Redox report,* 9(1):57-61.

TANNER, C.M. & LANGSTON, J.W. 1990. Do environmental toxins cause Parkinson's disease? A critical review. *Neurology, supplement 3,* 40(10):17-31.

TOGO, T., KATSUSE, O. & ISEKI, E. 2004. Nitric oxide pathways in Alzheimer's disease and other neurodegenerative dementias. *Neurological research,* 26(5):563-566.

VAN DEN BERG, D., ZOELLNER, K.R., OGUNROMBI, M.O., MALAN, S.F., TERRE'BLANCHE, G., CASTAGNOLI, N., Jr., BERGH, J.J. & PETZER, J.P. 2007. Inhibition of monoamine oxidase B by selected benzimidazole and caffeine analogues. *Bioorganic & medicinal chemistry,* 15(11):3692-3702.

VAN DER SCHYF, C.J., GELDENHUYS, W.J. & YOUDIM, M.B.H. 2006. Multifunctional drugs with different CNS targets for neuropsychiatric disorders. *Journal of neurochemistry,* 99(4):1033-1048.

VLOK, N., MALAN, S.F., CASTAGNOLI, N., Jr., BERGH, J.J. & PETZER, J.P. 2006. Inhibition of monoamine oxidase B by analogues of the adenosine A_{2A} receptor antagonist (E)-8-(3-chlorostyryl)caffeine (CSC). *Bioorganic & medicinal chemistry,* 14(10):3512-3521.

WEI, Y.-H., KAO, S.-H. & LEE, H.-C. 1996. Simultaneous increase of mitochondrial DNA deletions and lipid peroxidation in human aging. *Annals of the New York academy of sciences,* 786:24-43.

WOUTERS, J., OOMS, F., JEGHAM, S., KOENIG, J., GEORGE, P. & DURANT, F. 1997. Reversible inhibition of type B monoamine oxidase. Theoretical study of model diazo heterocyclic compound. *European journal of medicinal chemistry,* 32(9):721-730.

WU, R.M., CHIEUH, C.C., PERT, A. & MURPHY, D.L. 1993. Apparent antioxidant effect of $_L$-deprenyl on hydroxyl radical formation and nigral injury elicited by MPP^+ in vivo. *European journal of pharmacology,* 243(3):241-247.

YOUDIM, M.B.H. & BUCCAFUSCO, J.J. 2005. Multi-functional drugs for various CNS targets in the treatment of neurodegenerative disorders. *Trends in pharmacological sciences,* 26(1):27-35.

YOUDIM, M.B.H., GROSS, A. & FINBERG, J.P.M. 2001. Rasagiline [N-propargyl-1R(+)-aminoindan], a selective and potent inhibitor of mitochondrial monoamine oxidase B. *British journal of pharmacology,* 132(2):500-506.

YU, P.H., DAVIS, B.A., DURDEN, D.A., BARBER, A., TERLECKYJ, I., NICKLAS, W.G. & BOULTON, A.A. 1994. Neurochemical and neuroprotective effects of some aliphatic propargylamines: New selective nonamphetamine-like monoamine oxidase B inhibitors. *Journal of neurochemistry,* 62(2):697-704.

ZORATTI, M. & SZABÒ, I. 1995. The mitochondrial permeability transition. *Biochimica et biophysica acta (reviews on biomembranes),* 1241(2):139-176.

CHAPTER 2
MONOAMINE OXIDASE (MAO)

2.1 Introduction

Amine oxidases are generally divided into two groups based on the chemical structure of the attached cofactor. The flavin adenine dinucleotide (FAD)-containing enzymes are intracellular enzymes and include MAO-A and -B as well as polyamine oxidases (PAOs) (Shih *et al.*, 1999:197). The cofactor for the other class of amine oxidases is topa-quinone (TPQ) in most cases (Klinman, 1996:27189, Lyles, 1996:259), and include diamine oxidases, lysyl oxidase, plasma membrane and soluble MAOs.

MAO-A and -B are integral proteins situated in the outer mitochondrial membrane, and catalyse the oxidative deamination of catecholamine neurotransmitters (dopamine, adrenaline, noradrenaline, serotonin) and *β*-phenylethylamine in the CNS. Kinetic studies have indicated that the reaction involves the binding of the amine substrate to the MAO enzyme before oxygen and that it proceeds in two steps. Firstly (eq. 1), reduction of enzyme-bound FAD results in the formation of the aldehyde product and ammonia, whereas in the second step (eq. 2) the enzyme-bound FAD is reoxidised by O_2 with the formation of H_2O_2.

$$R\text{-}CH_2NH_2 + MAO \xrightarrow[+H_2O]{-2H^+} R\text{-}CHO + NH_3 + \text{Reduced-MAO} \quad (1)$$

$$\text{Reduced-MAO} + O_2 \longrightarrow MAO + H_2O_2 \quad (2)$$

The two isoforms of MAO are distinguished based upon their substrate specificity and sensitivity towards inhibition by the MAO inhibitor, clorgyline (Johnston, 1968:1285):

- **MAO-A** primarily metabolises serotonin and noradrenalin in the CNS and is inhibited by clorgyline at low concentrations.
- **MAO-B** primarily metabolises dopamine and *β*-phenylethylamine in the CNS and is relatively insensitive to clorgyline.

Because of this selectivity, MAO-A inhibitors are mainly used as antidepressants whereas MAO-B inhibitors are used and further developed as treatment for neurological disorders such as PD.

2.2 Why MAO-B Inhibition?

As mentioned earlier $_L$-dopa remains a key compound in PD treatment, acting as a precursor of dopamine. Drugs used in combination with $_L$-dopa include COMT and MAO-B inhibitors since they alter the metabolism of dopamine *in vivo* by increasing its plasma half-life. The well known MAO-B inhibitor rasagiline (**4**) has been shown to protect neurons *in vivo* as well as *in vitro* against a variety of neurotoxic assaults (Cavalli *et al.*, 2008:347). Rasagiline inhibits the enzyme irreversibly, which has certain disadvantages including the fact that recovery requires synthesis of new enzyme, possible loss of selectivity as a result of repeated administration and an inhibition that is not affected by changes in substrate concentration. The rate of turnover, and hence recovery from irreversible inhibition is fairly slow and differs substantially between tissues and species. For example, the turnover rate for MAO-B in the human brain is close to 40 days. Reversible inhibition may be of a competitive, mixed, non-competitive or uncompetitive nature and possesses the following advantages: the enzyme recovers as the inhibitor is eliminated from the tissues, the risk of loss of selectivity is far less because of a shorter duration of action and, in the case of competitive reversible inhibition, the inhibition is relieved if the substrate concentration increases (Tipton *et al.*, 2004:1965). As additional information on the behaviour of the MAO enzymes become available, it may be appropriate to design more effective inhibitors thereof.

β-phenylethylamine is found in the CNS where it is neither stored nor actively released. In the synaptic cleft, *β*-phenylethylamine is thought to potentiate the actions of dopamine (Boulton, 1991:139). As mentioned earlier *β*-phenylethylamine is preferentially metabolised by MAO-B, and it has been suggested that chronic (*R*)-deprenyl (**5**) administration increases striatal *β*-phenylethylamine levels, which then facilitates dopamine activity (Paterson *et al.*, 1991:1019). At doses that selectively inhibit MAO-B, compounds such as (*R*)-deprenyl and lazabemide have been reported to elevate striatal *β*-phenylethylamine levels in both rodents and primates (Berry *et al.*, 1994:1159).

As described in equations 1 and 2 the MAO-catalysed oxidation of amine substrates, including dopamine, leads to the production of H_2O_2. This compound is usually a harmless cellular metabolite, however, in the presence of free iron cations (Fe^{2+}, Fe^{3+}) it can be converted to highly reactive hydroxyl radicals ($^{\bullet}OH$) through Fenton chemistry. It may therefore be deduced that MAO-B inhibitors reduce oxidative stress in healthy dopaminergic neurons in humans by inhibiting H_2O_2 production, thus functioning as neuroprotective agents. A study performed by Cohen *et al.* (1989:689) indicated that treatment of mice with (*R*)-deprenyl reduced oxidative stress associated with increased dopamine turnover. Tissue glutathione disulfide was used as an index of changes in redox state in the striatum and its concentration tripled after provoking increased dopamine release and subsequent turnover with haloperidol. (*R*)-deprenyl reduced this rise in tissue glutathione disulfide by 71.9 %. In another study (De la Cruz *et al.*, 1996:1756) chronic treatment with (*R*)-deprenyl protected rats against age-related protein oxidation in the rat substantia nigra. (*R*)-deprenyl has also been shown to be a possible neurorescuer by increasing the survival rate of motor neurons following axotomy of rat facial nerve (Salo *et al.*, 1992:394) or subjection to spinal cord ischaemia (Ravikumar *et al.*, 1998:123). Tatton *et al.* (1996:S171) reported at least 50 glial and neuronal proteins whose synthesis is modulated by (*R*)-deprenyl, of which 10 have been identified: the levels of both forms of superoxide dismutase, glutathione peroxidase, tyrosine hydroxylase, BCL-2, BCL-X_L and c-FOS mitochondrial NADH dehydrogenase were increased whereas the levels of BAX and c-JUN, proteins associated with initiation of apoptosis, were decreased. From these findings it was proposed that (*R*)-deprenyl initiates a transcriptional program that inhibits the apoptotic pathway, most likely by stabilising the mitochondrial membrane and inhibiting oxidative stress.

As described earlier, the MAO isoform predominantly found in human brain is MAO-B (Saura *et al.*, 1996:755) where it may be involved in age-related neuropsychiatric diseases such as PD and AD. It has been demonstrated that MAO-B activity, but not MAO-A activity in the brain increases during the aging process (Fowler *et al.*, 1980:1), which may be due to the increase in the number of glial cells observed with aging. This enzyme isoform plays a dual role in the pathophysiology of PD as it is the main enzyme implicated in the metabolism of dopamine as well as being involved in the formation of

free radicals and other neurotoxic species. Increased MAO-B levels have been observed in plaque-associated astrocytes in the brains of AD patients. This increase in MAO-B activity produces an elevation in $^{\bullet}OH$, which has been correlated with Aβ plaque formation. Hence, the therapeutic potential of selective reversible MAO-B inhibitors does not rely solely on their ability to increase the biological half–life of dopamine (symptomatic effects) but also on their ability to slow down PD progression (neuroprotective effects) and their potential ability to inhibit Aβ plaque formation.

From the above discussion it is clear that the model MAO-B inhibitor, (*R*)-deprenyl, has an array of biological attributes which makes it a good candidate for the treatment and possible prevention of neurodegenerative disorders. The fact that it inhibits MAO-B in an irreversible fashion is however a disadvantage. Current focus should thus be on the development of selective reversible MAO-B inhibitors that possess additional properties such as antioxidant activity and neuroprotective effects.

Comparison of the effects of various MAO-B inhibitors may shed some light on the underlying nature of PD and perhaps that of neurodegeneration as well.

2.3 MAO-B Active Site

Mammalian MAO enzymes are bound to the outer mitochondrial membrane and therefore classified as non-soluble enzymes. Human MAO-B (and –A) has a mass of about 59 kDa with the FAD cofactor covalently bound through the flavin C8 α-position to a cysteine side chain (Cys 397). The crystal structure of this enzyme reveals that it crystallises as a dimer in two different crystal forms (orthorhombic and triclinic), suggesting that it may also occur as a dimer in its membrane environment (Binda *et al.*, 2002:23973). Figure 18 is a ribbon diagram demonstrating the MAO-B dimer with the two-fold axis vertical in the plane of the paper. Monomer A is on the right and monomer B on the left. 'N' and 'C' indicate the observed N-terminal (Lys 4 in both monomers) and C-terminal (Thr 500 in monomer A and Ile 496 in monomer B) amino acids, respectively. The dimer is anchored to the outer mitochondrial membrane through the C-terminal α-helix and the neighbouring residues of each monomer.

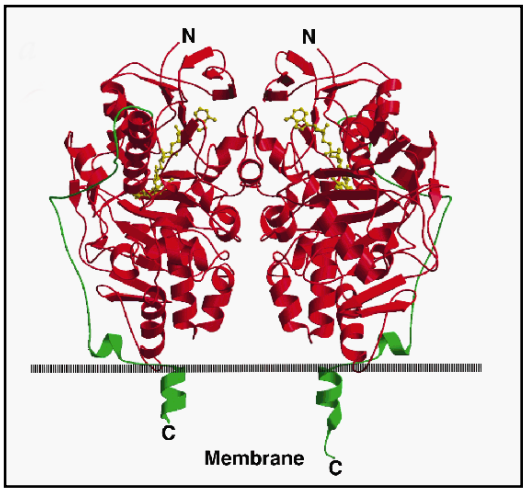

Figure 18: Structure of the human MAO-B enzyme (Binda *et al.*, 2002:22). (Red = Residues 4-460; Green = Residues 461-500 (C-terminal α-helix); Yellow = FAD cofactor (ball-and-stick representation))

The access channel stretching from the protein surface to the enzyme active site consists of two cavities: the entrance cavity and the substrate (active site) cavity. The entrance cavity is slightly smaller than the adjacent substrate cavity with a volume of 290 $Å^3$. It is lipophilic in nature and lined by residues Phe 103, Pro 104, Trp 119, Leu 164, Leu 167, Phe 168, Leu 171, Ile 199, Ile 316 and Tyr 326. The substrate cavity has a larger volume of 420 $Å^3$ and is lined by a number of aromatic and aliphatic amino acids giving it a highly lipophilic environment. It does however contain hydrophilic areas near the flavin, which direct the substrate amine moiety for binding and catalysis. The recognition site for the amine group of enzyme substrates is an "aromatic sandwich" formed by two aromatic amino acid side chains, Tyr 398 and Tyr 435 (Binda *et al.*, 2002:22). These amino acids face each other in a perpendicular orientation to the flavin plane with their aromatic rings slightly turned towards the flavin. The distance between them is in the region of 8 Å. Another aromatic amino acid, Tyr 60 is positioned at the top of the flavin ring and is coplanar to the respective pyrimidine rings of the flavin coenzyme. The flavin ring plays an important role in substrate recognition as its C4a atom is in Van der Waals contact with the substrate nitrogen. The combination of the "aromatic sandwich" and flavin produces an "aromatic cage" that is suggested to recognise the deprotonated amine group of the substrate.

In a study wherein the crystal structure of human MAO-B in complex with *trans,trans*-farnesol was elucidated to 1.8 Å resolution (Hubalek *et al.*, 2005:15761), it was shown that the abovementioned compound together with 1,4-diphenyl-2-butene span both the entrance and substrate cavities with the side chain of Ile 199 rotated out of its normal configuration, suggesting that Ile 199 acts as a gate to the substrate cavity. Both *trans,trans*-farnesol (**34**, fig. 19) and 1,4-diphenyl-2-butene (**35**) are selective, reversible MAO-B inhibitors and it was deduced that this Ile 199 "gate" is a determinant for the specificity of these (and other) MAO-B inhibitors. Structural and functional data demonstrated that reversible inhibitors traversing the entrance and substrate cavities of MAO-B exhibit specificity for this isozyme, providing a molecular basis for the development of reversible inhibitors specific for the MAO-B enzyme that do not interfere with MAO-A function in neurotransmitter metabolism.

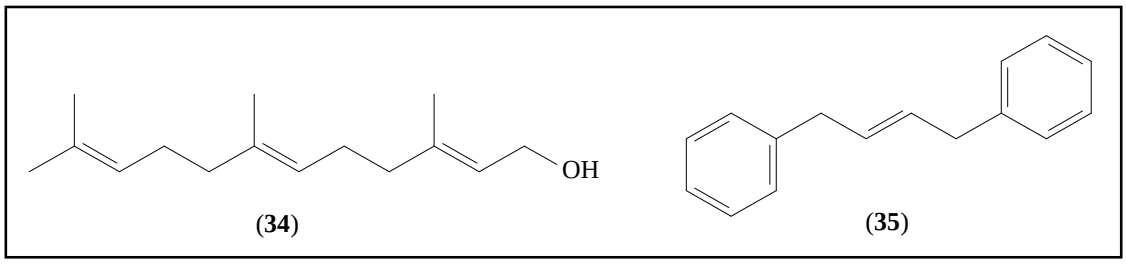

(**34**) (**35**)

Figure 19: Chemical structures of *trans,trans*-farnesol (**34**) and 1,4-diphenyl-2-butene (**35**).

2.4 Rational MAO-B Inhibitor Design

Prototypical MAO-B inhibitors of the aryl diazo heterocyclic chemical series were studied with regard to their structural and electronic properties (Wouters *et al.*, 1997:721). This provided a theoretical basis for structure-inhibition relationships of compounds with potential MAO-B inhibitory activity. Conclusions drawn were as follows:

1) The lipophilicity of these compounds was the most important parameter governing their affinity for the MAO-B enzyme as indicated by the benzyloxy chain interacting with the lipophilic binding site of the protein.

2) The possibility to stabilise (*via* hydrogen (H) bonds) the relevant inhibitor in the lipophilic binding site pocket through fixed anchoring points was also important for MAO-B inhibition.

3) A planar support presenting a conserved pattern of H-bonding acceptor sites, substituted by a functionalised (CN, OR) ethyl lateral chain being able to reach the catalytic site of the enzyme without reacting with it, was also indicated as essential.

These findings were confirmed when Binda *et al.* (2006:S5) indicated that the chemical requirements for MAO-B inhibitors were, amongst others, a lipophilic nature and structural rigidity to be accommodated in both the entrance and substrate cavities.

A MAO-B pharmacophore has been designed that satisfies the relative three dimensional positions of inhibitor hetero-atoms involved in H-bonding with amino acid residues within the MAO-B active site (fig. 20). These hetero-atoms are located in the same plane as the aromatic moiety and by applying this pharmacophore model a highly potent and selective MAO-B inhibitor, namely 3-methyl-8-(4,4,4-trifluoro-butoxy)indeno[1,2-*c*]pyridazin-5-one (**36**, fig. 21), was developed. This compound was found to be approximately 7000 fold more selective for MAO-B than MAO-A, with a K_i value of 14 nM rendering it among the most potent and selective reversible MAO-B inhibitors yet reported. Docking study results indicated that **36** positions in the vicinity of the FAD cofactor and that the carbonyl and pyridazine functional groups of the indeno[1,2-*c*]pyridazin-5-one nucleus form H-bonds with Tyr 188, 398 and 435 (Ooms *et al.*, 2003:69).

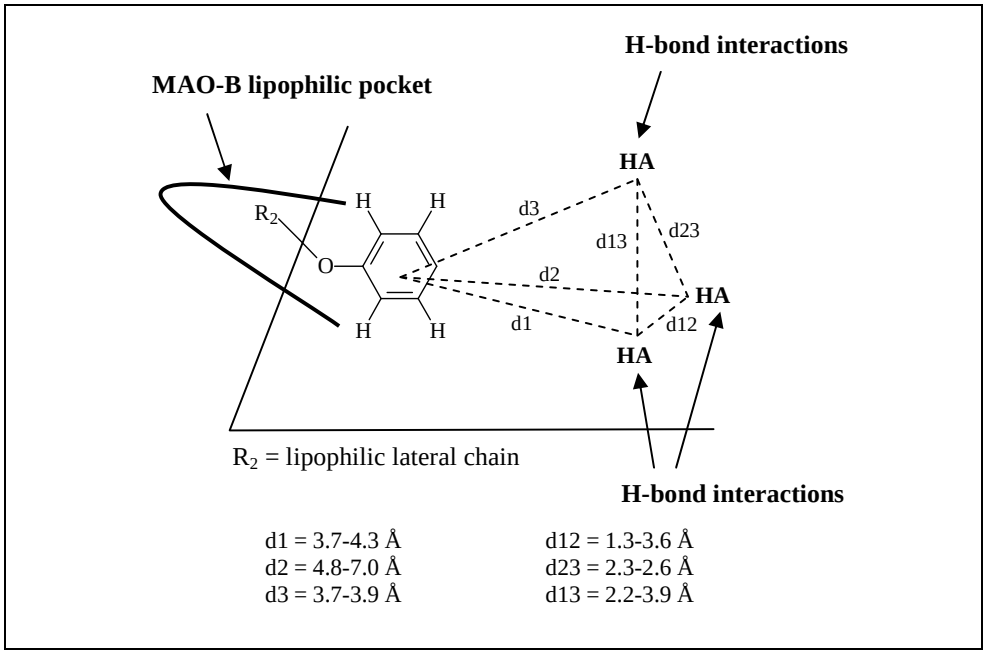

Figure 20: MAO-B pharmacophore model (Ooms *et al.*, 2003:69). (HA = relative position of the hydrogen accepting group)

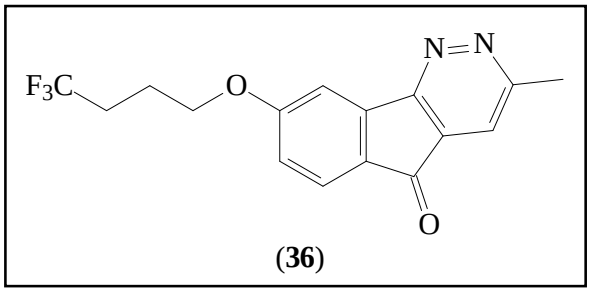

(**36**)

Figure 21: Chemical structure of 3-methyl-8-(4,4,4-trifluoro-butoxy)indeno[1,2-*c*]pyridazin-5-one (**36**) (Ooms *et al.*, 2003:69).

As discussed earlier the combination of the amino acids Tyr 398 and Tyr 435 is known as the so-called "aromatic sandwich", which is the only area in the substrate cavity that is hydrophilic in nature. In contrast, the entrance cavity of MAO-B is highly hydrophobic and is thought to interact tighty with aromatic ring systems, especially when substituted with electron withdrawing substituents such as chlorine. Examples of compounds that undergo such interactions with MAO-B are (*E*)-8-(3,4-dichlorostyryl)-caffeine (**37**, fig. 22) and CSC (**38**) (Van den Berg *et al.*, 2007:3692). These compounds are proposed to

bind with the caffeine ring located in the substrate cavity while the styryl substituent extends into the entrance cavity where the phenyl ring binds.

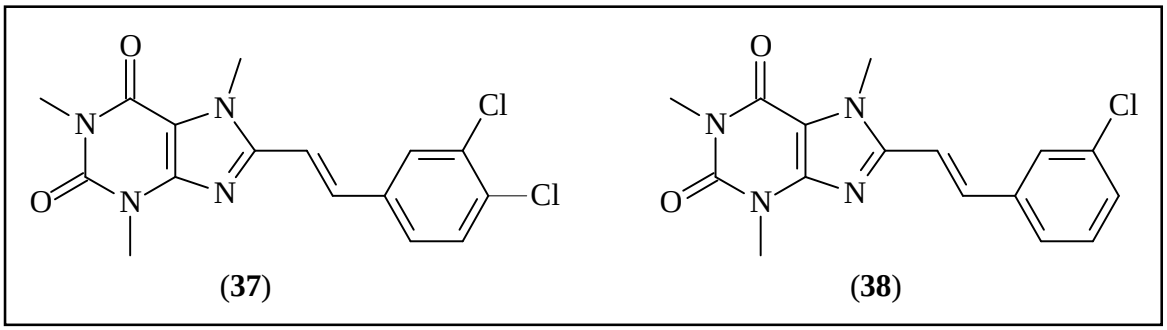

(**37**) (**38**)

Figure 22: Structural representation of (*E*)-8-(3,4-dichlorostyryl)-caffeine (**37**) and CSC (**38**).

The MAO-B active site is filled with several ordered, captive water molecules and therefore it has been suggested that future MAO-B inhibitor design should consider hydrophilic substituents that may displace these water molecules resulting in increased affinity and specificity (Binda *et al.*, 2003:9750).

A previous modelling study has however indicated that a relatively large portion of the MAO-B substrate cavity on the rear side, with respect to the flavin ring, is left unoccupied by the benzylamine substrate (Binda *et al.*, 2002:22). This explains the broad substrate specificity associated with MAO-B, which is able to oxidise several aromatic amines with side chains of different length. Keeping this in mind it is clear that predictions regarding the MAO-B inhibitory activity of any proposed compounds is difficult to accurately make.

2.5 Conclusion

In this chapter it is shown that MAO-B is an important drug target for the treatment of neurodegenerative diseases. Two irreversible MAO-B inhibitors, (*R*)-deprenyl and rasagiline, are currently used clinically in PD therapy. It may however be argued that reversible inhibitors could be more advantageous as therapeutic agents. While the design of selective MAO-B inhibitors remains a challenge, the knowledge of the three-dimensional structure of the enzyme may greatly facilitate the discovery of new PD drugs.

References

BERRY, M.D., SCARR, E., ZHU, M.-Y., PATERSON, I.A. & JUORIO, A.V. 1994. The effects of administration of monoamine oxidase B inhibitors on rat striatal neurone responses to dopamine. *British journal of pharmacology,* 113(4):1159-1166.

BINDA, C., HUBÁLEK, F., LI, M., CASTAGNOLI, N., Jr., EDMONDSON, D.E. & MATTEVI, A. 2006. Structure of the human mitochondrial monoamine oxidase B: New chemical implications for neuroprotective drug design. *Neurology,* 67(7):S5-S7.

BINDA, C., LI, M., HUBÁLEK, F., RESTELLI, N., EDMONDSON, D.E. & MATTEVI, A. 2003. Insights into the mode of inhibition of human mitochondrial monoamine oxidase-B from high-resolution crystal structures. *Proceedings of the national academy of sciences,* 100(17):9750-9755.

BINDA, C., MATTEVI, A. & EDMONDSON, D.E. 2002. Structure-function relationships in flavoenzyme-dependent amine oxidations. A comparison of polyamine oxidase and monoamine oxidase. *Journal of biological chemistry,* 277(27):23973-23976.

BOULTON, A.A. 1991. Phenylethylaminergic modulation of catecholaminergic neurotransmission. *Progress in neuro-psychopharmacology and biological psychiatry,* 15(2):139-156.

CAVALLI, A., BOLOGNESI, M.L., MINARINI, A., ROSINI, M., TUMIATTI, V., RECANATINI, M. & MELCHIORRE, C. 2008. Multi-target-directed ligands to combat neurodegenerative diseases. *Journal of medicinal chemistry,* 51(3):347-372.

COHEN, G. & SPINA, M.B. 1989. Deprenyl suppresses the oxidant stress associated with increased dopamine turnover. *Annals of neurology,* 26(5):689-690.

DE LA CRUZ, C.P., REVILLA, E., STEFFEN, V., RODRÍGUEZ-GÓMEZ, J.A., CANO, J. & MACHADO, A. 1996. Protection of the aged substantia nigra of the rat against oxidative damage by (-)-deprenyl. *British journal of pharmacology,* 117(8):1756-1760.

FOWLER, C.J., WIBERG, A., ORELAND, L., MARCUSSON, J. & WINBLAD, B. 1980. The effect of age on the activity and molecular properties of human brain monoamine oxidase. *Journal of neural transmission (general section),* 49(1-2):1-20.

HUBÁLEK, F., BINDA, C., KHALIL, A., LI, M., MATTEVI, A., CASTAGNOLI, N., Jr., & EDMONDSON, D.E. 2005. Demonstration of isoleucine 199 as a structural determinant for the selective inhibition of human monoamine oxidase B by specific reversible inhibitors. *Journal of biological chemistry,* 280(16):15761-15766.

JOHNSTON, J.P. 1968. Some observations upon a new inhibitor of monoamine oxidase in brain tissue. *Biochemical pharmacology,* 17(7):1285-1297.

KLINMAN, J.P. 1996. New quinocofactors in eukaryotes. *Journal of biological chemistry,* 271(44):27189-27192.

LYLES, G.A. 1996. Mammalian plasma and tissue-bound semicarbazide-sensitive amine oxidases: Biochemical, pharmacological and toxicological aspects. *The international journal of biochemistry & cell biology,* 28(3):259-274.

OOMS, F., FRÉDÉRICK, R., DURANT, F., PETZER, J.P., CASTAGNOLI, N., Jr., VAN DER SCHYF, C.J. & WOUTERS, J. 2003. Rational approaches towards reversible inhibition of type B monoamine oxidase. Design and evaluation of a novel 5H-indeno[1,2-c]pyridazin-5-one derivative. *Bioorganic & medicinal chemistry letters,* 13(1):69-73.

PATERSON, I.A., JUORIO, A.V., BERRY, M.D. & ZHU, M.Y. 1991. Inhibition of monoamine oxidase B by (-)-deprenyl potentiates neuronal responses to dopamine agonists but does not inhibit dopamine catabolism in the rat striatum. *Journal of pharmacology and experimental therapeutics,* 258(3):1019-1026.

RAVIKUMAR, R., LAKSHMANA, M.K., SHANKARANARAYANA RAO, B.S., METI, B.L., BINDU, P.N. & RAJU, T.R. 1998. (−)-Deprenyl attenuates spinal motor neuron degeneration and associated locomotor deficits in rats subjected to spinal cord ischaemia. *Experimental neurology,* 149(1):123-129.

SALO, P.T. & TATTON, W.G. 1992. Deprenyl reduces the death of motoneurons caused by axotomy. *Journal of neuroscience research.,* 31(2):394-400.

SAURA, J., BLEUEL, Z., ULRICH, J., MENDELOWITSCH, A., CHEN, K., SHIH, J.C., MALHERBE, P., DA PRADA, M. & RICHARDS, J.G. 1996. Molecular neuroanatomy of human monoamine oxidases A and B revealed by quantitative enzyme radioautography and in situ hybridization histochemistry. *Neuroscience,* 70(3):755-774.

SHIH, J.C., CHEN, K. & RIDD, M.J. 1999. Monoamine oxidase: From genes to behaviour. *Annual review of neuroscience,* 22(1):197.

TATTON, W.G. & CHALMERS-REDMAN, R.M. 1996. Modulation of gene expression rather than monoamine oxidase inhibition: (-)-deprenyl-related compounds in controlling neurodegeneration. *Neurology,* 47(6):S171-S183.

TIPTON, K.F., BOYCE, S., O'SULLIVAN, J., DAVEY, G.P. & HEALY, J. 2004. Monoamine oxidases: Certainties and uncertainties. *Current medicinal chemistry,* 11(15):1965-1982.

VAN DEN BERG, D., ZOELLNER, K.R., OGUNROMBI, M.O., MALAN, S.F., TERRE'BLANCHE, G., CASTAGNOLI, N., Jr., BERGH, J.J. & PETZER, J.P. 2007. Inhibition of monoamine oxidase B by selected benzimidazole and caffeine analogues. *Bioorganic & medicinal chemistry,* 15(11):3692-3702.

WOUTERS, J., OOMS, F., JEGHAM, S., KOENIG, J., GEORGE, P. & DURANT, F. 1997. Reversible inhibition of type B monoamine oxidase. Theoretical study of model diazo heterocyclic compound. *European journal of medicinal chemistry,* 32(9):721-730.

CHAPTER 3
NITRIC OXIDE SYNTHASE (NOS)

3.1 Introduction

NOS is a cytochrome P450-like heme protein that requires tetrahydrobiopterin (H_4B), flavin mononucleotide (FMN) and FAD to catalyse the NADPH- and O_2-dependent oxidation of $_L$-arginine to $_L$-citrulline and NO (fig. 23) (Marletta, 1993:12231).

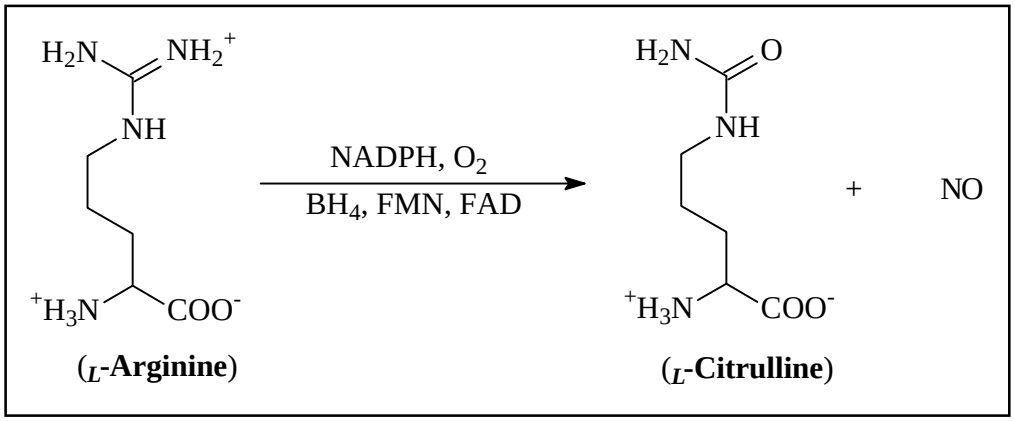

Figure 23: The NOS catalysed oxidation of $_L$-arginine to $_L$-citrulline and NO.

NO is known to be an important cell signalling agent that regulates an array of physiological functions. These include blood pressure by regulation of smooth muscle relaxation (Palmer *et al.*, 1987:524), platelet aggregation by acting as an antithrombotic agent (Moncada *et al.*, 1989:1709), antitumor, antibacterial, and antiviral action of macrophages (Hibbs *et al.*, 1987:550), brain development, learning and memory (Garthwaite, 1990:115), and it is also the neuronal mediator of penile erection (Burnett *et al.*, 1992:401). However, since NO is a free radical, overproduction thereof can result in deleterious effects ranging from septic shock and pain (Cheshire, 2001:795) to ischaemia (Endres *et al.*, 2004:283) and several neurodegenerative disorders (Togo *et al.*, 2004:563) such as PD and AD (Cheshire, 2001:795).

Because of the harmful effects linked to NO overproduction, the inhibition of NO biosynthesis emerges as an important approach for the treatment of NO associated diseases. Its inhibition could however be detrimental to other essential physiological functions of NO, but as it is not produced from a single source this dilemma is somewhat abated. As described earlier three separate NOS isoforms have been identified: neuronal NOS (nNOS), endothelial NOS (eNOS) and inducible NOS (iNOS). These isoforms share approximately 50% sequence identity and have identical overall architecture (Hobbs *et al.*, 1999:191).

3.2 Why NOS Inhibition?

The harmful effects caused by an overproduction of NO are thought to be mediated by $ONOO^-$, the product obtained when NO and $O_2^{\bullet -}$ react with one another. $ONOO^-$ causes injury to the mitochondrial electron transport chain resulting in damage and eventual death of neurons. Evidence that NO and $ONOO^-$ are neurotoxic is provided in the ability of superoxide dismutase to protect cortical cultures from both glutamate and NO donors. Removal of nNOS neurons from culture with a low dose of quisqualate or elimination of nNOS through transgenic technology, results in cell cultures that are resistant to NMDA neurotoxicity indicating that nNOS neurons are the source of neurotoxic NO (Dawson *et al.*, 1996:179, Dawson *et al.*, 1993:2651).

Since the NOS isoforms possess a distinct cellular localisation and are differentially regulated, they represent specific targets for potential therapeutic approaches. The development of isoform-selective inhibitors is therefore of considerable interest, not only for therapeutic purposes but also for their use as specific pharmacological tools. NO of neuronal origin is involved in pain transmission (Moore *et al.*, 1993:219, Moore *et al.*, 1991:198) and therefore constitutes a potential target for antinociceptive drugs. It has also been indicated that overstimulated nNOS is implicated in ischaemia-reperfusion injury following a stroke (Strijbos *et al.*, 1996:5004), migraine headache (Lassen *et al.*, 1997:401) and a variety of neurodegenerative diseases (Dawson *et al.*, 1996:179). Neuroprotection against ischaemia may be achieved by selectively targeting nNOS and/or iNOS (Parmentier *et al.*, 1999:546), while the eNOS isoform, which has been shown to

be critical for angiogenesis and for maintaining proper vascular tone (Huang *et al.*, 1995:239), should not be affected (Erdal *et al.*, 2005:603).

A range of studies were performed during the 1990s using transgenic mice to clarify the contributions made by nNOS and eNOS in cerebral ischaemia and other neurodegenerative disorders. Results from these studies indicated that there was a profound reduction in infarct volume after middle cerebral artery occlusion in nNOS deficient mice when compared with normal individuals (Huang *et al.*, 1994:1883). Another study concluded that striatal malonate lesions were also attenuated in nNOS knockout mice whereas the lesion size increased in mice deficient of eNOS (Schulz *et al.*, 1996:430).

From the above discussion it is clear that because of the opposite biological effects that may be evoked by NO produced by nNOS and eNOS, the development of isoform-specific NOS inhibitors is a highly advantageous goal (Salerno *et al.*, 2002:177).

3.3 NOS Active Site

Native NOS is an enzyme that has a homodimeric nature where each monomer polypeptide contains an N-terminal and C-terminal domain (Stuehr, 1999:217). The N-terminal section of the enzyme is the heme-binding domain (or oxygenase domain), which is similar to that of the cytochrome P450 enzyme family. The N-terminal domain also contains H_4B and $_L$-arginine-binding sites. H_4B appears to have a dual role in that it stabilises the dimer as well as participating in catalysis (Alderton *et al.*, 2001:593). The heme-binding domain may therefore be classified as the catalytic centre of NOS. The C-terminal section is the flavin-binding domain, also known as the reductase domain and contains the FAD-, FMN-, and NADPH-binding sites (Bredt *et al.*, 1991:714). The FAD and FMN of the reductase domain are responsible for electron transfer from NADPH to the heme (Roman *et al.*, 2002:1179). The reductase domain can be divided further into two subdomains, each containing one of the two flavins. The FMN-containing subdomain is situated at the N-terminal side, whereas the FAD- and NADPH-binding sites are situated at the C-terminal side. A calmodulin (CaM)-binding region is found at the junction between the catalytic N-terminal oxygenase domain and the C-terminal electron-supplying reductase domain. As a result of the reversible binding of CaM, the

constitutive NOS isoforms (nNOS and eNOS) display Ca^{2+} dependence in their enzymatic activities (Förstermann *et al.*, 1991:1788). iNOS on the other hand binds CaM tightly and is almost independent of the Ca^{2+} concentration (Cho *et al.*, 1992:599).

There is significant sequence identity between the different NOS isoforms and the crystallographic structures of the different isoforms show similar active site structures. Figure 24 is a schematic representation of the NOS active site, where the amino acids that differ among the three isoforms are indicated.

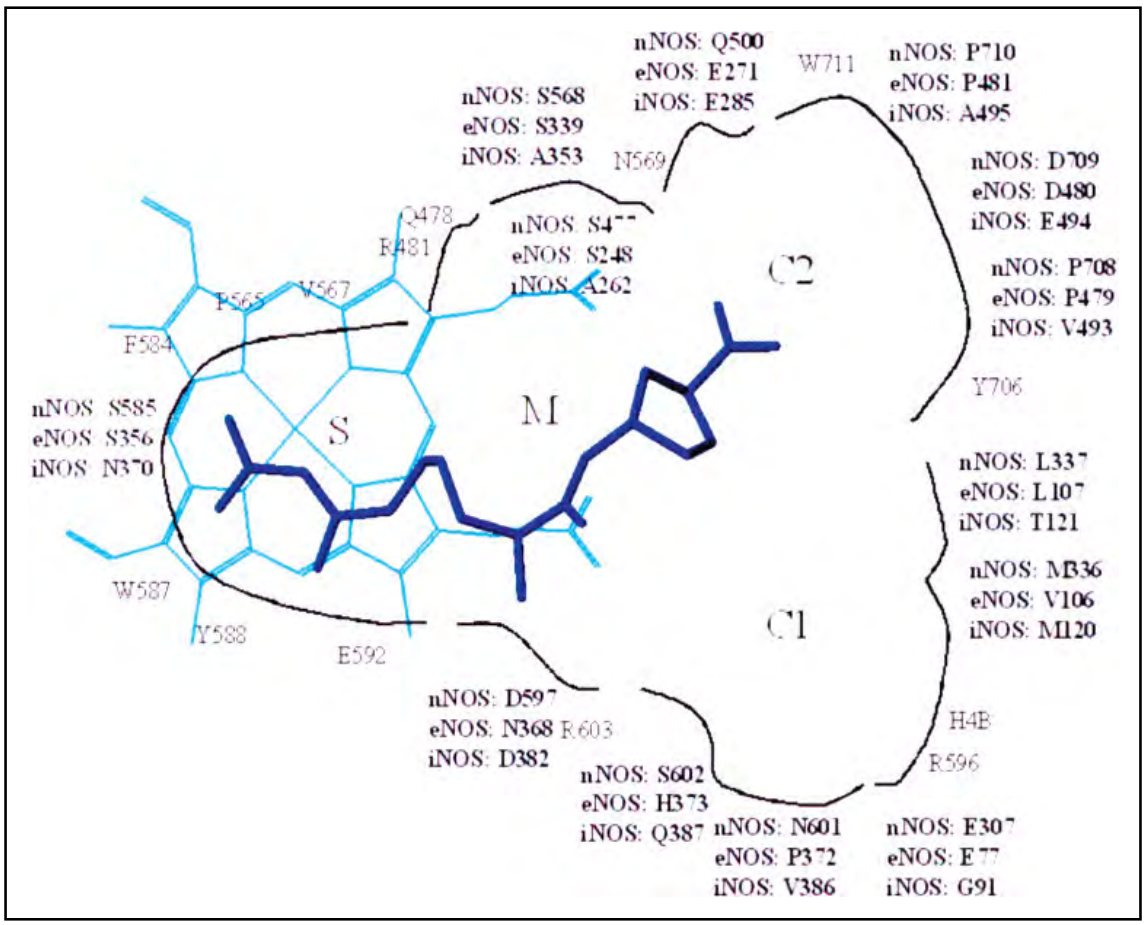

Figure 24: Schematic representation of NOS active site with the S-, M-, C1- and C2-pockets indicated by the binding mode of IV-1 (dark blue). Amino acids important for inhibitor binding are indicated and numbering is in accordance with rat nNOS sequence. Residues differing between NOS are in bold (Ji *et al.*, 2003:5700).

The NOS active site is typically divided into four pockets, namely S, M, C1 and C2 (fig. 24). The S-pocket is located directly above the heme ring and functions as the catalytic site for *L*-arginine. All the residues in this pocket are identical, except for Ser 585 (S585) in nNOS, which corresponds to Asn 370 (N370) in iNOS (Ji *et al.*, 2003:5700). The side chains of Phe 584 (F584), Val 567 (V567) and Pro 565 (P565) collectively produce a hydrophobic region located within the S-pocket (Li *et al.*, 2000:133). The region situated in the middle of the substrate catalytic site and the substrate access channel is known as the M-pocket. Certain residues within this pocket differ among the NOS isoforms, but there are also conserved polar/charged residues that play an important role in substrate and inhibitor binding. These include Gln 478 (Q478), Arg 481 (R481), Asn 569 (N569) and Arg 603 (R603) of nNOS (fig. 24). The C1 and C2 pockets are situated slightly away from the substrate binding cavity and they collectively constitute the substrate access channel (Raman *et al.*, 2001:26486). In these two pockets there are more residues that differ among the NOS isoforms. These pockets also contain exposed polar/charged residues such as Arg 596 (R596) and Tyr 706 (Y706) which interact via hydrogen bonding with the bound ligands.

In a study conducted by Masters *et al.* (1996:552) it was confirmed that a zinc ion is bound in the structure of nNOS. Zinc forms an important and strategically located metal centre as it is equidistant from both H_4B molecules (~12 Å) and both heme iron atoms (21.8 Å) of the dimer. This underscores its important structural roles, which includes maintaining the integrity of the pterin-binding pocket and possibly providing a docking surface for the flavin-binding domain (Raman *et al.*, 1998:939). Zinc is also involved in maintaining dimer stability. This notion is supported by the observation that there is a net gain of eight hydrogen bonds when going from the zinc-free to the zinc–bound state, contributing favourably to the free energy of dimer stabilisation (Schwabe *et al.*, 1994:345). It has also been reported (Demura *et al.*, 1998:314) that zinc may inhibit nNOS activity (K_i ~ 30 µM) by binding to the reductase domain (flavin-binding domain) or directly to CaM.

Constitutive NOS (cNOS), namely eNOS and nNOS, possess a polypeptide insert within their FMN binding modules that acts as an autoinhibitory control element. This insert is

unique to NOS isoforms and is regulated by transitory CaM binding. Since this insert is positioned adjacent to the CaM binding domain, it obstructs CaM binding and hence, NOS activation. When CaM binds this insert is displaced. This structure molecularly defines cNOSs and offers a unique target for the development of novel, peptide-like NOS inhibitors (Salerno et al., 1997:29769.).

3.4 Rational NOS Inhibitor Design

Huang *et al.* (1999:3147) synthesised a series of N^{ω}-nitroarginine-containing dipeptide amides and screened them for *in vitro* activity against the three NOS isoforms. The following were revealed from this study:

1) The NOS active sites are large enough to accommodate inhibitors as large as dipeptides.
2) There are very subtle differences in the active sites of the NOS isoforms and minor structural modifications can produce highly diverse inhibition results. These differences can be applied to direct the rational design of isoform-selective NOS inhibitors.
3) A possible electrostatic or hydrogen bonding interaction exists between the side chains of dipeptide inhibitors and nNOS. This notion is supported by the fact that the dipeptides containing an amino group side chain, present with high inhibitory potency for nNOS and excellent selectivity over both eNOS and iNOS.
4) Multiple hydrogen bond donors may be present at the active site of nNOS.
5) Steric as well as electronic factors influence inhibitory potency and isoform selectivity of these dipeptide inhibitors to a great extent.

The majority of NOS inhibitors described to date bind to the oxygenase (heme-binding) domain of the enzyme and interact with the guanidinium region of the $_L$-arginine binding site. Other guanidine-, amidine- and isothiourea-based inhibitors also seem to bind to this same region of the $_L$-arginine-binding site, but their interactions with NOS are not entirely understood. It does however seem to primarily involve lipophilic interactions with the adjacent regions of the NOS enzyme (Babu *et al.*, 1998:491). Both amino acid and non-amino acid NOS inhibitors occupy the guanidinium-binding site near the heme

cofactor and some have also been shown to interact covalently with heme iron, which leads to increased binding affinity (Salerno *et al.*, 1995:27423). A few aromatic heterocycles that do not contain guanidine-like structures have also been shown to bind near the heme cofactor and to interact with the adjacent lipophilic region. It is postulated that NOS inhibitors interacting with both the substrate and non-substrate binding sites may produce the best combination of potency and NOS isoform selectivity.

Raman *et al.* (2001:13448) hypothesised that compounds with little or no structural similarity to $_L$-arginine could exhibit unique modes of binding to NOS and that conformational changes induced by these compounds might provide key insights that could not otherwise be obtained from those inhibitors that bound without perturbing the binding site. Two conclusions were drawn from the crystal structure of the catalytic heme domain of endothelial NOS complexed with 3-bromo-7-nitroindazole. Firstly, Glu 363 (E363) is completely removed from engaging in direct H-bonded contact with the inhibitor. Secondly, by competing simultaneously for both the substrate and cofactor binding sites, 3-bromo-7-nitroindazole is able to occupy one site and subsequently alter the specificity of a second site. Also, designing an inhibitor that avoids hydrogen-bonded contact with one of the heme propionates, can serve as a potential template for designing isoform-selective NOS inhibitors. This is because compounds that interact with the heme propionates dramatically weaken the affinity of the cofactor site for H_4B, rendering it promiscuous. Although 3-bromo-7-nitroindazole targets the highly conserved substrate- and cofactor-binding sites, its high specificity is a result of adapting to a unique and altered protein conformation. This provides useful information for the further development of therapeutically useful, isoform-selective NOS inhibitors.

3.5 Conclusion

From the above discussions it is clear that while the active site geometries of the NOS isoform are known it remains a challenge to design isoform-selective inhibitors (Fischmann *et al.*, 1999:233, Li *et al.*, 1999:21276).

References

ALDERTON, W.K., COOPER, C.E. & KNOWLES, R.G. 2001. Nitric oxide synthases: Structure, function and inhibition. *Biochemical journal,* 357(3):593-615.

BABU, B.R. & GRIFFITH, O.W. 1998. Design of isoform-selective inhibitors of nitric oxide synthase. *Current opinion in chemical biology,* 2(4):491-500.

BREDT, D.S., HWANG, P.M., GLATT, C.E., LOWENSTEIN, C., REED, R.R. & SNYDER, S.H. 1991. Cloned and expressed nitric oxide synthase structurally resembles cytochrome P-450 reductase. *Nature,* 351(6329):714-718.

BURNETT, A.L., LOWENSTEIN, C.J., BREDT, D.S., CHANG, T.S.K. & SNYDER, S.H. 1992. Nitric oxide: A physiologic mediator of penile erection. *Science,* 257(5068):401-403.

CHESHIRE, D.R. 2001. Use of nitric oxide synthase inhibitors for the treatment of inflammatory disease and pain. *IDrugs,* 4(7):795-803.

CHO, H., XIE, Q., CALAYCAY, J., MUMFORD, R., SWIDEREK, K., LEE, T. & NATHAN, C. 1992. Calmodulin is a subunit of nitric oxide synthase from macrophages. *Journal of experimental medicine,* 176(2):599-604.

DAWSON, V.L., DAWSON, T.M., BARTLEY, D., UHL, G. & SNYDER, S. 1993. Mechanisms of nitric oxide-mediated neurotoxicity in primary brain cultures. *Journal of neuroscience,* 13(6):2651-2661.

DAWSON, V.L. & DAWSON, T.M. 1996. Nitric oxide neurotoxicity. *Journal of chemical neuroanatomy,* 10(3-4):179-190.

DEMURA, Y., AMESHIMA, S., ISHIZAKI, T., OKAMURA, S., MIYAMORI, I. & MATSUKAWA, S. 1998. The activation of eNOS by copper ion (Cu^{2+}) in human pulmonary arterial endothelial cells (HPAEC). *Free radical biology and medicine,* 25(3):314-320.

ENDRES, M., LAUFS, U., LIAO, J.K. & MOSKOWITZ, M.A. 2004. Targeting eNOS for stroke protection. *Trends in neurosciences,* 27(5):283-289.

ERDAL, E.P., LITZINGER, E.A., SEO, J., ZHU, Y., JI, H. & SILVERMAN, R.B. 2005. Selective neuronal nitric oxide synthase inhibitors. *Current topics in medicinal chemistry,* 5(7):603-624.

FISCHMANN, T.O., HRUZA, A., NIU, X.D., FOSSETTA, J.D., LUNN, C.A., DOLPHIN, E., PRONGAY, A.J., REICHERT, P., LUNDELL, D.J., NARULA, S.K. & WEBER, P.C. 1999. Structural characterization of nitric oxide synthase isoforms reveals striking active-site conservation. *Nature structural biology,* 6(3):233.

FÖRSTERMANN, U., POLLOCK, J.S., SCHMIDT, H.H., HELLER, M. & MURAD, F. 1991. Calmodulin-dependent endothelium-derived relaxing factor/nitric oxide synthase activity is present in the particulate and cytosolic fractions of bovine aortic endothelial cells. *Proceedings of the national academy of sciences of the United States of America,* 88(5):1788-1792.

GARTHWAITE, J. 1990. (In Moncada, S. & Higgs, E.A., eds. Nitric oxide from $_{L}$-arginine: A bioregulatory system. Amsterdam: Elsevier. p. 115-137.).

HIBBS, J.B., Jr., VAVRIN, Z. & TAINTOR, R.R. 1987. $_{L}$-arginine is required for expression of the activated macrophage effector mechanism causing selective metabolic inhibition in target cells. *Journal of immunology,* 138(2):550-565.

HOBBS, A.J., HIGGS, A. & MONCADA, S. 1999. Inhibition of nitric oxide synthase as a potential therapeutic target. *Annual review of pharmacology & toxicology,* 39(1):191.

HUANG, H., MARTASEK, P., ROMAN, L.J., MASTERS, B.S.S. & SILVERMAN, R.B. 1999. Nω-nitroarginine-containing dipeptide amides. Potent and highly selective inhibitors of neuronal nitric oxide synthase. *Journal of medicinal chemistry,* 42(16):3147-3153.

HUANG, P.L., HUANG, Z., MASHIMO, H., BLOCH, K.D., MOSKOWITZ, M.A., BEVAN, J.A. & FISHMAN, M.C. 1995. Hypertension in mice lacking the gene for endothelial nitric oxide synthase. *Nature,* 377(6546):239-242.

HUANG, Z., HUANG, P.L., PANAHIAN, N., DALKARA, T., FISHMAN, M.C. & MOSKOWITZ, M.A. 1994. Effects of cerebral ischemia in mice deficient in neuronal nitric oxide synthase. *Science,* 265(5180):1883-1885.

JI, H., LI, H., FLINSPACH, M., POULOS, T.L. & SILVERMAN, R.B. 2003. Computer modeling of selective regions in the active site of nitric oxide synthases: Implication for the design of isoform-selective inhibitors. *Journal of medicinal chemistry,* 46(26):5700-5711.

LASSEN, L., ASHINA, M., CHRISTIANSEN, I., ULRICH, V. & OLESEN, J. 1997. Nitric oxide synthase inhibition in migraine. *The lancet,* 349(9049):401-402.

LI, H., RAMAN, C.S., GLASER, C.B., BLASKO, E., YOUNG, T.A., PARKINSON, J.F., WHITLOW, M. & POULOS, T.L. 1999. Crystal structures of zinc-free and -bound heme domain of human inducible nitric-oxide synthase. Implications for dimer stability and comparison with endothelial nitric oxide synthase. *Journal of biological chemistry,* 274(30):21276-21284.

LI, H., RAMAN, C.S., MARTÁSEK, P., KRÁL, V., MASTERS, B.S.S. & POULOS, T.L. 2000. Mapping the active site polarity in structures of endothelial nitric oxide synthase heme domain complexed with isothioureas. *Journal of inorganic biochemistry,* 81(3):133-139.

MARLETTA, M. 1993. Nitric oxide synthase structure and mechanism. *Journal of biological chemistry,* 268(17):12231-12234.

MASTERS, B., MCMILLAN, K., SHETA, E., NISHIMURA, J., ROMAN, L. & MARTASEK, P. 1996. Neuronal nitric oxide synthase, a modular enzyme formed by convergent evolution: Structure studies of a cysteine thiolate-liganded heme protein that hydroxylates $_L$-arginine to produce $NO^{\bullet}$ as a cellular signal. *FASEB Journal,* 10(5):552-558.

MONCADA, S., PALMER, R.M.J. & HIGGS, E.A. 1989. Biosynthesis of nitric oxide from $_L$-arginine. A pathway for the regulation of cell function and communication. *Biochemical pharmacology,* 38(11):1709-1715.

MOORE, P.K., OLUYOMI, A.O., BABBEDGE, R.C., WALLACE, P. & HART, S.L. 1991. $_L$-N(G)-nitro arginine methyl ester exhibits antinociceptive activity in the mouse. *British journal of pharmacology,* 102(1):198-202.

MOORE, P.K., WALLACE, P., GAFFEN, Z., HART, S.L. & BABBEDGE, R.C. 1993. Characterization of the novel nitric oxide synthase inhibitor 7-nitro indazole and related indazoles: Antinociceptive and cardiovascular effects. *British journal of pharmacology.,* 110(1):219-224.

PALMER, R.M.J., FERRIGE, A.G. & MONCADA, S. 1987. Nitric oxide release accounts for the biological activity of endothelium-derived relaxing factor. *Nature,* 327(6122):524-526.

PARMENTIER, S., BÖHME, G.A., LEROUET, D., DAMOUR, D., STUTZMANN, J.M., MARGAILL, I. & PLOTKINE, M. 1999. Selective inhibition of inducible nitric oxide synthase prevents ischaemic brain injury. *British journal of pharmacology,* 127(2):546-552.

RAMAN, C.S., LI, H., MARTÁSEK, P., KRÁL, V., MASTERS, B.S.S. & POULOS, T.L. 1998. Crystal structure of constitutive endothelial nitric oxide synthase: A paradigm for pterin function involving a novel metal center. *Cell,* 95(7):939-950.

RAMAN, C.S., LI, H., MARTASEK, P., SOUTHAN, G., MASTERS, B.S.S. & POULOS, T.L. 2001. Crystal structure of nitric oxide synthase bound to nitro indazole reveals a novel inactivation mechanism. *Biochemistry,* 40(45):13448-13455.

ROMAN, L.J., MARTASEK, P. & MASTERS, B.S.S. 2002. Intrinsic and extrinsic modulation of nitric oxide synthase activity. *Chemical reviews,* 102(4):1179-1190.

SALERNO, J.C., FREY, C., MCMILLAN, K., WILLIAMS, R.F., MASTERS, B.S.S. & GRIFFITH, O.W. 1995. Characterization by electron paramagnetic resonance of the interactions of $_L$-arginine and $_L$-thiocitrulline with the heme cofactor region of nitric oxide synthase. *Journal of biological chemistry,* 270(46):27423-27428.

SALERNO, J.C., HARRIS, D.E., IRIZARRY, K., PATEL, B., MORALES, A.J., SMITH, S.M.E., MARTASEK, P., ROMAN, L.J., MASTERS, B.S.S., JONES, C.L., WEISSMAN, B.A., LANE, P., LIU, Q. & GROSS, S.S. 1997. An autoinhibitory control element defines calcium-regulated isoforms of nitric oxide synthase. *Journal of biological chemistry,* 272(47):29769-29777.

SALERNO, L., SORRENTI, V., DI GIACOMO, C., ROMEO, G. & SIRACUSA, M.A. 2002. Progress in the development of selective nitric oxide synthase (NOS) inhibitors. *Current pharmaceutical design,* 8(3):177.

SCHULZ, J.B., HUANG, P.L., MATTHEWS, R.T., PASSOV, D., FISHMAN, M.C. & BEAL, M.F. 1996. Striatal malonate lesions are attenuated in neuronal nitric oxide synthase knockout mice. *Journal of neurochemistry,* 67(1):430-433.

SCHWABE, J.W. & KLUG, A. 1994. Zinc mining for protein domains. *Nature structural biology,* 1(6):345-349.

STRIJBOS, P.J.L.M., LEACH, M.J. & GARTHWAITE, J. 1996. Vicious cycle involving Na^+ channels, glutamate release, and NMDA receptors mediates delayed neurodegeneration through nitric oxide formation. *Journal of neuroscience,* 16(16):5004-5013.

STUEHR, D.J. 1999. Mammalian nitric oxide synthases. *Biochimica et biophysica acta (bioenergetics),* 1411(2-3):217-230.

TOGO, T., KATSUSE, O. & ISEKI, E. 2004. Nitric oxide pathways in Alzheimer's disease and other neurodegenerative dementias. *Neurological research,* 26(5):563-566.

CHAPTER 4

ARTICLE 1 - BIOORGANIC & MEDICINAL CHEMISTRY

Article published online on 15 September 2009.

Bioorganic & Medicinal Chemistry 17 (2009) 7523–7530.

Synthesis and In Vitro Evaluation of Pteridine Analogues as Monoamine Oxidase B and Nitric Oxide Synthase Inhibitors

Louis H.A. Prins[a], Jacobus P. Petzer[a], and Sarel F. Malan[a*]

[a] Pharmaceutical Chemistry, School of Pharmacy, North-West University, Private Bag X6001, Potchefstroom, 2520, South Africa.

[*] Corresponding author.
Present address: School of Pharmacy, University of the Western Cape, Private Bag X17, Bellville, 7535, South Africa.
Tel: +27-21-9593190; fax: +27-21-9591588.
E-mail address: sfmalan@uwc.ac.za

Graphical abstract

A series of pteridine-2,4-dione analogues were synthesised and evaluated as inhibitors of monoamine oxidase B (MAO-B) and nitric oxide synthase (NOS).

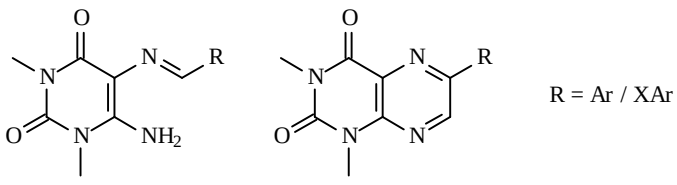

R = Ar / XAr

Synthesis and In Vitro Evaluation of Pteridine Analogues as Monoamine Oxidase B and Nitric Oxide Synthase Inhibitors

Louis H.A. Prins[a], Jacobus P. Petzer[a], and Sarel F. Malan[a]*

[a] Pharmaceutical Chemistry, School of Pharmacy, North-West University, Private Bag X6001, Potchefstroom, 2520, South Africa.

* Corresponding author.
Present address: School of Pharmacy, University of the Western Cape, Private Bag X17, Bellville, 7535, South Africa.
Tel: +27-21-9593190; fax: +27-21-9591588.
E-mail address: sfmalan@uwc.ac.za

Abstract

Monoamine oxidase B (MAO-B) and nitric oxide synthase (NOS) have both been implicated in the pathology of neurodegenerative diseases. In an attempt to design dual-target-directed drugs that inhibit both these enzymes, a series of pteridine-2,4-dione analogues were synthesised. The compounds were found to be relatively weak NOS inhibitors but showed promising MAO-B activity. For example, 6-amino-5-[(*E*)-3-(3-chloro-phenyl)-prop-2-en-(*E*)-ylideneamino]-1,3-dimethyl-1H-pyrimidine-2,4-dione and 6-[(*E*)-2-(3-chloro-phenyl)-vinyl]-1,3-dimethyl-1H-pteridine-2,4-dione inhibited MAO-B with IC_{50} values of 0.602 and 0.314 µM, respectively. The pteridine-2,4-dione analogues thus show promise as scaffolds for the development of potent reversible MAO-B inhibitors and as observed in earlier studies, the most potent inhibitors were obtained with 3-chlorostyryl substitution.

Keywords: Monoamine oxidase B; Nitric oxide synthase; Pteridine-2,4-dione; Dual-target-directed ligands

4.1 Introduction

Neurodegenerative disorders such as Parkinson's and Alzheimer's diseases, are affecting the lives of a growing number of people worldwide. These debilitating conditions lead to a general decrease in quality of life and the need for therapeutics to effectively prevent and treat these conditions are of increasing importance.[1]

It has become evident that neurodegenerative diseases are not the result of a single cause but that the processes involved are of a multifactorial nature. It is hypothesised that genetic, environmental and endogenous factors may be involved in neurodegenerative diseases such as Alzheimer's disease, Parkinson's disease, Huntington's disease and amyotrophic lateral sclerosis. A series of general pathways have been identified that may be involved in different pathogenic cascades and includes protein misfolding and aggregation, oxidative stress and free radical formation, metal dyshomeostasis, mitochondrial dysfunction and phosphorylation impairment. All of the above seem to occur simultaneously, leading to the demise of key neuronal cells.[2]

Keeping this in mind, the paradigm of targeting a single disease factor may not be an effective treatment strategy for neurodegenerative diseases. The polypharmaceutical approach, wherein several drugs that act independently on different etiological targets of a disease are combined, has been used as a means of multiple targeting in the clinical setting. However, this strategy of combining several drug molecules results in several challenges, such as a combined or even multiplied toxicity and side-effect profile and the occurrence of unforeseen drug-drug interactions.[3] For these reasons the design of single drug molecules that act on two or more specific etiological targets of a particular disease may be of value. The advantages associated with this strategy includes a lower likelihood of encountering unwanted side-effects and the possibility to 'design out' any side-effects when only using one drug, as opposed to using two or more drugs.[1]

One target for the treatment of neurodegenerative diseases is the enzyme monoamine oxidase B (MAO-B). It is the predominant isoform of MAO found in human brain[4] where it is implicated in age-related neurodegenerative diseases such as Parkinson's disease and Alzheimer's disease. It has been demonstrated that brain MAO-B activity, but not MAO-A activity, increases with aging,[5] and since MAO-B appears to be located in glial cells

this may be due to gliosis associated with aging. MAO-B plays a dual role in the pathophysiology of Parkinson's disease since it is a major dopamine metabolising enzyme and is also implicated in the formation of reactive oxygen species and other neurotoxic species.[6] MAO-B has also been implicated in the pathophysiology of Alzheimer's disease since increased MAO-B levels have been observed in plaque-associated astrocytes in the brains of Alzheimer's disease patients.[7] This increase in MAO-B activity may result in an elevation in hydroxyl radicals ($^{\bullet}OH$), which has been correlated with amyloid-β (Aβ) plaque formation. Hence, the therapeutic potential of selective reversible MAO-B inhibitors does not rely solely on their ability to increase the biological half–life of dopamine but also on their ability to reduce the levels of MAO-B generated reactive oxygen species in the brain and their potential ability to inhibit Aβ plaque formation.

Another enzyme implicated in the neurodegenerative process is nitric oxide synthase (NOS). Nitric oxide (NO) is known to be an important cell signalling agent that regulates an array of physiological functions. These include blood pressure by regulation of smooth muscle relaxation,[8] platelet aggregation by acting as an antithrombotic agent,[9] antitumor, antibacterial, and antiviral action of macrophages,[10] brain development, learning and memory,[11] and it is also the neuronal mediator of penile erection.[12] However, since NO is a free radical, overproduction thereof may result in deleterious effects ranging from septic shock and pain[13] to ischaemia[14] and it may also be involved in neurodegenerative processes[15] associated with Parkinson's and Alzheimer's diseases.[16] The harmful effects caused by an overproduction of NO are thought to be mediated by peroxynitrate ($ONOO^-$), the product obtained when NO and the superoxide radical ($O_2^{\bullet -}$) react. $ONOO^-$ causes injury to the mitochondrial electron transport chain resulting in damage and eventual death of neurons. Evidence that NO and $ONOO^-$ are neurotoxic is provided in the ability of superoxide dismutase to protect cortical cultures from both glutamate and NO donors. Removal of nNOS containing neurons from culture or elimination of nNOS through transgenic technology, results in a culture that is resistant to NMDA neurotoxicity indicating that nNOS neurons are the source of neurotoxic NO.[16,17]

Several 8-substituted caffeinyl derivatives have been reported to be moderate to potent reversible inhibitors of MAO-B.[18,19] For example the caffeine analogue (*E*)-8-(3-chlorostyryl)-caffeine (CSC) (**1**, Fig. 1), is an exceptionally potent MAO-B inhibitor, with enzyme-inhibitor dissociation constants (K_i values) of 100 nano molar (nM) for mouse brain mitochondrial MAO-B[20] and 128 nM for baboon liver mitochondrial MAO-B.[21] Pteridine-2,4-dione (**2**) bear structural resemblance to caffeine (**3**) and was therefore of interest in the design of novel reversible MAO-B inhibitors, possibly with comparable activity to the caffeinyl derivatives. The synthesis of pteridine-2,4-diones conjugated to styryl and other moieties was thus pursued, and the resulting compounds were evaluated as MAO-B inhibitors.

Pteridine-2,4-dione is also structurally similar to the essential NOS cofactor, tetrahydrobiopterin (BH_4) (**4**) and certain pterin analogues (**5**) have been developed to target this binding site.[22,23] Because of this structural relationship with BH_4, pteridine derivatives have been described as NOS inhibitors. Since BH_4 exhibits lower affinity and selectivity for other pterin dependent enzymes, this approach appears to be promising.[24] In a series of BH_4 analogues the 4-amino derivative, 5,6,7,8-tetrahydro-6-(D-*threo*-1,2-dihydroxypropyl)pterin (**6**), was reported to be a potent inhibitor of recombinant rat brain NOS in vitro (K_i = 13 nM) as well as in vivo.[25] Also of interest is the 6-phenyl derivative (**7**) which inhibits NOS with an IC_{50} value of 6 μM. Based on the NOS inhibition activity of pterin analogues, the structurally similar pteridine-2,4-dione analogues prepared in the present study were also evaluated as NOS inhibitors. Compounds that inhibit both MAO-B and NOS may find enhanced application in the treatment of neurodegenerative disorders.

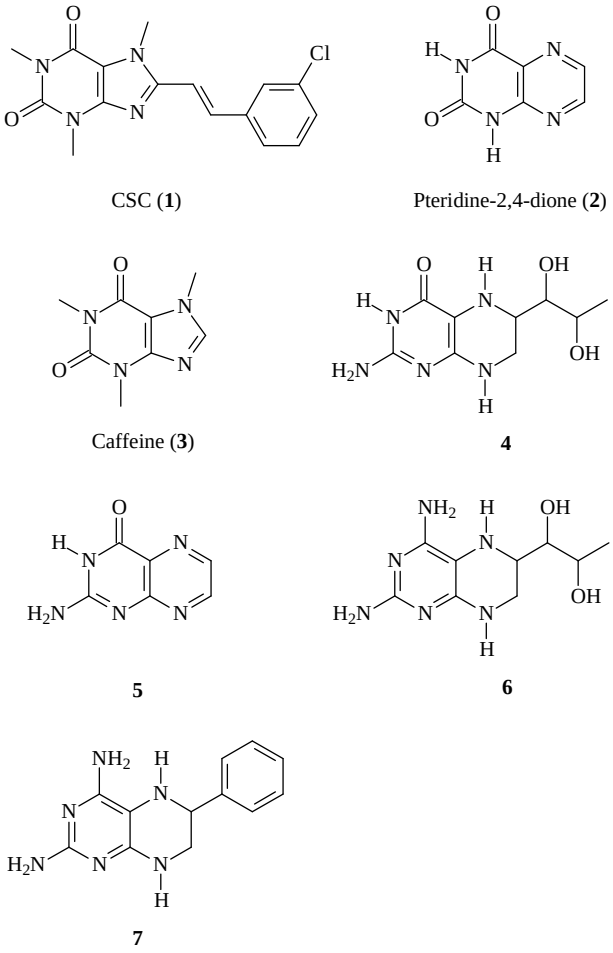

Figure 1. The structures of CSC (**1**), pteridine-2,4-dione (**2**), caffeine (**3**) and selected pterin analogues.

4.2 Results

4.2.1 Synthesis of pteridine-2,4-dione analogues

The target pteridine-2,4-dione derivatives were synthesised according to the literature procedure (Scheme 1).[26] The key starting material, 1,3-dimethyl-5,6-diaminouracil (**8**), was reacted with the appropriate aldehyde to yield the pyrimidines **9a-d**. The pyrimidines were cyclicised by the addition of triethyl orthoformate under reflux, to obtain the final pteridine-2,4-diones **10a-b**, **d**.[26] Cyclisation of **9c** using this procedure was not successful and the corresponding pteridine-2,4-dione could not be obtained. The structures of the newly synthesised compounds were confirmed by ^{1}H NMR, ^{13}C NMR, IR, MS and elemental analyses.

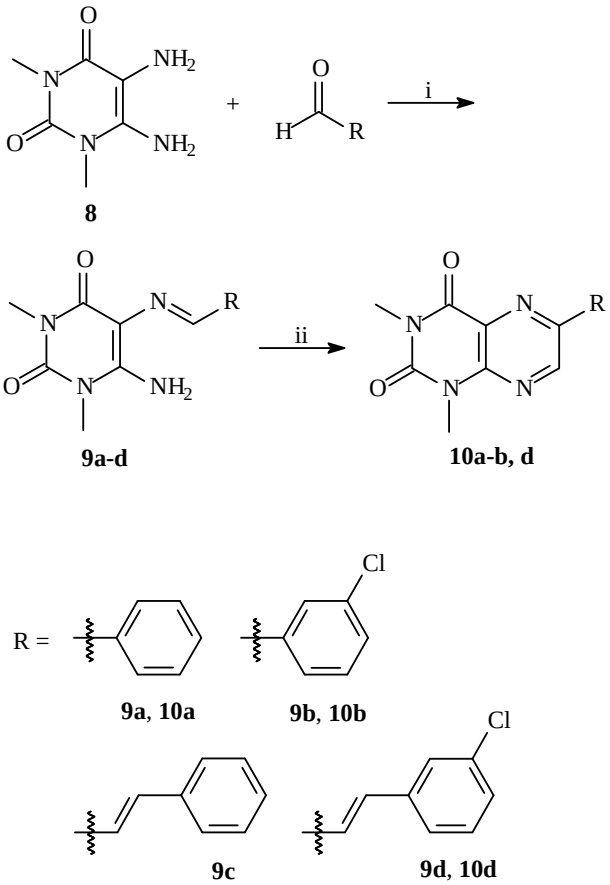

Scheme 1. Synthetic pathway to pteridine-2,4-dione (**10**) and pyrimidine (**9**) analogues: (i) EtOH, reflux, 4 h; (ii) $CH(OCH_2CH_3)_3$, DMF, reflux, 10 h.

4.2.2 MAO-B inhibition

It has previously been shown that baboon liver tissue is devoid of MAO-A activity while exhibiting a high degree of MAO-B catalytic activity.[27] The interaction of reversible inhibitors with baboon liver MAO-B also appears to be similar to human liver MAO-B.[19] Recent results from our laboratory (unpublished data) have also indicated that a variety of structurally unrelated compounds inhibit membrane bound baboon liver and recombinant human MAO-B with similar potencies. Mitochondrial fractions obtained from baboon liver were thus used to determine the extent by which the pteridine-2,4-dione analogues (**10a-b**, **d**) and the pyrimidines (**9a-d**) inhibit this enzyme.

IC_{50} values (concentration of the inhibitor that inhibits 50% of the enzyme activity) for the test compounds were determined by measuring the extent by which different concentrations thereof slowed the rate of α-carbon oxidation of 1-methyl-4-(1-

methylpyrrol-2-yl)-1,2,3,6-tetrahydropyridine (MMTP) to the corresponding dihydropyridinium metabolite, $MMDP^+$ (Fig. 2). The production of $MMDP^+$ was measured spectrophotometrically at a wavelength of 420 nm, at which neither the substrate nor the test compounds absorb UV light.

The results of the MAO-B activity measurements indicate that **10d** is the most potent MAO-B inhibitor of the analogues examined in this study, with an IC_{50} value of 0.314 µM (Table 1). The second most potent inhibitor was pyrimidine **9d** with with an IC_{50} value of 0.602 µM. It is noteworthy that **10d** and **9d** are structurally closely related to CSC (**1**), a known MAO-B inhibitor. Using the Cheng-Prusoff equation[28] the K_i values (enzyme-inhibitor dissociation constants) for the inhibition of MAO-B by **10d** and **9d** were calculated to be 181 and 348 nM respectively, indicating that **10d** is only slightly less potent than CSC (K_i = 128 nM)[21] as a MAO-B inhibitor.

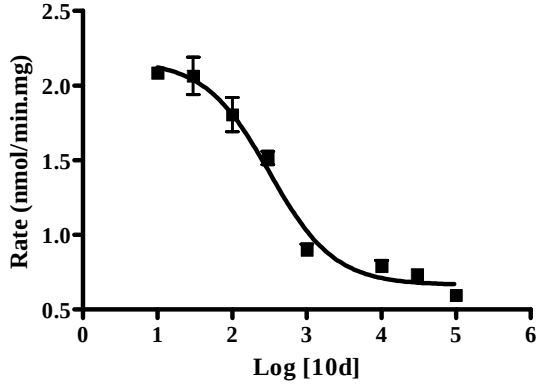

Figure 2. The sigmoidal dose-response curve of the initial rates of oxidation of MMTP versus the logarithm of concentration of inhibitor **10d** (expressed in nM). The concentration of the baboon liver mitochondrial preparation was 0.15 mg protein/mL. The rates are expressed as nmol $MPDP^+$ formed/mg protein/min and the concentration of MMTP used was 50 µM. The determinations were carried out in duplicate and the values are expressed as mean ± SEM.

4.2.3 NOS inhibition

In order to determine the NOS inhibition potencies of the pteridine-2,4-dione (**10a-b**, **d**) and pyrimidine (**9a-d**) analogues, the oxyhaemoglobin (Hb) assay[29] was used. This assay is based on the measurement of the conversion of oxyHb to metHb by NO (Fig. 3). Rat

brain homogenate was used as NOS enzyme source since it has been shown to have high constitutive NOS activity.[30] A disadvantage of brain homogenate as enzyme source is that isoform selectivity is unaccounted for since the crude rat brain extract contains several NOS isoforms. For the purpose of screening potential NOS inhibitors for central NOS inhibition activity, this enzyme source was deemed appropriate.

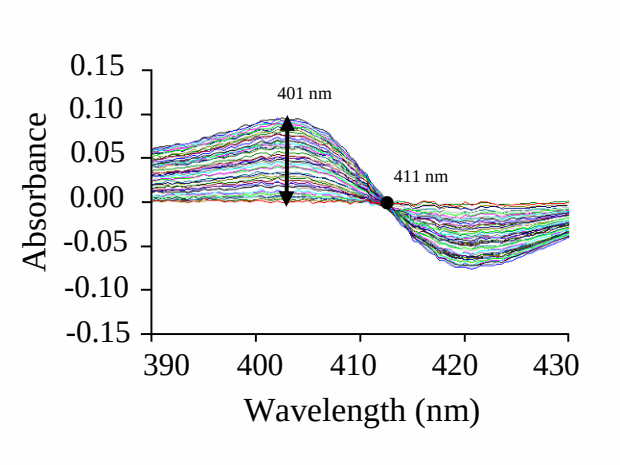

Figure 3. UV-vis scans of incubations containing rat brain homogenate, oxyHb, NADPH and *L*-arginine. The increase in absorbance intensity at a wavelength of 401 nm is indicative of metHb production as a result of NO formation by NOS present in the homogenate fraction.

Comparing the obtained IC_{50} values for the pteridine-2,4-diones (**10a-b**, **d**) and pyrimidines (**9a-d**) to those of two known NOS inhibitors, 7-nitroindazole (7-NI; IC_{50} = 0.111 µM) and aminoguanidine (AG; IC_{50} = 19.41 µM), reveals that none of the test compounds are promising as potential NOS inhibitors (Table 1). The most potent inhibitors were **10a** (IC_{50} = 443.3 µM) and **9a** (IC_{50} = 466.9 µM), which are approximately 23 fold less potent than AG. IC_{50} values could not be calculated for compounds **9c** and **10b** since these compounds absorb UV light in the detection range (390-430 nm) of the assay.

Table 1. MAO-B and NOS inhibition by pteridine-2,4-dione (**10**) and pyrimidine (**9**) analogues.

Compound	MAO-B Inhibition		NOS Inhibition
	IC_{50} (μM)	*K_i (μM)*[c]	*IC_{50} (μM)*
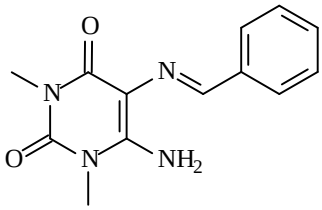 **9a**	Not determined[a]	Not determined[a]	466.9
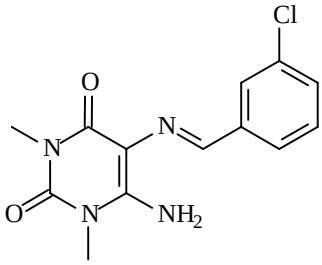 **9b**	7.033	4.060	6968
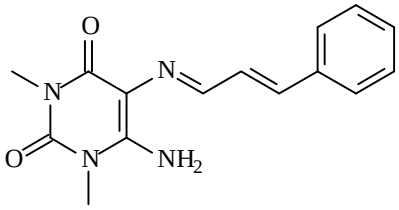 **9c**	12.052	6.958	Not determined[d]
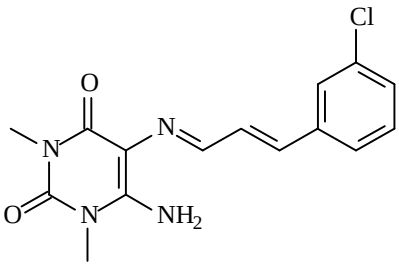 **9d**	0.602	0.348	577.2
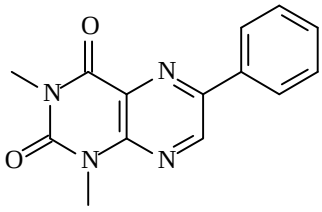 **10a**	Not determined[b]	Not determined[b]	443.3

Compound	MAO-B Inhibition		NOS Inhibition
	IC_{50} (μM)	*K_i (μM)*[c]	*IC_{50} (μM)*
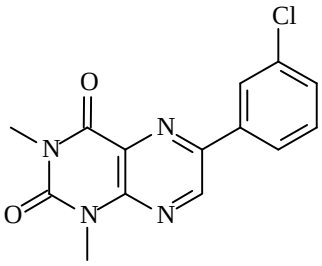 **10b**	4.889	2.823	Not determined[d]
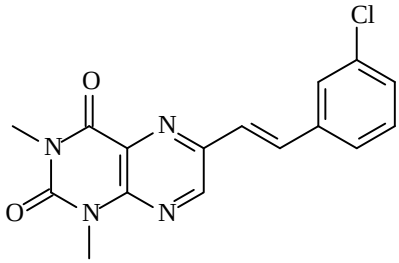 **10d**	0.314	0.181	1057
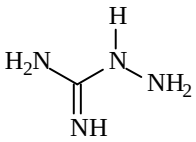 **AG**	-	-	19.41[e]
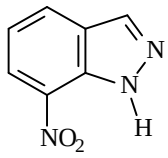 **7-NI**	-	-	0.111[e]

[a] At the limit of solubility (30 μM) 17.8% of the MAO-B activity was inhibited.

[b] At the limit of solubility (100 μM) 12.2% of the MAO-B activity was inhibited.

[c] The experimentally determined IC_{50} values were used to calculate the K_i values according to the equation by Cheng and Prusoff: $K_i = IC_{50}/(1 + [S]/K_m)$ with [S] = 50 μM and K_m (MMTP) = 68.3±1.60 μM.[28]

[d] Values could not be calculated as these compounds absorb UV light within the assay detection range (390-430 nm).

[e] Values obtained from Joubert *et al.* (2008).[31]

4.2.4 Molecular modelling study

In an attempt to clarify the relationships between the observed MAO-B inhibition potencies and the structures of the inhibitors examined here, molecular docking studies with the active pyrimidine (**9b**–**d**) and pteridine (**10b**, **d**) analogues were performed. CSC (**1**) and safinamide were also included in the docking study. The crystallographic structure of recombinant human MAO-B in complex with the reversible inhibitor safinamide (PDB code: 2V5Z)[32] was selected for the docking studies. Since safinamide spans both the entrance and substrate cavities of the enzyme active site, the side chain of the gating residue, Ile-199, is rotated out of its normal conformation to allow for the fusion of the two cavities and the accommodation of larger structures such as those examined in the present study.[33] To evaluate the accuracy of the docking procedure, the co-crystallised ligand was redocked within the active site using the LigandFit application within Discovery Studio® 1.7. This procedure was repeated three times and the best ranked solution of safinamide in each instance exhibited a RMSD of 1.73 Å from the co-crystallised ligand (Fig. 4). In general, RMSD values smaller than 2.0 Å indicate that the docking protocol is capable of accurately predicting the binding orientation of the co-crystallised ligand.[34] This protocol was thus deemed to be suitable for docking of the inhibitors into the active site model of MAO-B.

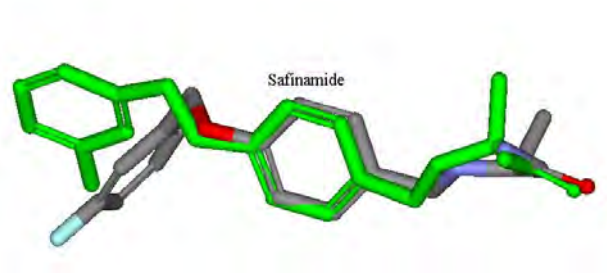

Figure 4. RMSD overlay of the best ranked solutions of safinamide on the original co-crystallised ligand, displayed in bright green.

The best-ranked docking solutions of the pyrimidine (**9b**–**d**) and pteridine (**10b**, **d**) analogues examined here show that all inhibitors span both the entrance and substrate cavities of the enzyme. As shown for example with **9d** (Fig. 5) and **10d** (Fig. 6), the

pyrimidine-2,4-dione rings of **9b**–**d** and the pteridine-2,4-dione rings of **10b**, **d** are located within the substrate cavity nearer to the FAD cofactor. The phenyl (**9b**, **10b**) and styryl (**9c**–**d**, **10d**) side chains extend towards the entrance cavity. These binding modes are expected since the polar regions in the substrate cavity would better accommodate the pyrimidine and pteridine rings while the phenyl and styryl moieties would be better stabilised within the hydrophobic entrance cavity. In addition, hydrogen bonding between the carbonyl oxygens of the pyrimidine and pteridine rings and integral water molecules within the substrate cavity would further promote these binding orientations.

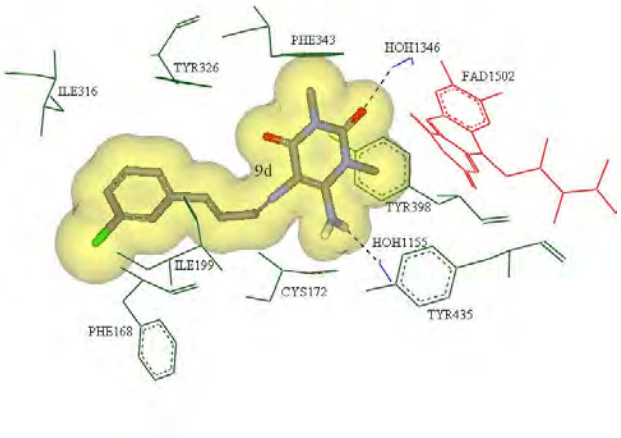

Figure 5. Putative binding mode of **9d** to the human MAO-B active site. Hydrogens are hidden, except those involved in hydrogen bonds, and selected amino acid residues are displayed in dark green. The FAD cofactor is indicated in red, interacting water molecules in blue and hydrogen bonds in black. The Van der Waals volume of **9d** is displayed as a transparent yellow surface.

For structures **9b**–**d** the possibility of hydrogen bond formation with the amino functional group on C6 of the pyrimidine ring also exists as demonstrated in Fig. 7. CSC adopts a similar binging mode to those observed for the pyrimidine (**9b**–**d**) and pteridine (**10b**, **d**) analogues and the caffeine ring of CSC is located in the substrate cavity of the MAO-B active site model while the styryl side chain extends into the entrance cavity (Fig. 8). As observed for the pyrimidine and pteridine analogues, the caffeine carbonyl oxygens can also act as potential hydrogen bond acceptors within the substrate cavity.

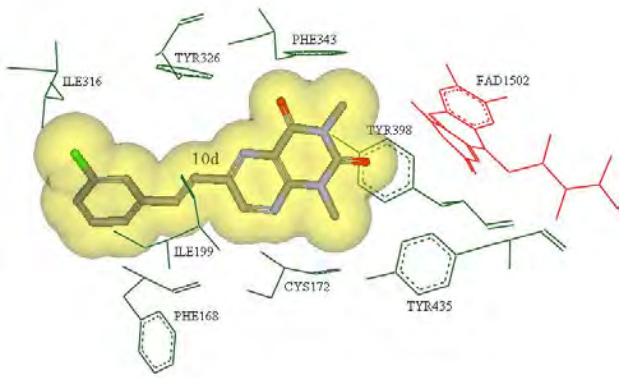

Figure 6. Putative binding mode of **10d** to the human MAO-B active site. Hydrogens are hidden, except those involved in hydrogen bonds, and selected amino acid residues are displayed in dark green. The FAD cofactor is indicated in red, interacting water molecules in blue and hydrogen bonds in black. The Van der Waals volume of **10d** is displayed as a transparent yellow surface.

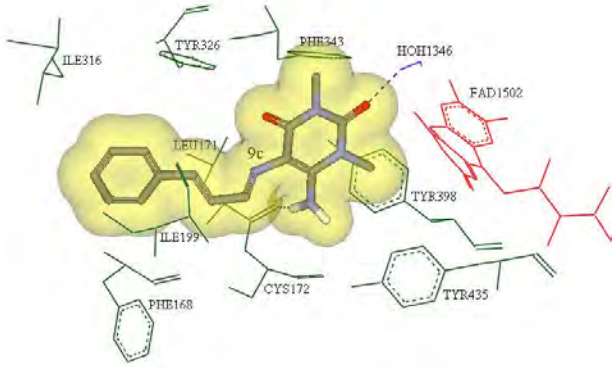

Figure 7. Putative binding mode of **9c** to the human MAO-B active site. Hydrogens are hidden, except those involved in hydrogen bonds, and selected amino acid residues are displayed in dark green. The FAD cofactor is indicated in red, interacting water molecules in blue and hydrogen bonds in black. The Van der Waals volume of **9c** is displayed as a transparent yellow surface.

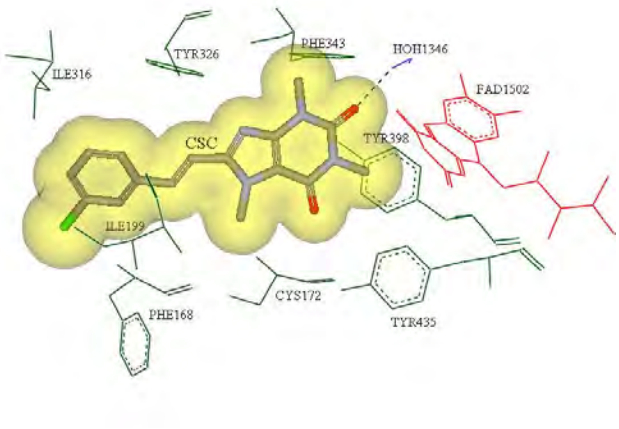

Figure 8. Putative binding mode of CSC to the human MAO-B active site. Hydrogens are hidden, except those involved in hydrogen bonds, and selected amino acid residues are displayed in dark green. The FAD cofactor is indicated in red, interacting water molecules in blue and hydrogen bonds in black. The Van der Waals volume of CSC is displayed as a transparent yellow surface.

The $\log IC_{50}$ values of the pyrimidine (**9c**–**d**) and pteridine (**10d**) analogues and of CSC correlated with the DockScore value with a correlation coefficient (r^2 value) of 0.97 (Table 2). Although it is extremely difficult to accurately rank compounds based on their binding affinity in a docking study, this observation may serve as additional evidence that this docking protocol is effective for examining the molecular interactions between the inhibitors studied here and the active site of MAO-B. This docking protocol also appears to have predictive value and may in the future be developed as a predictive model for MAO-B inhibition.

Table 2. Comparison of calculated affinities (DockScore values) of compounds **9c**, **9d**, **10d** and CSC with experimental MAO-B inhibitory activities (logIC_{50} values).

Ligand	*DockScore*	*logIC_{50} (µM)*
CSC	60.171	-0.836[a]
10d	59.898	-0.503
9d	57.842	-0.220
9c	54.249	1.081

[a] Value obtained from literature.[36]

4.3 Discussion

The current study has identified pteridine-2,4-diones as promising novel inhibitors of MAO-B. Analogue **10d** which is substituted with a 3-chlorostyryl functional group at C6 of the pteridine-2,4-dione ring was found to be the most potent inhibitor with an IC_{50} value of 0.314 µM. This inhibition potency is comparable to that of CSC, a potent reversible MAO-B inhibitor.[20,21,35] Interestingly, the pteridine-2,4-diones were found to be more potent MAO-B inhibitors than their corresponding pyrimidine precursors. For example pyrimidine **9d**, the precursor of **10d,** has an IC_{50} value of 0.602 µM compared to the 0.314 µM of **10d**. The same trend is observed for pteridine-2,4-dione **10b**, which is more potent than pyrimidine **9b**. A possible reason for this observation is that the amino functional group at C6 of the pyrimidine ring might be protonated at physiological pH. This may hinder access to the active site or prevent effective binding within the site.

The current study also shows that styryl substitution at C6 of the pteridine-2,4-dione results in better MAO-B inhibitors than phenyl substitution. For example **10d** was approximately 16 fold more potent as a MAO-B inhibitor than was **10b**. Chlorine substitution at C3 of the styryl ring was again found to be important for binding to the active site of MAO-B[19,20] and throughout both the pyrimidine and pteridine series, the chlorine substituted compounds exhibited higher activity as MAO-B inhibitors. This concurs with the reported findings that CSC is approximately 22 fold more potent than the corresponding unsubstituted (*E*)-8-styrylcaffeines.[21] This data suggests that the

inhibitors examined here have a similar binding mode as CSC. In general, substitution of the styryl ring appears to improve the binding interactions within the entrance cavity.

As has been the case in numerous other enzymatic studies, the limited solubility of the test compounds in this study restricted the full exploration of their biological profile. In the MAO-B assay for example, compound **10a** and its pyrimidine precursor **9a** were insoluble in the buffer medium at 100 and 30 µM respectively. Another factor specifically relating to the NOS oxyHb assay, which hindered biological evaluation, was the UV absorption properties of the test inhibitors. Compounds **9c** and **10b** were both shown to absorb UV light in the assay detection range stretching from 390 to 430 nm. As a result, NOS inhibition data could not be calculated for either of these compounds. As none of the pteridine analogues showed promise as NOS inhibitors, neither the obtained results nor the assay procedure were optimised any further.

4.4 Conclusion

Although multifunctional drugs are a promising strategy for the treatment of neurodegenerative diseases,[36,37,1] designing drugs that act at multiple targets remains a challenge. Designing pteridine analogues to target the BH_4 binding site of NOS was not successful in this study and it is hypothesised that the styryl phenyl may be sterically hindering binding of the test compounds to NOS.

Comparing the calculated MAO-B K_i values for the synthesised pteridines (Table 1) with those experimentally determined for a series of benzimidazoles,[38] reveals that pteridines may be better scaffolds for MAO-B inhibition than benzimidazoles and in general exhibit MAO-B inhibition only slightly less potent than that observed with the corresponding caffeine structures. These compounds thus show potential for the design of potent reversible MAO-B inhibitors and might, with optimisation, be attractive alternatives to the caffeine analogues.

4.5 Experimental

Caution: *MMTP is a structural analogue of the nigrostriatal neurotoxin, 1-methyl-4-phenyl-1,2,3,6-tetrahydropyridine (MPTP) and it should be handled using disposable latex gloves and protective eyewear. Procedures for the safe handling of neurotoxic compounds were followed as described previously.*[39]

4.5.1 Materials and instrumentation

All chemicals and reagents were purchased from commercial sources and solvents were dried using standard methods. 1,3-Dimethyl-5,6-diaminouracil (**8**),[40] *trans*-3-chloro-cinnamaldehyde[41] and the oxalate salt of MMTP[42] were prepared according to previously reported methods. Because of chemical instability, **8** was used within 24 hours of preparation. Thin-layer chromatography was performed on 0.20 mm thick aluminium silica gel sheets (Alugram® SIL G/UV_{254}, Kieselgel 60, Macherey-Nagel® Düren, Germany) with an appropriate mobile phase and visualisation was achieved using UV light (254 and 366 nm) and iodine vapour. All melting points (mp) were obtained using a Stuart® SMP10 melting point apparatus and are uncorrected. ^{1}H and ^{13}C NMR spectra were recorded using a Bruker® Avance III 600 spectrometer at a frequency of 600 and 150 MHz, respectively. Chemical shifts are expressed in parts per million (δ) relative to the signal from tetramethylsilane (Me_4Si), added to an appropriate deuterated solvent ($CDCl_3$ or DMSO-d_6). Spin multiplicities are given as s (singlet), d (doublet), dd (doublet of doublets) and m (multiplet). Mass spectra were obtained by direct insertion electron impact ionisation mass spectrometry (EI-MS) using an analytical VG 7070E mass spectrometer. IR spectra were recorded in KBr on a Nicolet® Nexus™ 470-FT IR spectrometer over the range 400-4000 cm^{-1} employing the diffuse reflectance method. Elemental analyses were done using a Perkin-Elmer® 2400 Series II CHNS elemental analyser with argon gas as carrier.

4.5.2 Synthesis

General procedure for the synthesis of pyrimidines **9a**-**d**: 1,3-Dimethyl-5,6-diaminouracil (17.6 mmol) was suspended in 10 mL ethanol (anhydrous). The appropriate aldehyde (20.6 mmol) was dissolved in 5 mL ethanol (anhydrous) and added to the above suspension. After heating the mixture under reflux for 4 hours it was allowed to cool to room temperature. The reaction was cooled on an ice bath for 30 minutes and the precipitate was collected by filtration and washed with ethanol. Recrystallisation from DMF/H_2O gave the pure intermediary compounds (**9a**-**d**) in excellent yield.

General procedure for the synthesis of pteridine-2,4-dione analogues **10a**-**d**: The appropriate pyrimidine compound (**9a**-**b**, **d**, 8.5 mmol) was dissolved in 10 mL *N*,*N*'-

dimethylformamide at ambient temperature and triethyl orthoformate (43 mmol) was added. The solution was refluxed for 10 hours and then allowed to cool to room temperature. The reaction was incubated on an ice bath for 30 minutes and the resulting precipitate was collected by filtration. The pteridine-2,4-diones were recrystallised from *N*,*N'*-dimethylformamide (**10a**, **10b**) or acetone (**10d**).

4.5.2.1 6-Amino-1,3-dimethyl-5-{[1-phenylmeth-(*E*)-ylidene]-amino}-1H-pyrimidine-2,4-dione (9a)

Compound **9a** was prepared from 1,3-dimethyl-5,6-diaminouracil (**8**) and benzaldehyde in a yield of 59.2%. $C_{13}H_{14}N_4O_2$; **mp:** 225 °C (DMF/H_2O). The measured melting point was in accordance with the literature value (225 °C).[26]

4.5.2.2 6-Amino-5-{[1-(3-chlorophenyl)-meth-(*E*)-ylidene]-amino}-1,3-dimethyl-1H-pyrimidine-2,4-dione (9b)

Compound **9b** was prepared from 1,3-dimethyl-5,6-diaminouracil (**8**) and 3-chloro-benzaldehyde in a yield of 78.6%. $C_{13}H_{13}ClN_4O_2$; **mp:** 253 °C (DMF/H_2O); **^{1}H NMR** (600 MHz, DMSO-d_6) δ_H: 9.71-9.67 (s, 1H), 8.07-7.71 (m, 2H), 7.46-7.33 (m, 4H), 3.42-3.37 (s, 3H), 3.19-3.14 (s, 3H); **^{13}C NMR** (150 MHz, DMSO-d_6) δ_C: 157.70 (C), 154.20 (C), 150.00 (CH), 148.00 (C), 141.20 (C), 134.10 (C), 130.60 (CH), 129.00 (CH), 126.90 (CH), 126.20 (CH), 99.10 (C), 30.90 (CH_3), 27.50 (CH_3); **MS** (EI, 70 eV) m/z: 292 (M^+); **IR** (KBr) ν_{max}: 3414, 3297, 3081, 1690, 1551, 1593, 1518, 1449, 1263, 1226, 1207, 1067, 876, 789, 760, 748, 711 cm^{-1}; Anal. calcd for $C_{13}H_{13}ClN_4O_2$: C, 53.34; H, 4.48; N, 19.14. Found: C, 54.20; H, 4.30; N, 19.40.

4.5.2.3 6-Amino-1,3-dimethyl-5-[(*E*)-3-phenyl-prop-2-en-(*E*)-ylideneamino]-1H-pyrimidine-2,4-dione (9c)

Compound **9c** was prepared from 1,3-dimethyl-5,6-diaminouracil (**8**) and *trans*-cinnamaldehyde in a yield of 76.1%. $C_{15}H_{16}N_4O_2$; **mp:** 235 °C (DMF/H_2O); **^{1}H NMR** (600 MHz, DMSO-d_6) δ_H: 9.48-9.45 (d, 1H, J = 8.21 Hz), 7.55-7.52 (d, 2H, J = 8.62 Hz), 7.39-7.25 (m, 5H), 7.00-6.97 (d, 2H, J = 8.00 Hz), 3.36 (s, 3H), 3.15 (s, 3H); **^{13}C NMR** (150 MHz, DMSO-d_6) δ_C: 156.81 (C), 153.26 (C), 151.32 (CH), 149.63 (2 x C), 136.53 (CH), 131.62 (CH), 128.73 (2 x CH), 128.12 (2 x CH), 126.59 (CH), 99.39 (C), 30.21 (CH_3), 26.99 (CH_3); **MS** (EI, 70 eV) m/z: 285 (M^+); **IR** (KBr) ν_{max}: 3498, 3374,

3061, 3032, 2996, 1680, 1608, 1585, 1518, 1448, 1226, 1162, 1068, 973, 916, 840, 766, 747, 694 cm^{-1}; Anal. calcd for $C_{15}H_{16}N_4O_2$: C, 63.37; H, 5.67; N, 19.71. Found: C, 62.60; H, 5.60; N, 18.80.

4.5.2.4 6-Amino-5-[(*E*)-3-(3-chloro-phenyl)-prop-2-en-(*E*)-ylideneamino]-1,3-dimethyl-1H-pyrimidine-2,4-dione (9d)

Compound **9d** was prepared from 1,3-dimethyl-5,6-diaminouracil (**8**) and *trans*-3-chlorocinnamaldehyde in a yield of 59.9%. $C_{15}H_{15}ClN_4O_2$; **mp:** 222 °C (DMF/H_2O); **^{1}H NMR** (600 MHz, DMSO-d_6) δ_H: 9.44-9.42 (d, 1H, J = 8.76 Hz), 7.61-7.49 (m, 2H), 7.42-7.28 (m, 4H), 7.10-7.02 (dd, 1H, J = 8.79, 16.13 Hz), 6.98-6.92 (d, 1H, J = 16.18 Hz), 3.40-3.36 (s, 3H), 3.19-3.14 (s, 3H); **^{13}C NMR** (150 MHz, DMSO-d_6) δ_C: 157.20 (C), 154.00 (C), 151.10 (CH), 150.09 (C), 139.50 (C), 135.00 (C), 134.10 (CH), 133.70 (CH), 131.10 (CH), 128.10 (CH), 125.75 (CH), 100.00 (CH), 30.90 (CH_3), 27.80 (CH_3); **MS** (EI, 70 eV) m/z: 318 (M^+); **IR** (KBr) ν_{max}: 3411, 3323, 3125, 3054, 3029, 1684, 1611, 1559, 1509, 1438, 1280, 1218, 1165, 1068, 898, 871, 791, 749, 702 cm^{-1}; Anal. calcd for $C_{15}H_{15}ClN_4O_2$: C, 56.52; H, 4.74; N, 17.58. Found: C, 56.20; H, 4.40; N, 17.90.

4.5.2.5 1,3-Dimethyl-6-phenyl-1H-pteridine-2,4-dione (10a)

Compound **10a** was prepared from 6-amino-1,3-dimethyl-5-{[1-phenylmeth-(*E*)-ylidene]-amino}-1H-pyrimidine-2,4-dione (**9a**) and triethyl orthoformate in a yield of 29.3%. $C_{14}H_{12}N_4O_2$; **mp:** 258 °C (DMF); **^{1}H NMR** (600 MHz, DMSO- d_6) δ_H: 8.16-8.12 (m, 1H), 7.53-7.50 (m, 2H), 7.50-7.48 (m, 2H), 7.48-7.45 (m, 1H), 3.52-3.50 (s, 3H), 3.28-3.26 (s, 3H); **^{13}C NMR** (150 MHz, DMSO- d_6) δ_C: 155.00 (2 x C), 151.80 (CH), 150.10 (C), 148.90 (C), 142.00 (2 x C), 130.10 (CH), 129.25 (2 x CH), 127.00 (2 x CH), 30.10 (CH_3), 28.20 (CH_3); **MS** (EI, 70 eV) m/z: 268 (M^+); **IR** (KBr) ν_{max}: 3165, 1697, 1659, 1561, 1525, 1472, 1356, 1298, 1229, 1060, 786, 758, 746, 707 cm^{-1}; Anal. calcd for $C_{14}H_{12}N_4O_2$: C, 62.68; H, 4.51; N, 20.88. Found: C, 62.00; H, 4.70; N, 20.30.

4.5.2.6 6-(3-Chlorophenyl)-1,3-dimethyl-1H-pteridine-2,4-dione (10b)

Compound **10b** was prepared from 6-amino-5-{[1-(3-chlorophenyl)-meth-(*E*)-ylidene]-amino}-1,3-dimethyl-1H-pyridine-2,4-dione (**9b**) and triethyl orthoformate in a yield of 27.1%. $C_{14}H_{11}ClN_4O_2$; **mp:** 233-236 °C (DMF); **^{1}H NMR** (600 MHz, $CDCl_3$) δ_H: 9.06-9.04 (s, 1H), 8.11-8.09 (s, 1H), 7.99-7.95 (m, 1H), 7.48-7.45 (m, 2H), 3.79-3.72 (s, 3H),

3.60-3.55 (s, 3H); **^{13}C NMR** (150 MHz, $CDCl_3$) δ_C: 160.00 (C), 150.02 (C), 147.00 (C, CH), 144.90 (C), 136.30 (C), 135.10 (C), 130.02 (CH), 130.00 (CH), 127.00 (CH), 126.80 (CH), 125.00 (C), 29.22 (CH_3), 29.00 (CH_3); **MS** (EI, 70 eV) m/z: 302 (M^+); **IR** (KBr) ν_{max}: 3066, 1717, 1669, 1545, 1505, 1424, 1336, 1218, 1105, 1010, 908, 794, 750, 739, 687 cm^{-1}; Anal. calcd for $C_{14}H_{11}ClN_4O_2$: C, 55.55; H, 3.66; N, 18.51. Found: C, 56.20; H, 3.60; N, 18.60.

4.5.2.7 6-[(*E*)-2-(3-Chlorostyryl)]-1,3-dimethyl-1H-pteridine-2,4-dione (10d)

Compound **10d** was prepared from 6-amino-5-[(*E*)-3-(3-chlorophenyl)-prop-2-en-(*E*)-ylideneamino]-1,3-dimethyl-1H-pyrimidine-2,4-dione (**9d**) and triethyl orthoformate in a yield of 7.2%. $C_{16}H_{13}ClN_4O_2$; **mp:** 270 °C (Acetone); **^{1}H NMR** (600 MHz, $CDCl_3$) δ_H: 8.65 (s, 1H), 7.65 (d, 1H, *J* = 15.97 Hz), 7.61-7.36 (m, 4H), 7.27 (d, 1H, *J* = 15.29 Hz), 3.70 (s, 3H), 3.50 (s, 3H); **^{13}C NMR** (150 MHz, $CDCl_3$) δ_C: 159.06 (C), 149.68 (C), 146.43 (CH), 145.14 (C), 138.23 (C), 135.57 (C), 133.78 (C), 129.84 (2 x CH), 127.51 (2 x CH), 125.63 (C), 123.49 (CH), 122.24 (CH), 29.06 (CH_3), 27.00 (CH_3); **MS** (EI, 70 eV) m/z: 328 (M^+); **IR** (KBr) ν_{max}: 3096, 3062, 2954, 1719, 1670, 1539, 1501, 1460, 1346, 1287, 1220, 1010, 889, 794, 750, 727, 681 cm^{-1}; Anal. calcd for $C_{16}H_{13}ClN_4O_2$: C, 58.46; H, 3.99; N, 17.04. Found: C, 59.80; H, 4.10; N, 16.70.

4.5.3 Biological evaluation

Approval for this study was obtained from the Ethics Committee for Research on Experimental Animals of the North-West University (Potchefstroom Campus).

4.5.3.1 MAO-B inhibition study

Mitochondria from baboon liver tissue were isolated as follows:[43] Baboon liver tissue (200 g) was grinded through a Foley mill and homogenised with a glass/teflon homogeniser in 356 mL potassium phosphate buffer (10 mM, pH 7–7.2) containing sucrose (0.25 M) and ethylenediaminetetra-acetic acid (EDTA) (0.5 mM). The homogenate was diluted to 620 mL with the above solution and centrifuged at 600 *g* for 15 minutes. The supernatant was decanted through a cheese cloth and again centrifuged at 10,400 *g* for 15 minutes. The pellet obtained was homogenised in a small volume of a potassium phosphate buffer (10 mM, pH 7–7.2) containing sucrose (0.25 M) and diluted to a final volume of 124 mL with the same buffer. The homogenate was centrifuged at

7,500 *g* for 15 minutes and the resulting pellet was homogenised in a small volume of a buffer containing tris (10 mM, pH 7–7.2) and potassium chloride (0.15 M). The homogenate was diluted to a final volume of 52 mL, centrifuged at 7,500 *g* for 15 minutes and the pellet obtained was stored at –70 °C in 300 µL aliquots. Before use, the mitochondrial isolate was suspended in 300 µL of sodium phosphate buffer (100 mM, pH 7.4) containing glycerol (50%, w/v) and the protein concentration was determined by the Bradford method[44] using bovine serum albumin as reference standard. As noted earlier, the mitochondrial fraction obtained from baboon liver tissue is devoid of MAO-A activity[27] and therefore inactivation of the enzyme with clorgyline was unnecessary. The MAO-A and –B mixed substrate MMTP (K_m = 60.9 µM for baboon liver MAO-B)[25] was used as substrate for the inhibition studies. All incubations were performed in sodium phosphate buffer (100 mM, pH 7.4) and contained MMTP (50 µM), the mitochondrial isolate (0.15 mg protein/mL), and various concentrations of the test inhibitors, producing a final incubation volume of 500 µL. Stock solutions of the test inhibitors were prepared in DMSO and added to the incubation mixtures to yield a final DMSO concentration of 4% (v/v). DMSO concentrations higher than 4% are reported to inhibit MAO-B.[45] Samples were incubated at 37 °C for 10 minutes, a time period for which dihydropyridinium metabolite formation is reported to be linear.[27] The enzyme reactions were terminated by the addition of 10 µL perchloric acid (70%) and centrifuged at 16,000*g* for 10 minutes. The supernatant fractions were removed and the concentrations of the MAO-B generated product, $MMDP^+$, were measured spectrophotometrically at 420 nm using a Shimadzu® MultiSpec-1501 spectrophotometer (ε = 25,000 M^{-1}). The IC_{50} values were determined from plots of the rate of MAO-B catalysed $MMDP^+$ formation versus the logarithm of the inhibitor concentration. For this purpose the Prism® 4.02 (GraphPad, Sorrento Valley, CA) software package was employed. At least 8 different concentrations of the test inhibitor, spanning 3 orders of magnitude were used to construct the sigmoidal dose-response curve. The IC_{50} values are reported as mean ± standard error of the mean (SEM) of duplicate determinations.

4.5.3.2 NOS inhibition study

Brain tissue (1 g/5 mL) of male Sprague-Dawley rats were homogenised in a solution consisting of 4-(2-hydroxyethyl)piperazine-1-ethanesulfonic acid (HEPES) (100 mM, pH 7.4), sucrose (320 mM), EDTA (1 mM), D/L-dithiothretiol (1 mM), leupeptin (10 µg/mL), soybean-trypsin inhibitor (10 µg/mL) and aprotinin (2 µg/mL).

After 10 seconds of homogenation at 4 °C phenylmethylsulfonyl fluoride (PMSF) (10 µM/mL) was added and the mixture was homogenised for an additional 30 seconds. Thereafter the homogenate was centrifuged at 12,000 *g* for 10 minutes. The supernatant was collected and divided into 2 mL aliquots, which were assayed immediately or snap frozen and stored at -70 °C.

Haemoglobin was converted to its oxygenated form as follows: Crystallised haemoglobin (25 mg) was dissolved in 1 mL cold HEPES buffer[46] and reduced with an excess sodium dithionate (0.958 mg). Oxygen was blown over the surface and the solution gently swirled for 15 minutes. The gradual colour change from dark red to bright red was indicative of the oxygenation of haemoglobin. Purification and desalting of the resulting oxyHb solution was performed using a Sephadex® G-25 column.

The test compounds were dissolved in DMSO to yield a concentration of 5% DMSO in the final incubation mixtures. The incubations contained HEPES (500 µM), test inhibitor, $CaCl_2$ (250 µM) and tissue homogenate (2.36 mg of the original brain tissue) and were preincubated for 3 minutes at 37 °C before the reaction was started by the addition of oxyHb (~1.09 µM), NADPH (100 µM) and $_L$-arginine (100 µM). UV-vis scans (1 scan every 10 seconds) were recorded between 390 and 430 nm for a period of 10 minutes. The metHb production was estimated by subtracting the absorbance at 411 nm from the absorbance at 401 nm. The IC_{50} values for the inhibition of NOS were determined from plots of the rate of metHb formation versus the logarithm of the inhibitor concentration. For this purpose Prism® 4.02 was used.

4.5.4 Molecular modelling

All computational studies were carried out with Discovery Studio® 1.7 (Accelrys Software Inc., San Diego, CA). The crystal structure of human MAO-B (PDB code:

2V5Z)[32] recovered from the Brookhaven Protein Database (www.rcsb.org/pdb) was applied as receptor model for the docking procedure. Manipulation of the crystal structure followed wherein the valences of the co-crystallised ligand (safinamide) and FAD cofactor were corrected and hydrogen atoms added. The receptor protein was then typed by applying the CHARMm forcefield before performing a three-step minimisation protocol (steepest descent, conjugate gradient and adopted basis Newton-Rapheson), wherein the protein backbone was kept rigid and the Generalised Born with Simple Switching implicit solvation model was used to account for the effects of the aqueous environment. Minimisation of the receptor protein was considered necessary since the protein X-ray structure might contain residual energetic tensions from the crystallisation process. The safinamide (in the A chain) was subsequently eliminated from the energy-minimised receptor protein and the backbone constraint was removed, where after it was used as the starting model for the docking simulation. The ligands to be docked were first constructed within DS Visualizer Pro® and then prepared for the docking simulations employing the Prepare Ligands application of Discovery Studio® 1.7. The structures were docked into the receptor model with the LigandFit application, which applied total ligand flexibility whereby the final ligand conformations were determined by the Monte Carlo conformation search method set to a variable number of trial runs. The docked ligand conformations were further refined using in situ ligand minimisation with the Smart Minimizer algorithm. The best solution for each docked ligand was adjudged by the DockScore scoring function of LigandFit. All the application modules within Discovery Studio® 1.7 were set to their default values and 10 docking solutions were allowed for each ligand.

Acknowledgements

The authors would like to express their gratitude towards the National Research Foundation (South Africa) for financial support.

References

1. Van der Schyf, C.J.; Geldenhuys, W.J.; Youdim, M.B.H. *J. Neurochem.* **2006**, *99*, 1033.
2. Jellinger, K.A. *J. Neural Transm. (Suppl.)* **2003**, *65*, 101.
3. Smid, P.; Coolen, H.K.A.C.; Keizer, H.G.; Van Hes, R.; De Moes, J.-P.; Den Hartog, A.P.; Stork, B.; Plekkenpol, R.H.; Niemann, L.C.; Stroomer, C.N.J.; Tulp, M.T.M.; Van Stuivenberg, H.H.; McCreary, A.C.; Hesselink, M.B.; Herremans, A.H.J.; Kruse, C.G. *J. Med. Chem.* **2005**, *48*, 6855.
4. Saura, J.; Bleuel, Z.; Ulrich, J.; Mendelowitsch, A.; Chen, K.; Shih, J.C.; Malherbe, P.; Da Prada, M.; Richards, J.G. *Neurosci.* **1996**, *70*, 755.
5. Fowler, C.J.; Wiberg, A.; Oreland, L.; Marcusson, J.; Winblad, B. *J. Neural Transm. (Gen. Sect.)* **1980**, *49*, 1.
6. Maimone, D.; Dominici, R.; Grimaldi, L.M.E. *Eur. J. Pharmacol.* **2001**, *413*, 11.
7. Saura, J.; Luque, J.M.; Cesura, A.M.; Da Prada, M.; Chan-Palay, V.; Huber, G.; Loffler, J.; Richards, J.G. *Neuroscience* **1994**, *62*, 15.
8. Palmer, R.M.J.; Ferrige, A.G.; Moncada, S. *Nature* **1987**, *327*, 524.
9. Moncada, S.; Palmer, R.M.J.; Higgs, E.A. *Biochem. Pharmacol.* **1989**, *38*, 1709.
10. Hibbs, J.B., Jr.; Vavrin, Z.; Taintor, R.R. *J. Immunol.* **1987**, *138*, 550.
11. Garthwaite, J. In *Nitric Oxide from L-Arginine: A Bioregulatory System*; Moncada, S., Higgs, E.A., Eds.; Elsevier: Amsterdam, 1990; pp 115-137.
12. Burnett, A.L.; Lowenstein, C.J.; Bredt, D.S.; Chang, T.S.K.; Snyder, S.H. *Science* **1992**, *257*, 401.
13. Cheshire, D.R. *IDrugs* **2001**, *4*, 795.
14. Endres, M.; Laufs, U.; Liao, J.K.; Moskowitz, M.A. *Trends Neurosci.* **2004**, *27*, 283.

15. Togo, T.; Katsuse, O.; Iseki, E. *Neurol. Res.* **2004**, *26*, 563.

16. Dawson, V.; Dawson, T.; Bartley, D.; Uhl, G.; Snyder, S. *J. Neurosci.* **1993**, *13*, 2651.

17. Dawson, V.L.; Dawson, T.M. *J. Chem. Neuroanat.* **1996**, *10*, 179.

18. Chen, J.-F.; Xu, K.; Petzer, J.P.; Staal, R.; Xu, Y.-H.; Beilstein, M.; Sonsalla, P.K.; Castagnoli, K.; Castagnoli, N., Jr.; Schwarzschild, M.A. *J. Neurosci.* **2001**, *21*, 143.

19. Petzer, J.P.; Steyn, S.; Castagnoli, K.P.; Chen, J.-F.; Schwarzschild, M.A.; Van der Schyf, C.J.; Castagnoli, N., Jr. *Bioorg. Med. Chem.* **2003**, *11*, 1299.

20. Chen, J.-F.; Steyn, S.; Staal, R.; Petzer, J.P.; Xu, K.; Van der Schyf, C.J.; Castagnoli, K.; Sonsalla, P.K.; Castagnoli, N., Jr.; Schwarzschild, M.A. *J. Biol. Chem.* **2002**, *277*, 36040.

21. Vlok, N.; Malan, S.F.; Castagnoli, N., Jr.; Bergh, J.J.; Petzer, J.P. *Bioorg. Med. Chem.* **2006**, *14*, 3512.

22. Crane, B.R.; Arvai, A.S.; Ghosh, D.K.; Wu, C.; Getzoff, E.D.; Stuehr, D.J.; Tainer, J.A. *Science* **1998**, *279*, 2121.

23. Raman, C.S.; Li, H.; Martásek, P.; Král, V.; Masters, B.S.S.; Poulos, T.L. *Cell* **1998**, *95*, 939.

24. Mayer, B.; Werner, E.R. *Naunyn-Schmiedeberg's Arch. Pharmacol.* **1995**, *351*, 453.

25. Werner, E.R.; Pitters, E.; Schmidt, K.; Wachter, H.; Werner-Felmayer, G.; Mayer, B. *Biochem J.* **1996**, *320*, 193.

26. Yoneda, F.; Higuchi, M. *J. Chem. Soc., Perkin Trans. 1* **1977**, *11*, 1336.

27. Inoue, H.; Castagnoli, K.; Van der Schyf, C.; Mabic, S.; Igarashi, K.; Castagnoli, N., Jr. *J. Pharmacol. Exp. Ther.* **1999**, *291*, 856.

28. Cheng, Y.C.; Prusoff, W.H. *Biochem. Pharmacol.* **1973**, *22*, 3099.

29. Salter, M.; Knowles, R.G. In *Nitric Oxide Protocols*; Titheradge, M.A., Ed.; Humana Press: Totowa, NJ, 1998; pp 61-65.

30. Salter, M.; Knowles, R.G.; Moncada, S. *FEBS lett.* **1991**, *291*, 145.

31. Joubert, J.; Van Dyk, S.; Malan, S.F. *Bioorg. Med. Chem.* **2008**, *16*, 8952.

32. Binda, C.; Wang, J.; Pisani, L.; Caccia, C.; Carotti, A.; Salvati, P.; Edmondson, D.E.; Mattevi, A. *J. Med. Chem.* **2007**, *50*, 5848.

33. Binda, C.; Li, M.; Hubálek, F.; Restelli, N.; Edmondson, D. E.; Mattevi, A. *Proc. Natl. Acad. Sci. U. S. A.* **2003,** *100*, 9750.

34. Boström, J.; Greenwood, J.R.; Gottfries, J. *J. Mol. Graph. Model.* **2003**, *21*, 449.

35. Pretorius, J.; Malan, S.F.; Castagnoli, N., Jr.; Bergh, J.J.; Petzer, J.P. *Bioorg. Med. Chem.* **2008**, *16*, 8676.

36. Morphy, R.; Rankovic, Z. *J. Med. Chem.* **2005**, *48*, 6523.

37. Youdim, M.B.H.; Buccafusco, J.J. *J. Neural Transm.* **2005a**, *112*, 519.

38. Van den Berg, D.; Zoellner, K.R.; Ogunrombi, M.O.; Malan, S.F.; Terre'Blanche, G.; Castagnoli, N., Jr.; Bergh, J.J.; Petzer, J.P. *Bioorg. Med. Chem.* **2007**, *15*, 3692.

39. Pitts, S.M.; Markey, S.P.; Murphy, D.L.; Weisz, A. In *MPTP: A Neurotoxin Producing a Parkinsonian Syndrome*; Markey, S.P., Castagnoli, N. Jr., Trevor, A.J., Kopin, I.J., Eds.; Academic Press: New York, 1986; pp 703-716.

40. Blicke, F.F.; Godt, H.C. *J. Am. Chem. Soc.* **1954**, *76*, 2798.

41. Baker, B.R.; Janson, E.E.; Vermeulen, N.M.J. *J. Med. Chem.* **1969**, *12*, 898.

42. Bissel, P.; Bigley, M.C.; Castagnoli, K.; Castagnoli, N., Jr. *Bioorg. Med. Chem.* **2002**, *10*, 3031.

43. Salach, J.I.; Weyler, W. *Methods Enzymol.* **1987**, *142*, 627.

44. Bradford, M.M. *Anal.Biochem.* **1976**, *72*, 248.

45. Gnerre, C.; Catto, M.; Leonetti, F.; Weber, P.; Carrupt, P.-A.; Altomare, C.; Carotti, A.; Testa, B. *J. Med. Chem.* **2000**, *43*, 4747.

46. Corbett, J.A.; McDaniel, M.L. *Methods* **1996**, *10*, 21.

CHAPTER 5
ARTICLE 2 - EUROPEAN JOURNAL OF MEDICINAL CHEMISTRY

Article published online on 31 July 2010.

European Journal of Medicinal Chemistry DOI: 10.1016/j.ejmech.2010.07.005.

Inhibition of Monoamine Oxidase by Indole and Benzofuran Derivatives

Louis H.A. Prins, Jacobus P. Petzer, and Sarel F. Malan*

Pharmaceutical Chemistry, School of Pharmacy, North-West University, Private Bag X6001, Potchefstroom, 2520, South Africa.

* Corresponding author at present address. School of Pharmacy, University of the Western Cape, Private Bag X17, Bellville, 7535, South Africa. Tel: +27-21-9593190; fax: +27-21-9591588.
E-mail address: sfmalan@uwc.ac.za

Graphical abstract

A series of indole and benzofuran derivatives were synthesised and evaluated for their ability to inhibit monoamine oxidase (MAO) A and B.

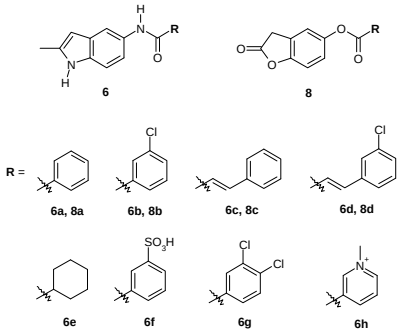

Inhibition of Monoamine Oxidase by Indole and Benzofuran Derivatives

Louis H.A. Prins, Jacobus P. Petzer, and Sarel F. Malan*

Pharmaceutical Chemistry, School of Pharmacy, North-West University, Private Bag X6001, Potchefstroom, 2520, South Africa.

* Corresponding author at present address. School of Pharmacy, University of the Western Cape, Private Bag X17, Bellville, 7535, South Africa. Tel: +27-21-9593190; fax: +27-21-9591588.
E-mail address: sfmalan@uwc.ac.za

Abstract

Monoamine oxidase (MAO) is an important drug target for the treatment of neurological disorders. A series of indole and benzofuran derivatives were synthesised and evaluated as inhibitors of the two MAO isoforms, MAO-A and MAO-B. In general, the derivatives were found to be selective MAO-B inhibitors with K_i values in the nanomolar (nM) to micromolar (μM) concentration range. The most potent MAO-B inhibitor, 3,4-dichloro-N-(2-methyl-1H-indol-5-yl)benzamide, exhibited a K_i value of 0.03 μM and was 99 fold more selective for the B isoform. We conclude that these indole and benzofuran derivatives are promising reversible MAO-B inhibitors with a possible role in the treatment of neurodegenerative diseases such as Parkinson's disease (PD).

Keywords: Monoamine oxidase (MAO); Indole derivatives; Benzofuran derivatives; Parkinson's disease (PD); Molecular docking; LigandFit

5.1 Introduction

Parkinson's disease (PD) is a condition associated with the degeneration of the dopamine containing nigrostriatal neurons [1]. The resulting depletion of striatal dopamine is responsible for the characteristic PD symptoms such as bradykinesia (slowness of movement), rigidity (stiffness), hypokinesia (reduction in movement amplitude), akinesia (absence of normal unconscious movements) and other extrapyramidal effects. Since monoamine oxidase A and B (MAO-A and –B) are involved in the metabolic degradation of dopamine in the brain, inhibitors of these enzymes are considered useful for the treatment of PD [2].

The MAO isoform predominantly found in the human brain is MAO-B [3]. It has also been demonstrated that brain MAO-B activity, but not MAO-A activity, increases with aging [4]. As MAO-B appears to be located in glial cells [5], this may be due to gliosis associated with aging. Not only is MAO-B a major dopamine metabolising enzyme but it is also involved in the formation of free radicals and other potentially neurotoxic species. In the catalytic cycle of MAO-B, one mole of hydrogen peroxide (H_2O_2) and dopaldehyde is produced for every mole of dopamine metabolised [6]. Both these metabolic by-products are toxic and may contribute to the pathogenesis of PD [7]. Increased MAO-B levels have also been observed in plaque-associated astrocytes in the brains of Alzheimer's disease (AD) patients. This increase in MAO-B activity produces an elevation in hydroxyl radicals ($^{\bullet}OH$), which has been correlated with amyloid-β (Aβ) plaque formation. Hence, the therapeutic potential of selective reversible MAO-B inhibitors does not rely solely on their ability to increase the biological half–life of dopamine (symptomatic effects) but also on their ability to potentially slow PD progression (neuroprotective effects) and to inhibit Aβ plaque formation. [4]

(*R*)-Deprenyl (selegiline) (**1**) (Figure 1) was one of the first selective MAO-B inhibitors to be identified [8] and has since been shown to possess neuroprotective properties [9,10]. These properties may, in part, be dependent on the ability of (*R*)-deprenyl to inhibit the MAO-B catalysed formation of H_2O_2 and dopaldehyde in the brain [11]. In 1981 it was found that an *N*-demethylated aminoindan propargylamine derivative, AGN 1135, also was a potent and selective inhibitor of MAO-B [12]. Unlike (*R*)-deprenyl, this

compound is not an amphetamine derivative and therefore did not present with amphetamine associated sympathomimetic side-effects. The *R*(+)-enantiomer of AGN 1135, now called rasagiline (**2**), is nearly three orders of a magnitude more potent than the *S*(-)-enantiomer in inhibiting MAO-B [13]. Rasagiline is considered useful as an adjuvant to levodopa for the treatment of PD, as this compound enhances dopamine levels in the primate brain following systemic administration of levodopa. Youdim and co-workers [14] showed that rasagiline also activates enzymes that play a key role in cellular events including mitochondrial viability, modulation of apoptotic processes and neuronal plasticity. These effects may further contribute to the observed protective effects of rasagiline.

Irreversible inhibition of MAO, however, have certain disadvantages including the fact that enzyme recovery requires the synthesis of new enzyme, the possible loss of selectivity as a result of repeated administration and an inhibition that is not affected by changes in substrate concentration [15]. The rate of enzyme biosynthesis, and hence recovery from irreversible inhibition is relatively slow and differs substantially between tissues and species. For example, a study by Fowler and co-workers [16] showed that the turnover rate for the synthesis of MAO-B in the human brain is close to 40 days. This was done by measuring the half-time for brain MAO-B synthesis in PD and in normal subjects after withdrawal from (*R*)-deprenyl. Reversible inhibition may be of a competitive, mixed, non-competitive or uncompetitive nature and possess the following advantages: the enzyme recovers as the inhibitor is eliminated from the tissues, the risk of loss of selectivity is far less because of a shorter duration of action and, in the case of competitive reversible inhibition, the inhibition is relieved when the substrate concentration is increased [15].

From the above discussion it is clear that the MAO-B inhibitors, (*R*)-deprenyl (**1**) and rasagiline (**2**), have an array of biological attributes that make them good candidates for the treatment and possible prevention of neurodegenerative disorders. Both of these are however irreversible MAO-B inhibitors, which is undesirable and current focus has however shifted to the development of selective reversible MAO-B inhibitors [17-19].

Several previous studies [20-22] have indicated that the indole nucleus (**3**) may be useful as a scaffold for the design of MAO inhibitors. For example, a variety of indolylmethylamine derivatives have been shown to act as irreversible MAO inhibitors [23]. Of importance is the observation that bulky C5 substituents generally increase potency and selectivity for the MAO-B isoform. An example of such a substituent is the benzyloxy moiety (for example structure **4**) which is thought to enhance the selectivity towards MAO-B by increasing the molecular lipophilicity [24]. In the present study, we evaluated the possibility that the indole nucleus may be used in the design of reversible MAO inhibitors by synthesising a series of indole (**6a**–**d**) and structurally related benzofuran (**8a**–**d**) derivatives and evaluating them as inhibitors of recombinant human MAO-A and –B (Scheme 1). As shown in scheme 1, the indole and benzofuran derivatives were substituted with a variety of C5 side chains. Based on the results of this study, a second series of indole derivatives (**6e**–**h**), which are structural analogues of compound **6b**, were synthesised and evaluated as MAO-A and –B inhibitors.

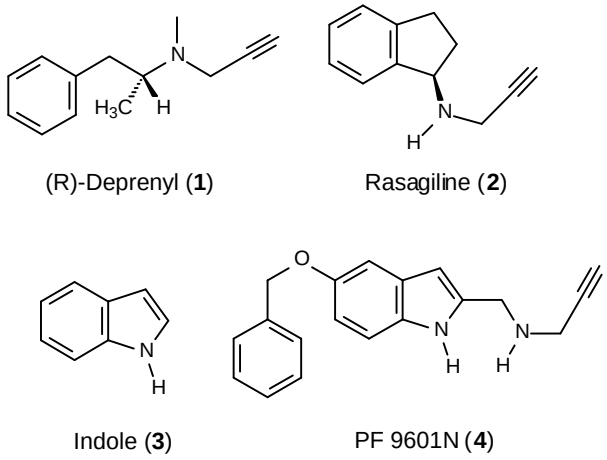

Figure 1. Chemical structures of (*R*)-deprenyl (**1**), rasagiline (**2**), indole (**3**) and PF 9601N (**4**).

5.2 Results and discussion

5.2.1 Chemistry

The indole derivatives **6a**–**d**, **6f** and **6h** were synthesised by reacting 5-amino-2-methylindole (**5**) with the appropriate carboxylic acid in the presence of *N*-(3-

dimethylaminopropyl)-*N′*-ethylcarbodiimide (EDC) as dehydrating agent [25-27]. For the synthesis of compounds **6e** and **6g** a similar procedure was followed, but in this instance *N*,*N′*-dicyclohexylcarbodiimide (DCC) was employed as dehydrating agent. The benzofuran derivatives (**8a**–**d**) were prepared according to the procedure reported by Scriven and co-workers [28] by reacting 5-hydroxy-3H-benzofuran-2-one (**7**) with the appropriate carboxylic acid in the presence of DCC to yield the esters (Scheme 1). The structures of the target compounds were confirmed by ^{1}H NMR, ^{13}C NMR, HRMS and IR while the purity was evaluated by HPLC analysis.

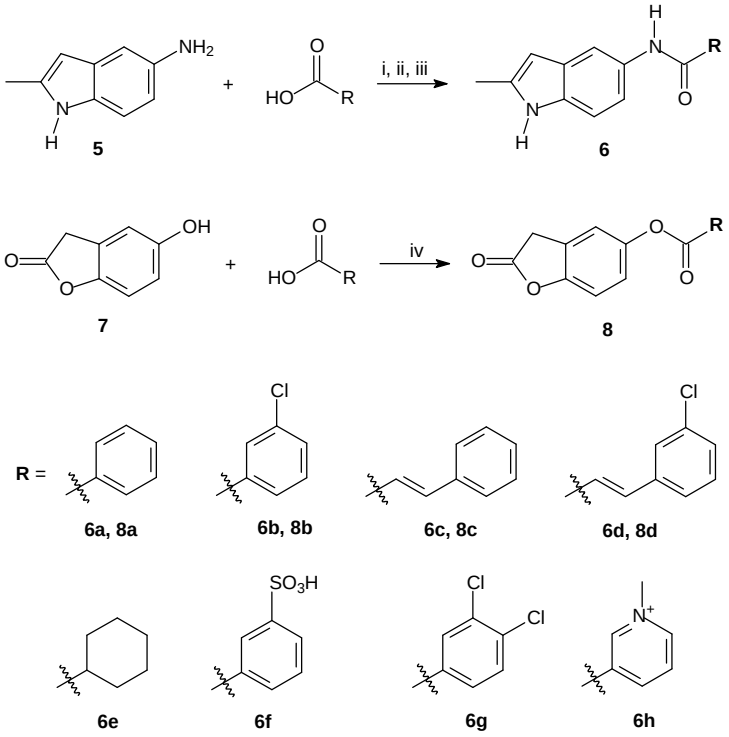

Scheme 1. Synthetic pathways to the indole (**6a**–**h**) and benzofuran (**8a**–**d**) derivatives: (i) EDC, dioxane/H_2O (**6a**–**d**); (ii) DCC, CH_2Cl_2 (**6e**, **6g**); (iii) EDC, MeOH (**6f**, **6h**) (iv) DCC, DMAP, CH_2Cl_2.

5.2.2 Enzyme inhibition studies

The MAO-A and –B activity measurements were based on the degree to which the MAO-A/B non-selective substrate, kynuramine (K_m = 16.1 µM and 22.67 µM for human recombinant MAO-A and –B, respectively), is oxidised by recombinant human MAO-A

and –B to yield 4-hydroxyquinoline [29]. Kynuramine is non-fluorescent until undergoing oxidative deamination by MAO to produce the fluorescent metabolite 4-hydroxyquinoline (λ_{Ex} = 310 nm, λ_{Em} = 400 nm). Quantification of product formation was achieved by comparing the fluorescence emission of the samples to that of known amounts of authentic 4-hydroxyquinoline [29]. The IC_{50} values (concentration of the inhibitor that inhibits 50% of the enzyme activity) for the test compounds were determined by measuring the extent by which different concentrations of a test inhibitor slow the rate of the MAO catalysed deamination of kynuramine (Figure 2). To allow for the calculation of the selectivity index (SI), the K_i values for the inhibition of MAO-A and –B were estimated from the experimentally determined IC_{50} values according to the Cheng-Prusoff equation [30].

The results of the MAO inhibition studies with compounds **6a**–**d** and **8a**–**d** are presented in table 1. With the exception of **6d** and **8a** all of the derivatives were selective inhibitors of the MAO-B isozyme. Compound **8a** was essentially non-selective. Interestingly, chlorine substitution of the C5 phenyl side chain of the indoles and benzofuranes enhances both MAO-A and –B inhibition potencies since the unsubstituted homologues were less potent MAO inhibitors than the corresponding chlorine substituted compounds (for example compare **6b** with **6a**). The most potent MAO-B inhibitor was benzofuran **8d** with a K_i value of 0.19 µM. Compound **8d** was also the most potent MAO-A inhibitor of the test compounds. The most selective MAO-B inhibitor was indole **6b** with a SI of 25. Compound **6b** was also found to be a potent MAO-B inhibitor with a K_i value of 0.33 µM. Two other inhibitors, **8b** and **8c**, also exhibited MAO-B inhibition potencies in the submicroMolar range. Compared to indole **6b**, the other potent MAO-B inhibitors of the series, benzofuranes **8b**–**d**, displayed relatively low selectivity for MAO-B (5–6 fold). Based on high inhibition potency and MAO-B selectivity as selection criteria, **6b** was considered a promising lead compound for the development of further reversible MAO-B inhibitors.

In the second series, four structural derivatives (**6e**–**h**) of **6b** were synthesised and evaluated as inhibitors of recombinant human MAO-A and –B. The results of the MAO inhibition studies with compounds **6e**–**h** are presented in table 1. Compound **6g** was found to be the most potent MAO-B inhibitor with a K_i value of 0.03 µM. Compound **6g**

was also the most selective MAO-B inhibitor with a SI of 99. Since **6g** is the most potent and selective MAO-B inhibitor identified in this study, it can be concluded that the addition of an additional chlorine substituent to the phenyl ring at C5 of the indole ring is a suitable strategy to enhance binding affinity to the MAO-B active site. As mentioned above, chlorine substitution at the phenyl ring of the C5 side chain in general appears to enhance MAO-B inhibition activity of both the indoles and benzofuranes. By employing molecular docking studies, possible reasons for this observation are discussed in the next section. Interestingly, **6h** was found to inhibit MAO-A selectively (7 fold). This is in agreement with literature reports that positively charged structures, such as methylene blue, display affinity for the MAO-A active site [31,32]. The observation that **6e** is a relatively weaker MAO-B inhibitor than **6a** indicates that phenyl substitution is more favourable for MAO-B inhibition than cyclohexyl substitution. Also, the weak inhibition of both MAO-A and –B by the sulfonyl substituted homologue **6f** supports the proposal that side chains with a relatively high degree of lipophilicity generally enhances affinity of inhibitors for the MAO-A and –B active sites [33,34].

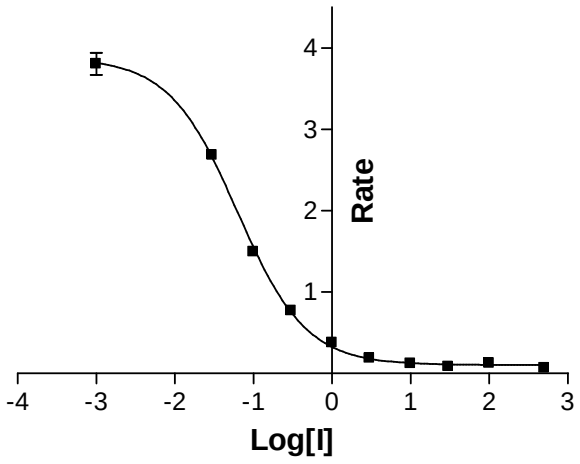

Figure 2. Sigmoidal dose-response curve of the rate of MAO-B catalysed 4-hydroxyquinoline formation versus the logarithm of concentration of inhibitor **6g** (expressed in nM). Rates are expressed as nmol 4-hydroxyquinoline formed/mg protein/min. All determinations were performed in duplicate and are expressed as mean ± SEM.

Table 1: MAO inhibition by the indole (**6a**–**h**) and benzofuran (**8a**–**d**) derivatives.

Compound	MAO-A Inhibition		MAO-B Inhibition		SI[c]
	IC_{50} (µM)	K_i (µM)[a]	IC_{50} (µM)	K_i (µM)[b]	
6a	149.71 ± 4.10	39.45	3.84 ± 0.75	1.65	24
6b	31.04 ± 0.11	8.18	0.76 ± 0.17	0.33	25
6c	662.71 ± 65.27	174.63	18.82 ± 3.28	8.01	22
6d	7.67 ± 0.55	2.02	9.83 ± 1.63	4.23	0.5
6e	69.42 ± 2.01	18.29	6.96 ± 0.09	3.0	6
6f	259.07 ± 8.27	68.27	175.94 ± 11.51	75.72	0.9
6g	9.79 ± 1.26	2.58	0.06 ± 0.01	0.03	99
6h	20.76 ± 0.4	5.47	92.62 ± 1.87	39.86	0.1
8a	11.57 ± 0.32	3.05	8.89 ± 0.99	3.83	0.8
8b	7.66 ± 0.63	2.02	0.99 ± 0.1	0.43	5
8c	12.5 ± 0.18	3.29	1.2 ± 0.17	0.52	6
8d	3.9 ± 0.36	1.03	0.44 ± 0.03	0.19	5

[a] The experimentally determined IC_{50} values were used to calculate the K_i values according to the equation by Cheng and Prusoff: $K_i = IC_{50}/(1 + [S]/K_m)$ with [S] = 45 µM and K_m (Kynuramine) = 16.1 µM [30].

[b] The experimentally determined IC_{50} values were used to calculate the K_i values according to the equation by Cheng and Prusoff: $K_i = IC_{50}/(1 + [S]/K_m)$ with [S] = 30 µM and K_m (Kynuramine) = 22.67 µM [30].

[c] Relative selectivity for MAO-B is defined by the ratio of K_i(MAO-A) / K_i(MAO-B) for each compound.

5.2.3 Reversibility of inhibition

Another goal of the present study was to determine if the indole and benzofuran derivatives investigated here act as reversible or irreversible enzyme inhibitors. Since the most active derivatives are MAO-B inhibitors with only moderate to weak MAO-A inhibition potencies, the time dependence of MAO-B inhibition was investigated with two potent derivatives, indole **6g** and benzofuran **8b**. Recombinant human MAO-B was preincubated with **6g** and **8b** for various periods of time (0–60 min). For this purpose the concentrations of the inhibitors were equal to 2 fold their respective IC_{50} values for the inhibition of MAO-B. The residual MAO-B activity was subsequently determined. As shown in figure 3, no time-dependent reduction in the rate of MAO-B catalysed oxidation of kynuramine is observed with both **6g** and **8b**. This indicated that the inhibition is reversible, at least for the time period (60 min) evaluated. Curiously, a marked increase of the MAO-B catalytic rate with increased preincubation time is observed for **8b**. One possible explanation for this observation is that **8b**, and probably the other benzofuran derivatives, is unstable in the potassium phosphate buffer used for the enzymatic reactions. The possibility exists that hydrolysis of the lactone and/or ester functional group may occur with the resulting loss of inhibition potential. Further studies are underway to investigate this observation.

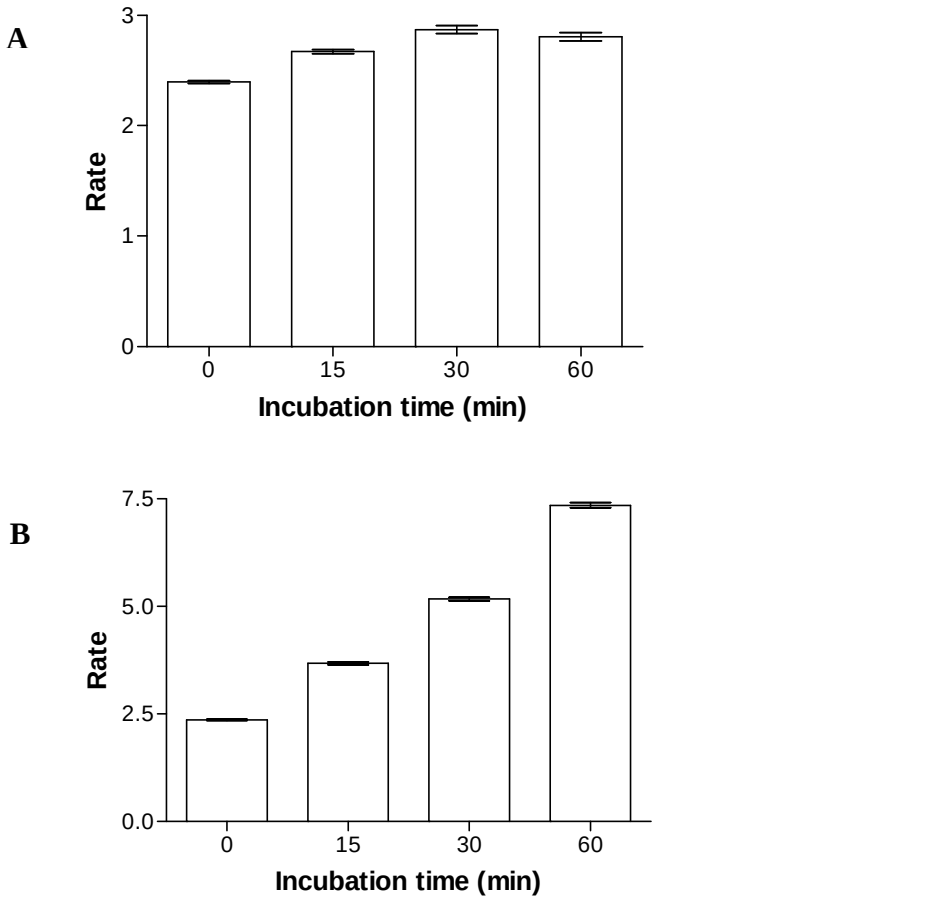

Figure 3. The time-dependence of the inhibition of the recombinant human MAO-B by **6g** (panel A) and **8b** (panel B). MAO-B was preincubated for different periods of time (0–60 min) with the inhibitors and the initial rates (nmoles 4-hydroxyquinoline formed/min/mg protein) were recorded.

To determine the mode of inhibition, sets of Lineweaver–Burk plots were constructed for the inhibition of MAO-B by **6g**. As shown in figure 4 the linear Lineweaver–Burk plots intersect on the y-axis for **6g,** which indicates that the mode of inhibition is competitive and therefore reversible.

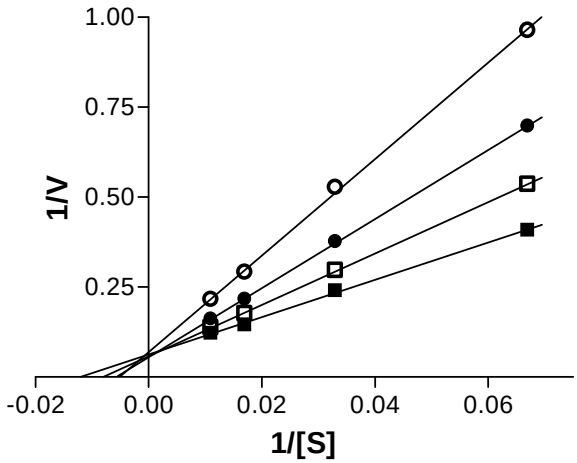

Figure 4. Lineweaver-Burk plots of the inhibition of recombinant human MAO-B by **6g**. The lines were constructed in the absence (open squares) and presence of 0.015 µM (filled squares), 0.03 µM (open circles) and 0.06 µM (filled circles) of **6g**. The rate (V) is expressed as nmol 4-hydroxyquinoline formed/min/mg protein.

5.2.4 Docking studies

While the indole and benzofuran derivatives investigated here were relatively weak MAO-A inhibitors, several derivatives were found to be potent inhibitors of MAO-B. Of these, compound **6g**, was the most potent and selective MAO-B inhibitor. To gain insight into the possible mode of binding of **6g** in the active site of MAO-B, molecular docking studies were performed. The most potent benzofuran derivative, **8d**, was also included in the docking study. For this purpose, the LigandFit application within Discovery Studio® 1.7 was used. The crystallographic structure of human recombinant MAO-B in complex with safinamide (PDB code: 2V5Z) [35], was selected as receptor model. The valences of the FAD co-factor and the co-crystallised ligand were corrected and the model was subjected to a three-step energy minimisation cascade while the protein backbone was constrained. Minimisation of the receptor proteins were considered necessary since the protein X-ray structure might contain residual energetic tensions from the crystallisation process. Following the energy minimisation cascade, the backbone constraint was removed and the co-crystallised ligand was deleted. With the exception of three highly conserved water molecules in the active site, all crystallographic waters were deleted from the protein model [35]. The structures of **6g** and **8d** were built, geometry optimised

within Discovery Studio and docked into the protein model with LigandFit. Following the docking, the orientations and conformations of the docked ligands were further refined with the Smart Minimizer algorithm in Discovery Studio. Ten possible binding orientations were computed. To determine the accuracy of this docking protocol, the co-crystallised ligand, safinamide, was redocked into the MAO-B active site. This procedure was repeated three times and the best ranked solutions of safinamide exhibited an RMSD value of 1.54 Å from the position of the co-crystallised ligand. Since RMSD values smaller than 2.0 Å generally indicate that the docking protocol is capable of accurately predicting the binding orientation of the co-crystallised ligand [36], this protocol was therefore deemed to be suitable for the docking of inhibitors into the active site of MAO-B. The docking solutions were ranked according to their respective DockScore values.

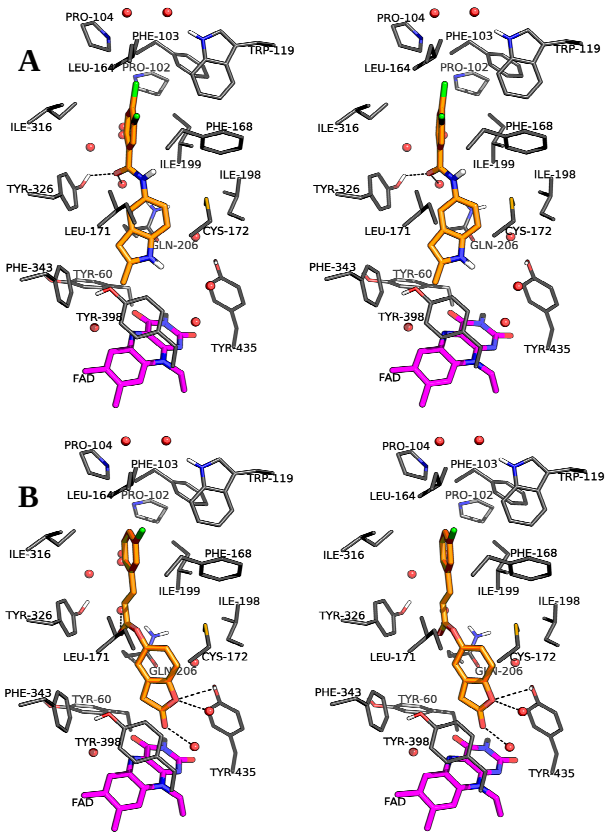

Figure 5. Stereo view of the predicted binding modes of **6g** (Panel A) and **8d** (Panel B) in the human MAO-B active site. Hydrogens are hidden, except those involved in hydrogen bonds, and selected amino acid residues are displayed in grey. The FAD co-factor is displayed in magenta and hydrogen bonds shown as black dashes.

Examination of the best-ranked docking solution for **6g**, reveals that the relatively polar indole nucleus is located in the substrate cavity, in the vicinity of the FAD co-factor, with the C5 side chain extending towards the entrance cavity space of MAO-B (Figure 5a). This binding orientation is similar to that observed for the co-crystallised ligand, safinamide, which also traverses both active site cavities [35]. The polar propanamidyl moiety of safinamide is also located in the substrate cavity while the apolar 3-fluorobenzyloxy side chain is stabilised within the entrance cavity space. As shown in figure 5a, the 3,4-dichlorophenyl moiety of **6g** is possibly stabilised by Van der Waals interactions in the hydrophobic entrance cavity defined by Phe-103, Trp-119, Leu-164, Leu-167, Phe-168 and Ile-316 [29]. Since the addition of chlorine would enhance the lipophilicity of a phenyl ring, these interactions may explain the observation that chlorine substitution of the phenyl side chains of the indoles and benzofuranes enhances MAO-B inhibition potency. Of importance is the observation that the amide carbonyl oxygen of **6g** is stabilised by hydrogen bond interaction with the phenolic hydrogen of Tyr-326 [37]. In MAO-A, the residue that corresponds to Tyr-326 (in MAO-B) is Ile-335 [38]. The resulting absence of these stabilising interactions may, in part, explain the lower MAO-A inhibition potencies of this inhibitor. Other significant interactions which may stabilise the MAO-B–**6g** complex include a possible π–π interaction [38] between the indole ring and the amide functional group of the Gln-206 side chain with an interplane distance of approximately 3.5 Å and a possible hydrogen bonding between the amide carbonyl oxygen of **6g** and an active site water molecule.

The best-ranked docking solution obtained for **8d** to the MAO-B active site is similar to that observed for **6g**. The polar benzofuran ring binds within the substrate cavity where it is stabilised by hydrogen bonding between the lactam functional group of the inhibitor and the phenolic hydrogen of Tyr-435 and two active site water molecules (Figure 5b). These are the principal interactions which stabilises the benzofuran derivatives in the MAO-B active site. The C5 side chain of **8d** extends towards the entrance cavity space of MAO-B where it is stabilised by hydrophobic interactions. Similar to the analysis for **6g** above, the observation that chlorine substitution improves the MAO-B inhibition potencies of the benzofuranes (**8a**–**d**) may be due to enhancement of the lipophilicity of the C5 side chain. In contrast to the amide carbonyl of indole **6g**, the ester carbonyl

oxygen of **8d** does not interact via hydrogen bonding with Tyr-326. The reason for this is that **8d** binds deeper (than **6g**) within the MAO-B active site in order to establish hydrogen bonding with the Tyr-435 and the two active site water molecules. It can therefore be concluded that hydrogen bonding with Tyr-326 is a major factor in stabilising the MAO-B–**6g** complex while polar interactions with Tyr-435 and the waters in the vicinity of the FAD co-factor are the major factors stabilising the MAO-B–**8d** complex. This analysis may explain why **8d** also exhibits affinity for the MAO-A active site. In MAO-A, the residue that corresponds to Tyr-435 (in MAO-B) is Tyr-444 [38]. Tyr-444 and water molecules present in the vicinity of the FAD co-factor may stabilise **8d** via hydrogen bonding in the MAO-A active site (Figure 6), similar to that observed for the MAO-B active site. The proposal that benzofuran derivatives are mainly stabilised by polar interactions in the substrate cavity may also explain the relatively small difference (~2 fold) in the MAO-B inhibition potencies of **8d** and its shorter side chain length homologue, **8b**. Regardless of the difference in chain lengths, both these homologues are expected to be stabilised to the same degree in the substrate cavity of MAO-B.

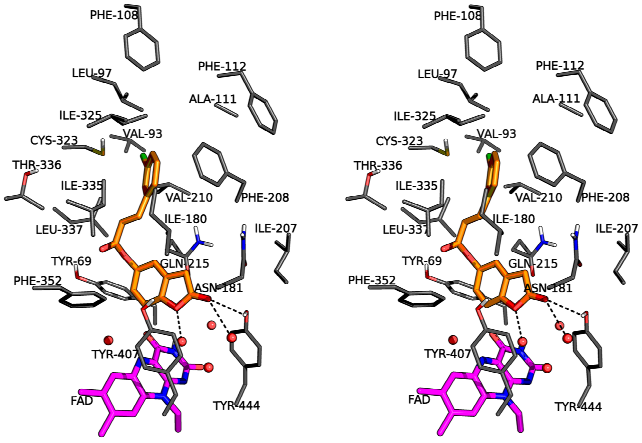

Figure 6. Stereo view of the predicted binding modes of **8d** in the human MAO-A active site. Hydrogens are hidden, except those involved in hydrogen bonds, and selected amino acid residues are displayed in grey. The FAD co-factor is displayed in magenta and hydrogen bonds shown as black dashes.

5.3 Conclusions

In the current study a series of indole and benzofuran derivatives were synthesised and evaluated as inhibitors of MAO-A and –B. In general, the derivatives were found to be selective for the MAO-B isoform with 3 benzofuranes and 2 indoles exhibiting inhibition potencies in the submicroMolar range. Indole derivative **6g** was found to be the most potent and selective MAO-B inhibitor with a K_i value of 0.03 µM and a selectivity index of 99. As suggested by the molecular docking studies, the selective binding of **6g** to MAO-B may be explained by hydrogen bond interaction between the inhibitor and the phenolic hydrogen of Tyr-326. The corresponding residue in MAO-A, Ile-335 [38], would not undergo this interaction with **6g**. The most potent MAO-B inhibitor among the benzofuran derivatives was **8d** with a K_i value of 0.19 µM and a selectivity index of 5. Molecular docking suggests that **8d** is stabilised in the MAO-B active site principally by hydrogen bonding with Tyr-435 and the waters in the vicinity of the FAD co-factor. The suggestion that similar polar interactions are possible between **8d** and the active site of MAO-A may explain the relatively low isoform selectivity of this inhibitor.

An important observation is that chlorine substitution at the C5 phenyl side chain of the indoles and benzofuranes enhances both MAO-A and –B inhibition potencies. This may be due to the enhancement of nonspecific hydrophobic interactions between the inhibitors and the active sites of the MAO isozymes. Halogen substitution of an aromatic ring may therefore be considered as a general strategy to improve the binding affinities of ligands to MAO-A and –B. An important consideration however, is that the binding of these ligands should place the halogen in the hydrophobic pockets located towards the entrance of the active site cavities of the two enzymes.

We conclude that the benzofuran nucleus, in general, is a good scaffold for designing potent, relatively non-selective MAO inhibitors and that the indole nucleus show promise as scaffold for developing potent, MAO-B selective inhibitors.

5.4 Experimental

5.4.1 General methods

Thin-layer chromatography was performed on 0.20 mm thick aluminium silica gel sheets (Alugram® SIL G/UV254, Kieselgel 60, Macherey-Nagel® Düren, Germany) with an

appropriate mobile phase and visualisation was achieved using UV light (254 and 366 nm) and iodine vapour. All melting points (mp) were obtained using a Stuart® Scientific SMP10 melting point apparatus and are uncorrected. ^{1}H and ^{13}C NMR spectra were recorded using a Bruker® Avance III 600 spectrometer at a frequency of 600 and 150 MHz, respectively. Chemical shifts are expressed in parts per million (δ) relative to the signal from tetramethylsilane (Me_4Si), added to the deuterated solvent DMSO-d_6. Spin multiplicities are given as s (singlet), d (doublet), dd (doublet of doublets) and m (multiplet). IR spectra were recorded in KBr on a Nicolet® Nexus™ 470-FT IR spectrometer over the range 400-4000 cm^{-1} employing the diffuse reflectance method. Direct insertion electron impact ionization (EIMS) and high resolution mass spectra (HRMS) were obtained on a DFS high resolution magnetic sector mass spectrometer (Thermo Electron Corporation).

HPLC analyses were performed using an Agilent® 1100 series HPLC equipped with a quaternary gradient pump, autosampler, diode array UV detector and Chemstation® data acquisition and analysis software. A Venusil XBP C18 column (4.60 × 150 mm, 5 µm) was used and elution was effected by means of a linear gradient starting at 30% acetonitrile to 85% acetonitrile after 5 min and holding at 85% acetonitrile until 10 min, where after the instrument was re-equilibrated at the starting conditions for 5 min. Standard solutions (1 mM) of each of the eight test compounds were prepared in analytical grade acetonitrile and analysed at wavelengths of 210, 254 and 300 nm over a 15 min time period. The mobile phase flow rate was 1 mL/min and the injection volume was 20 µL.

5.4.2 Synthesis

5.4.2.1 General synthetic method for indoles 6a–d

5-Amino-2-methylindole (500 mg, 3.42 mmol) and EDC hydrochloride (947 mg, 4.94 mmol) were dissolved in 20 mL dioxane/water (1:1). The appropriate benzoic acid or cinnamic acid (3.67 mmol) was added to the solution and the pH of the suspension adjusted to 5 with 2 M HCl (aq). The reaction mixture was stirred at room temperature for 2 h where after the pH was adjusted to 7 with 1 M NaOH (aq). Cooling the reaction with an external ice bath resulted in the final products (**6a-d**) precipitating from the

reaction mixture. The precipitates were collected by filtration, giving the amide products in good yield, without the need for further purification [27].

5.4.2.2 N-(2-Methyl-1H-indol-5-yl)benzamide (6a)

Yield: 230 mg (27%); R_f = 0.47 (diethyl ether); **mp:** 190–193 °C. **^{1}H NMR** [600 MHz, DMSO-d_6]: δ = 10.90 (s, 1H), 10.09 (s, 1H), 8.00 (s, 1H), 7.88 (s, 1H), 7.64–7.52 (m, 3H), 7.39–7.21 (m, 3H), 6.12 (s, 1H), 2.42 ppm (s, 3H); **^{13}C NMR** [150 MHz, DMSO-d_6]: δ = 164.0 (C), 137.0 (C), 136.0 (C), 134.0 (C), 131.6 (CH), 131.0 (C), 128.0 (3 x CH), 127.5 (C, CH), 115.0 (CH), 112.0 (CH), 110.0 (CH), 99.3 (CH), 13.5 ppm (CH_3); **IR** (KBr): ν_{max} = 3378, 3285, 2924, 2851, 1653, 1578, 1385, 912, 892, 856, 840, 797, 747, 713, 690 cm^{-1}. Compound purity (HPLC): 98.3%. EIMS m/z 250 ($M^{\bullet+}$); HRMS calcd. 250.1106, found 250.1102.

5.4.2.3 3-Chloro-N-(2-methyl-1H-indol-5-yl)benzamide (6b)

Yield: 369 mg (38%); R_f = 0.62 (diethyl ether); **mp:** 178–182 °C. **^{1}H NMR** [600 MHz, DMSO-d_6]: δ = 10.86 (s, 1H), 10.13 (s, 1H), 8.01–8.00 (m, 1H), 7.94–7.90 (m, 1H), 7.82 (s, 1H), 7.66–7.61 (m, 1H), 7.58–7.52 (m, 1H), 7.32–7.26 (m, 1H), 7.24–7.19 (m, 1H), 6.10 (s, 1H), 2.36 ppm (s, 3H); **^{13}C NMR** [150 MHz, DMSO-d_6]: δ = 163.5 (C), 137.5 (C), 136.3 (CH), 133.3 (CH), 133.2 (CH), 131.0 (C), 130.5 (C), 130.3 (C), 128.4 (C), 127.3 (C), 126.3 (CH), 114.9 (CH), 111.5 (CH), 110.1 (CH), 99.3 (CH), 13.5 ppm (CH_3); **IR** (KBr): ν_{max} = 3377, 3166, 2925, 2852, 1647, 1569, 1382, 913, 891, 869, 845, 799, 731, 675 cm^{-1}. Compound purity (HPLC): 98.6%. EIMS m/z 284 ($M^{\bullet+}$); HRMS calcd. 284.0716, found 284.0711.

5.4.2.4 (2E)-N-(2-methyl-1H-indol-5-yl)-3-phenylprop-2-enamide (6c)

Yield: 859 mg (91%); R_f = 0.49 (diethyl ether); **mp:** 198–200 °C (decomp). **^{1}H NMR** [600 MHz, DMSO-d_6]: δ = 10.88 (s, 1H), 10.02 (s, 1H), 7.90 (s, 1H), 7.70–7.60 (m, 2H), 7.57 (d, J = 15.63 Hz, 1H) 7.50–7.36 (m, 3H), 7.25 (dd, J = 7.85, 8.21 Hz, 2H), 6.91 ppm (d, J = 15.66 Hz, 1H); **^{13}C NMR** [150 MHz, DMSO-d_6]: δ = 162.9 (C), 139.0 (CH), 136.3 (C), 134.2 (C), 133.0 (C), 131.1 (C), 129.5 (CH), 129.0 (CH), 128.9 (CH), 127.5 (C, 2 x CH), 123.0 (CH), 113.5 (CH), 110.3 (CH), 109.8 (CH), 99.2 (CH), 13.4 ppm (CH_3); **IR** (KBr): ν_{max} = 3423, 3288, 3052, 2854, 1651, 1592, 1450, 992, 894, 887, 866,

811, 799, 784, 775, 748 cm^{-1}. Compound purity (HPLC): 97.6%. EIMS m/z 276 ($M^{\bullet+}$); HRMS calcd. 276.1263, found 276.1259.

5.4.2.5 (2E)-3-(3-chlorophenyl)-N-(2-methyl-1H-indol-5-yl)prop-2-enamide (6d)

Yield: 773 mg (73%); R_f = 0.51 (diethyl ether); **mp:** 155–160 °C. **^{1}H NMR** [600 MHz, DMSO-d_6]: δ = 10.86 (s, 1H), 10.00 (s, 1H), 7.90 (s, 1H), 7.70 (s, 1H), 7.63–7.57 (m, 1H), 7.54 (d, J = 16.03 Hz, 1H), 7.50–7.43 (m, 2H), 7.22 (s, 2H), 6.93 (d, J = 16.03 Hz, 1H), 6.10 (s, 1H), 2.37 ppm (s, 3H); **^{13}C NMR** [150 MHz, DMSO-d_6]: δ = 163.0 (C), 137.8 (2 x CH), 136.8 (C), 134.2 (C), 133.5 (C), 131.5 (C), 131.3 (C), 129.6 (CH), 129.0 (CH), 127.7 (C), 126.5 (CH), 125.2 (CH), 114.0 (CH), 110.8 (CH), 110.3 (CH), 99.8 (CH), 13.9 ppm (CH_3); **IR** (KBr): ν_{max} = 3410, 3236, 3049, 2853, 1655, 1595, 1485, 997, 984, 912, 884, 859, 800, 783, 745, 687, 671 cm^{-1}. Compound purity (HPLC): 98.0%. EIMS m/z 310 ($M^{\bullet+}$); HRMS calcd. 310.0873, found 310.0866.

5.4.2.6 General synthetic method for indoles 6e–h

Compounds **6e** and **6g**: The appropriate benzoic acid (4.1 mmol) was dissolved in 10 mL CH_2Cl_2 (anhydrous) where after DCC (932 mg, 4.52 mmol) was dissolved in an additional 10 mL CH_2Cl_2 (anhydrous) and added to the benzoic acid solution. The mixture was stirred on an external ice bath for 6 h and the *N*,*N*′-dicyclohexylurea (DCU) produced during activation of the carboxylic acid, was removed by filtration. 5-Amino-2-methylindole (600 mg, 4.1 mmol) was dissolved in 10 mL CH_2Cl_2 (anhydrous) and added to the reaction mixture. After allowing the reaction to stir at room temperature for 80 h, purification was performed with column chromatography using diethyl ether as mobile phase.

Compounds **6f** and **6h**: 5-Amino-2-methylindole (500 mg, 3.42 mmol) and the appropriate benzoic acid (3.49 mmol) were dissolved in 40 mL methanol. EDC hydrochloride (720 mg, 3.49 mmol) was added and the reaction allowed to stir at room temperature for 85 h. Compound **6h** was collected from the reaction mixture by filtration, without the need for further purification. Compound **6f** was purified by column chromatography with ethanol (anhydrous) as mobile phase [25].

5.4.2.7 N-(2-methyl-1H-indol-5-yl)cyclohexanecarboxamide (6e)

Yield: 258 mg (25%); R_f = 0.66 (diethyl ether); **mp:** 198–200 °C. **^{1}H NMR** [600 MHz, DMSO-d_6]: δ = 10.74 (s, 1H), 9.49 (s, 1H), 7.70 (s, 1H), 7.11 (dd, J = 8.44, 8.54 Hz, 2H), 6.02 (s, 1H), 2.33 (s, 4H), 1.78–1.63 (m, 2H), 1.44–1.38 (m, 2H), 1.28–1.09 ppm (m, 6H); **^{13}C NMR** [150 MHz, DMSO-d_6]: δ = 173.6 (C), 136.0 (C), 132.7 (C), 131.3 (C), 128.4 (C), 113.7 (CH), 110.0 (CH), 109.8 (CH), 99.1 (CH), 44.8 (CH), 29.3 (2 x CH_2), 25.3 (3 x CH_2), 13.4 ppm (CH_3); **IR** (KBr): ν_{max} = 3253, 3089, 2930, 2856, 1656, 1587, 1518, 1481, 1448, 897, 795, 770 cm^{-1}. Compound purity (HPLC): 97.7%. EIMS m/z 256 ($M^{\bullet+}$); HRMS calcd. 256.1576, found 256.1569.

5.4.2.8 3-[(2-Methyl-1H-indol-5-yl)carbamoyl]benzene-1-sulfonic acid (6f)

Yield: 1 g (94%); R_f = 0.71 (ethanol); **mp:** 222–225 °C. **^{1}H NMR** [600 MHz, DMSO-d_6]: δ = 10.85 (s, 1H), 10.15 (s, 1H), 8.22 (s, 1H), 7.92 (d, J = 7.39 Hz, 1H), 7.84 (s, 1H), 7.79 (d, J = 7.39 Hz, 1H), 7.47 (t, 1H), 7.26 (dd, J = 9, 9 Hz, 2H), 6.09 (s, 1H), 2.36 (s, 3H), 1.05 ppm (t, 1H); **^{13}C NMR** [150 MHz, DMSO-d_6]: δ = 164.8 (C), 148.3 (C), 136.2 (C), 135.1 (C), 133.2 (C), 130.8 (C), 128.4 (CH), 127.8 (CH), 127.6 (CH), 124.9 (C, CH), 115.0 (CH), 111.4 (CH), 110.1 (CH), 99.3 (CH), 13.5 ppm (CH_3); **IR** (KBr): ν_{max} = 3630, 3259, 3072, 2921, 1642, 1542, 1481, 1451, 1195, 1043, 917, 875, 803, 771, 752, 739, 676 cm^{-1}. Compound purity (HPLC): 91.2%.

5.4.2.9 3,4-Dichloro-N-(2-methyl-1H-indol-5-yl)benzamide (6g)

Yield: 201 mg (15%); R_f = 0.74 (diethyl ether); **mp:** 200 °C. **^{1}H NMR** [600 MHz, DMSO-d_6]: δ = 10.88 (s, 1H), 10.19 (s, 1H), 8.21 (s, 1H), 7.86 (dd, J = 8.17, 8.15 Hz, 2H), 7.82 (s, 1H), 7.25 (dd, J = 8.57, 8.34 Hz, 2H), 6.10 (s, 1H), 2.36 ppm (s, 3H); **^{13}C NMR** [150 MHz, DMSO-d_6]: δ = 162.6 (C), 136.4 (C), 135.8 (C), 133.9 (C), 133.4 (C), 131.2 (C), 130.7 (CH), 130.3 (C), 129.5 (CH), 128.4 (C), 127.9 (CH), 114.8 (CH), 111.5 (CH), 110.1 (CH), 99.3 (CH), 13.5 ppm (CH_3); **IR** (KBr): ν_{max} = 3304, 3090, 2922, 2854, 1928, 1855, 1824, 1794, 1741, 1707, 1632, 1587, 914, 873, 849, 836, 786, 762, 751, 680 cm^{-1}. Compound purity (HPLC): 97.7%. EIMS m/z 318 ($M^{\bullet+}$); HRMS calcd. 318.0327, found 318.0315.

5.4.2.10 1-Methyl-N-(2-methyl-1H-indol-5-yl)-1λ4- pyridine-3-carboxamide (6h)

Yield: 410 mg (55%); R_f = not calculable; **mp:** 258–260 °C (decomp). **^{1}H NMR** [600 MHz, DMSO-d_6]: δ = 11.05 (s, 1H), 10.86 (s, 1H), 9.81 (s, 1H), 9.12 (s, 2H), 8.22–8.19 (m, 1H), 7.91 (s, 1H), 7.35 (dd, J = 8.58, 8.57 Hz, 2H), 6.11 (s, 1H), 4.45 (s, 3H), 2.38 ppm (s, 3H); **^{13}C NMR** [150 MHz, DMSO-d_6]: δ = 159.3 (C), 146.4 (CH), 145.3 (CH), 143.2 (CH), 136.3 (C), 134.1 (C), 133.4 (C), 129.7 (C), 128.2 (C), 126.8 (CH), 114.4 (CH), 111.2 (CH), 109.9 (CH), 99.0 (CH), 47.8 (CH_3), 13.0 ppm (CH_3); **IR** (KBr): ν_{max} = 3349, 3079, 2860, 1674, 1633, 1592, 1549, 1508, 1480, 1428, 1387, 904, 882, 856, 808, 745, 731, 693 cm^{-1}.

5.4.2.11 General synthetic method for benzofuranes 8a–d

The appropriate benzoic acid or cinnamic acid (4.54 mmol) was dissolved in 10 mL CH_2Cl_2 (anhydrous) where after 4-dimethylaminopyridine (DMAP) (37 mg, 0.3 mmol) was added to the solution at room temperature. 5-Hydroxy-3H-benzofuran-2-one (500 mg, 3.33 mmol) was dissolved in 5 mL *N*,*N*'-dimethylformamide (DMF) (anhydrous) and added to the reaction mixture. The reaction was cooled with an external ice bath for 5 min. DCC (687 mg, 3.33 mmol) was dissolved in 5 mL CH_2Cl_2 (anhydrous) and added to the reaction while on ice. The reaction was stirred on ice for 5 min and the DCU produced during activation of the carboxylic acid, was removed by filtration. The external ice bath was removed and the reaction was stirred at room temperature for 24 h. The pure benzofuran derivatives (**8a-d**) were obtained through column chromatography with ethyl acetate/petroleum ether (1:1) as mobile phase [28].

5.4.2.12 Benzoic acid 2-oxo-2,3-dihydro-benzofuran-5-yl ester (8a)

Yield: 393 mg (46%); R_f = 0.71 (ethyl acetate/petroleum ether (1:1)); **mp:** 83–85 °C. **^{1}H NMR** [600 MHz, DMSO-d_6]: δ = 8.12-8.11 (m, 2H), 7.59–7.57 (m, 1H), 7.46–7.30 (m, 3H), 7.08 (s, 1H), 7.05 (s, 1H), 3.71 ppm (s, 2H); **^{13}C NMR** [150 MHz, DMSO-d_6]: δ = 173.7 (C), 165.3 (C), 152.1 (C), 147.1 (C), 133.8 (CH), 130.7 (CH), 130.1 (CH), 129.1 (C), 128.6 (CH), 128.5 (CH), 124.0 (C), 122.2 (CH), 118.7 (CH), 111.4 (CH), 33.3 ppm (CH_2); **IR** (KBr): ν_{max} = 1805, 1738, 1479, 1264, 1138, 1120, 1052, 1023, 895, 875, 822,

809, 768, 713, 685, 669 cm^{-1}. Compound purity (HPLC): 96.4%. EIMS m/z 254 ($M^{\bullet+}$); HRMS calcd. 254.0579, found 254.0576.

5.4.2.13 3-Chlorobenzoic acid 2-oxo-2,3-dihydro-benzofuran-5-yl ester (8b)

Yield: 563 mg (59%); R_f = 0.68 (ethyl acetate/petroleum ether (1:1)); **mp:** 90–93 °C. **^{1}H NMR** [600 MHz, DMSO-d_6]: δ = 8.14 (m, 1H), 8.05–8.04 (m, 1H), 7.61 (m, 1H), 7.41–7.39 (m, 1H), 7.16–7.10 (m, 3H), 3.77 ppm (s, 2H); **^{13}C NMR** [150 MHz, DMSO-d_6]: δ = 173.6 (C), 164.1 (C), 152.3 (C), 146.9 (C), 134.8 (C), 133.8 (CH), 130.1 (C), 130.0 (CH), 129.8 (CH), 128.3 (CH), 124.1 (C), 122.1 (CH), 118.5 (CH), 111.4 (CH), 33.3 ppm (CH_2); **IR** (KBr): ν_{max} = 1801, 1734, 1480, 1249, 1136, 1106, 1073, 1053, 898, 877, 817, 780, 747, 708, 679, 660 cm^{-1}. Compound purity (HPLC): 97.4%. EIMS m/z 288 ($M^{\bullet+}$); HRMS calcd. 288.0189, found 288.0201.

5.4.2.14 (E)-Cinnamic acid 2-oxo-2,3-dihydro-benzofuran-5-yl ester (8c)

Yield: 470 mg (50%); R_f = 0.66 (ethyl acetate/petroleum ether (1:1)); **mp:** 75–80 °C. **^{1}H NMR** [600 MHz, DMSO-d_6]: δ = 7.75 (d, J = 15.97 Hz, 1H), 7.47–7.45 (m, 2H), 7.37–7.23 (m, 3H), 6.97 (dd, J = 8.65, 8.81 Hz, 2H), 6.49 (d, J = 15.96 Hz, 1H), 3.63 ppm (s, 2H); **^{13}C NMR** [150 MHz, DMSO-d_6]: δ = 173.7 (C), 165.5 (C), 152.0 (C), 147.0 (CH), 133.9 (C), 130.9 (C), 129.0 (CH), 128.9 (CH), 128.7 (CH), 128.3 (CH), 127.9 (CH), 123.9 (C), 122.0 (CH), 118.5 (CH), 116.7 (CH), 111.3 (CH), 33.3 ppm (CH_2); **IR** (KBr): ν_{max} = 3059, 3026, 1825, 1708, 1478, 1307, 1261, 1233, 1149, 1067, 920, 879, 866, 801, 765, 738, 709, 686 cm^{-1}. Compound purity (HPLC): 97.3%.

5.4.2.15 (E)-3-Chlorocinnamic acid 2-oxo-2,3-dihydro-benzofuran-5-yl ester (8d)

Yield: 367 mg (35%); R_f = 0.62 (ethyl acetate/petroleum ether (1:1)); **mp:** 85–95 °C. **^{1}H NMR** [600 MHz, DMSO-d_6]: δ = 7.77 (d, J = 15.99 Hz, 1H), 7.56-7.53 (m, 2H), 7.43–7.27 (m, 3H), 7.60 (dd, J = 8.89, 8.60 Hz, 2H), 6.60 (d, J = 16.00 Hz, 1H), 3.75 ppm (s, 2H); **^{13}C NMR** [150 MHz, DMSO-d_6]: δ = 173.7 (C), 165.1 (C), 152.1 (C), 146.9 (C), 145.4 (CH), 135.7 (C), 135.0 (C), 130.7 (CH), 130.3 (CH), 127.6 (CH), 127.1 (CH), 126.0 (CH), 124.0 (C), 122.0 (CH), 118.5 (CH), 111.4 (CH), 33.3 ppm (CH_2); **IR** (KBr): ν_{max} = 3247, 3053, 1745, 1706, 1479, 1259, 1233, 1201, 1082, 1045, 893, 860, 842, 787, 753, 715, 688, 674 cm^{-1}. Compound purity (HPLC): 90.4%.

5.4.3 MAO activity measurements and inhibition

Human recombinant MAO-A and –B, expressed in baculovirus infected BTI insect cells, were used to evaluate the indole (**6a**–**h**) and benzofuran (**8a**–**d)** derivatives as potential MAO inhibitors. Both enzymes were purchased from Sigma-Aldrich® and stored at -70 °C until use. All incubations were performed in potassium phosphate buffer (100 mM, pH 7.4, made isotonic with KCl) and contained kynuramine (45 µM and 30 µM for MAO-A and –B, respectively), the enzyme (0.075 mg protein/mL), and various concentrations of the test inhibitors, producing a final incubation volume of 500 µL. Stock solutions of the test inhibitors were prepared in dimethyl sulfoxide (DMSO) and added to the incubation mixtures to yield a final DMSO concentration of 4% (v/v). DMSO concentrations higher than 4% are reported to inhibit MAO activity [39]. Samples were incubated at 37 °C for 20 min and the enzyme reactions were terminated by the addition of 200 µL sodium hydroxide (2 N) and centrifuged at 16,000*g* for 10 min. The supernatant fractions were removed and the concentrations of the MAO generated product, 4-hydroxyquinoline, were measured spectrofluorometrically at an excitation wavelength of 310 nm and an emission wavelength of 400 nm using a Varian® Cary Eclipse® fluorescence spectrophotometer. The IC_{50} values were determined from plots of the rate of MAO-A or –B catalysed 4-hydroxyquinoline formation versus the logarithm of the inhibitor concentration. For this purpose the Prism® 4.02 (GraphPad, Sorrento Valley, CA) software package was employed. Ten different concentrations of the test inhibitor, spanning three orders of magnitude were used to construct the sigmoidal dose-response curve. The IC_{50} values are reported as mean ± standard error of the mean (SEM) of duplicate determinations [29].

5.4.4 Time-dependent inhibition studies

Recombinant human MAO-B (0.03 mg protein/mL) was preincubated with **6g** (0.12 µM; 2 × IC_{50}) or **8b** (1.98 µM; 2 × IC_{50}) for periods of 0, 15, 30, 60 min. These preincubations were carried out at 37 ºC in potassium phosphate buffer (100 mM, pH 7.4, made isotonic with KCl). Kynuramine (30 µM) was added to the preincubations and the reactions were incubated for an additional 15 min at 37 °C. The reactions were terminated with the addition of sodium hydroxide (2N) and the rates of 4-hydroxyquinoline formation were

measured as described above. The final enzyme concentration in the incubations was 0.015 mg protein/mL and the final concentrations of **6g** and **8b** were 0.06 µM and 0.99 µM, respectively [40].

5.4.5 Examining the mode of inhibition

In order to determine the modes of inhibition of **6g**, Lineweaver–Burk plots were constructed by measuring the initial rates of MAO-B catalysed oxidation at four different kynuramine concentrations (15–90 µM) in the absence as well as in the presence of three different concentrations of the inhibitor. The concentration range chosen for **6g** was 0.015–0.06 µM. The reaction conditions and rate measurements were carried out as described above. Linear regression analysis was performed using the SigmaPlot software package (Systat Software Inc.).

5.4.6 Ligand docking

Manipulation of the crystal structure of MAO-B (PDB code: 2V5Z) [35] was performed with Discovery Studio® 1.7 (Accelrys Software Inc., San Diego, CA). The valences of the co-crystallised ligand (safinamide) and FAD co-factor were firstly corrected and hydrogen atoms were added. The receptor proteins were then typed by applying the CHARMm forcefield and a three-step minimisation protocol (steepest descent, conjugate gradient and adopted basis Newton-Rapheson) was performed while the protein backbone was kept rigid. During the minimisation cascade the Generalised Born with Simple Switching implicit solvation model was used to account for the effects of the aqueous environment. Minimisation of the receptor proteins were considered necessary since the protein X-ray structure might contain residual energetic tensions from the crystallisation process. Safinamide was subsequently eliminated from the energy-minimised receptor proteins and the backbone constraints were removed. The following conserved active site waters were retained: HOH 1155, 1169, 1346, 1351 (MAO-B, A-chain). The final modified proteins were used as the starting models for the docking simulation in Discovery Studio®. The structures of **6g** and **8d**, built and geometry optimised within Discovery Studio®, were docked into the protein model with LigandFit. Following the docking, the orientations and conformations of the docked ligands were further refined with the Smart Minimizer algorithm. All the parameters for the docking run were set to

their default values. A total of ten docking solutions were allowed and the top-ranked docking conformations were determined using the DockScore values.

Acknowledgements

Financial support received from the National Research Foundation (South Africa) is gratefully acknowledged.

References

[1] W. Dauer, S. Przedborski, Neuron, 39 (2003) 889-909.

[2] D. A. Di Monte, L. E. De Lanney, I. Irwin, Brain Res. 738 (1996) 53-59.

[3] J. Saura, Z. Bleuel, J. Ulrich, A. Mendelowitsch, K. Chen, J. C. Shih, P. Malherbe, M. Da Prada, J. G. Richards, Neuroscience 70 (1996) 755–774.

[4] C. J. Fowler, A. Wiberg, L. Oreland, J. Marcusson, B. Winblad, J. Neural Transm. Gen. Sect. 49 (1980) 1–20.

[5] K. N. Westlund, R. M. Denney, R. M. Rose, C. W. Abell, Neuroscience 25 (1988) 439-456.

[6] A. Parkinson, B. W. Ogilvie, Biotransformation of Xenobiotics, in: C .D. Klaassen (Ed.), Casarett & Doull's Toxicology: The Basic Science of Poisons, McGraw-Hill Inc., New York, 2008, pp. 204-206.

[7] G. Cohen, J. Neural. Transm. Suppl. 32 (1990) 229-238.

[8] J. Knoll, K. Magyar, Adv. Biochem. Psychopharm. 5 (1972) 393–408.

[9] R. E. Heikkila, L. Manzino, F.S. Cabbat, R. C. Duvoisin, Nature 311 (1984) 467–469.

[10] P. H. Yu, B. A. Davis, D. A. Durden, A. Barber, I. Terleckyj, W. G. Nicklas, A. A. Boulton, J. Neurochem. 62 (1994) 697–704.

[11] C. W. Olanow, Ann. Neurol. Suppl. 32 (1992) S2–S9.

[12] J. P. M. Finberg, M. Tenne, M. B. H. Youdim, Br. J. Pharmacol. 73 (1981) 65–74.

[13] M. B. H. Youdim, A. Gross, J. P. M. Finberg, Br. J. Pharmacol. 132 (2001) 500–506.

[14] M. B. H. Youdim, W. Maruyama, M. Naoi, Drugs of Today 41 (2005) 369–391.

[15] K. F. Tipton, S. Boyce, J. O'Sullivan, G. P. Davey, J. Healy, Curr. Med. Chem. 11 (2004) 1965–1982.

[16] J. S. Fowler, N. D. Volkow, J. Logan, G. J. Wang, R. R. MacGregor, D. Schyler, A. P. Wolf, N. Pappas, D. Alexoff, C. Shea, Synapse 18 (1994) 86-93.

[17] F. Ooms, R. Frédérick, F. Durant, J. P. Petzer, N. Castagnoli Jr., C. J. Van der Schyf, J. Wouters, Bioorg. Med. Chem. Lett. 13 (2003) 69–73.

[18] F. Stocchi, L. Vacca, P. Grassini, M. F. De Pandis, G. Battaglia, C. Cattaneo, R. G. Fariello, Neurology 67 (2006) S24–S29.

[19] M. J. Matos, D. Viña, C. Picciau, F. Orallo, L. Santana, E. Uriarte, Bioorg. Med. Chem. Lett. 19 (2009) 5053–5055.

[20] D. Balsa, E. Fernández-Álvarez, K. F. Tipton, M. Unzeta, J. Neural Transm. Suppl. 32 (1990) 103–105.

[21] D. Balsa, E. Fernández-Álvarez, K. F. Tipton, M. Unzeta, Biochem. Soc. Trans. 19 (1991) 215–218.

[22] C. Fernández García, J. L. Marco, E. Fernández-Álvarez, Eur. J. Med. Chem. 27 (1992) 909–918.

[23] J. A. Morón, M. Campillo, V. Pérez, M. Unzeta, L. Pardo, J. Med. Chem. 43 (2000) 1684–1691.

[24] V. Pérez, J. L. Marco, E. Fernández-Álvarez, M. Unzeta, Br. J. Pharmacol. 127 (1999) 869–876.

[25] C. E. Müller, J. Sandoval-Ramírez, U. Schobert, U. Geis, W. Frobenius, K. –N. Klotz, Bioorg. Med. Chem. 6 (1998) 707–719.

[26] D. van den Berg, K. R. Zoellner, M. O. Ogunrombi, S. F. Malan, G. Terre'Blanche, N. Castagnoli Jr., J. J. Bergh, J. P. Petzer, Bioorg. Med. Chem. 15 (2007) 3692–3702.

[27] F. Suzuki, J. Shimada, S. Shiozaki, S. Ichikawa, A. Ishii, J. Nakamura, H. Nonaka, H. Kobayashi, E. Fuse, J. Med. Chem. 36 (1993) 2508–2518.

[28] E. F. V. Scriven, Chem. Soc. Rev. 12 (1983) 129–161.

[29] L. Novaroli, M. Reist, E. Favre, A. Carotti, M. Catto, P.–A. Carrupt, Bioorg. Med. Chem. 13 (2005) 6212–6217.

[30] Y. C. Cheng, W. H. Prusoff, Biochem. Pharmacol. 22 (1973) 3099–3108.

[31] R. R. Ramsay, C. Dunford, P. K. Gillman, Br. J. Pharmacol. 152 (2007) 946-951.

[32] P. K. Gillman, Can. J. Anaesth. 55 (2008) 311-312.

[33] J. Wouters, F. Ooms, S. Jegham, J. Koenig, P. George, F. Durant, Eur. J. Med. Chem. 32 (1997) 721-730.

[34] U. Thull, S. Kneubühler, P. Gaillard, P.-A. Carrupt, B. Testa, C. Altomare, A. Carotti, P. Jenner, K. St. P. McNaught, Biochem. Pharmacol. 50 (1995) 869-877.

[35] C. Binda, J. Wang, L. Pisani, C. Caccia, A. Carotti, P. Salvati, D. E. Edmondson, A. Mattevi, J. Med. Chem. 50 (2007) 5848–5852.

[36] J. Boström, J. R. Greenwood, J. Gottfries, J. Mol. Graph. Model. 21 (2003) 449–462.

[37] F. Chimenti, R. Fioravanti, A. Bolasco, P. Chimenti, D. Secci, F. Rossi, M. Yanez, F. Orallo, F. Ortuso, S. Alcaro, J. Med. Chem. 52 (2009) 2818-2824.

[38] S.–Y. Son, J. Ma, Y. Kondou, M. Yoshimura, E. Yamashita, T. Tsukihara, Proc. Natl. Acad. Sci. USA 105 (2008) 5739–5744.

[39] C. Gnerre, M. Catto, F. Leonetti, P. Weber, P. –A. Carrupt, C. Altomare, A. Carotti, B. Testa, J. Med. Chem. 43 (2000) 4747–4758.

[40] H. Inoue, K. Castagnoli, C. J. van der Schyf, S. Mabic, K. Igarashi, N. Castagnoli Jr., J. Pharmacol. Exp. Ther. 291 (1999) 856-864.

Supporting Information:

Chromatograms of the HPLC analyses of the synthesised compounds.

Chromatograms are indicated at 210, 254 and 300 nm respectively.

6a

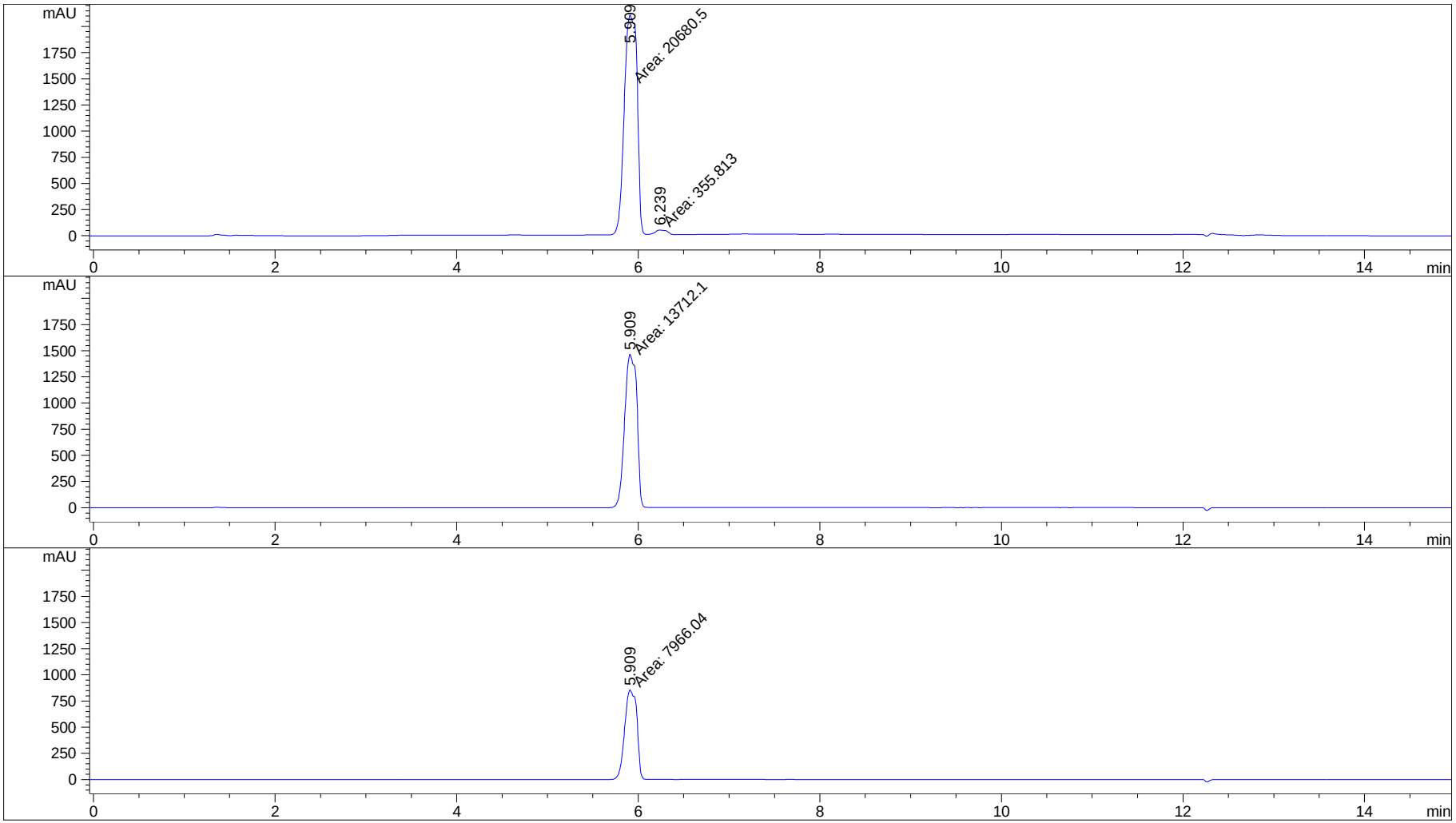
mAU
1750
1500
1250
1000
750
500
250
0
5.909
Area: 20680.5
6.239
Area: 355.813
0
2
4
6
8
10
12
14
min
mAU
5.909
Area: 13712.1
mAU
5.909
Area: 7966.04

6b

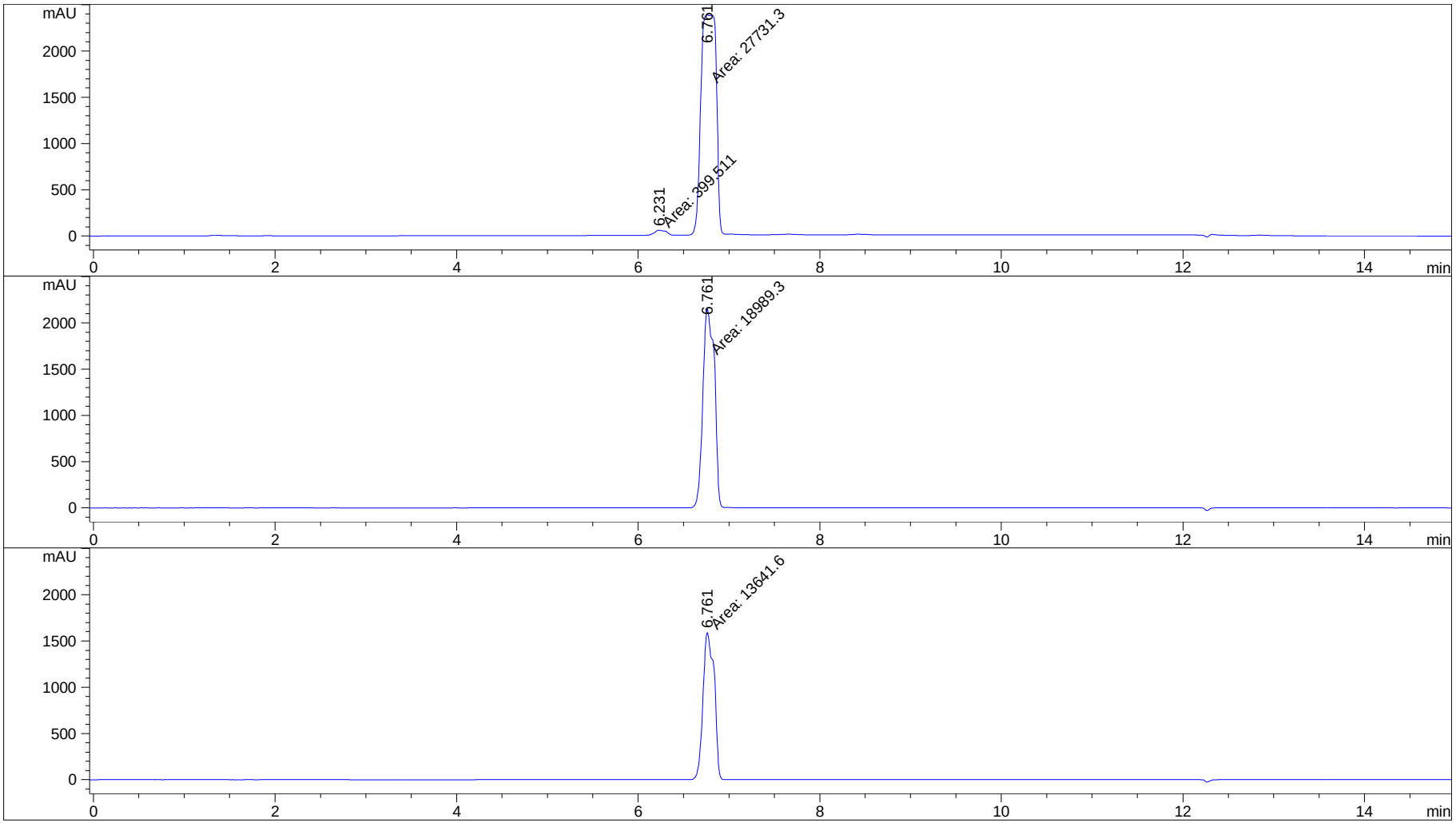
mAU
2000
1500
1000
500
0
6.761
Area: 27731.3
6.231
Area: 399.511
0
2
4
6
8
10
12
14
min
mAU
2000
1500
1000
500
0
6.761
Area: 18989.3
0
2
4
6
8
10
12
14
min
mAU
2000
1500
1000
500
0
6.761
Area: 13641.6
0
2
4
6
8
10
12
14
min

6c

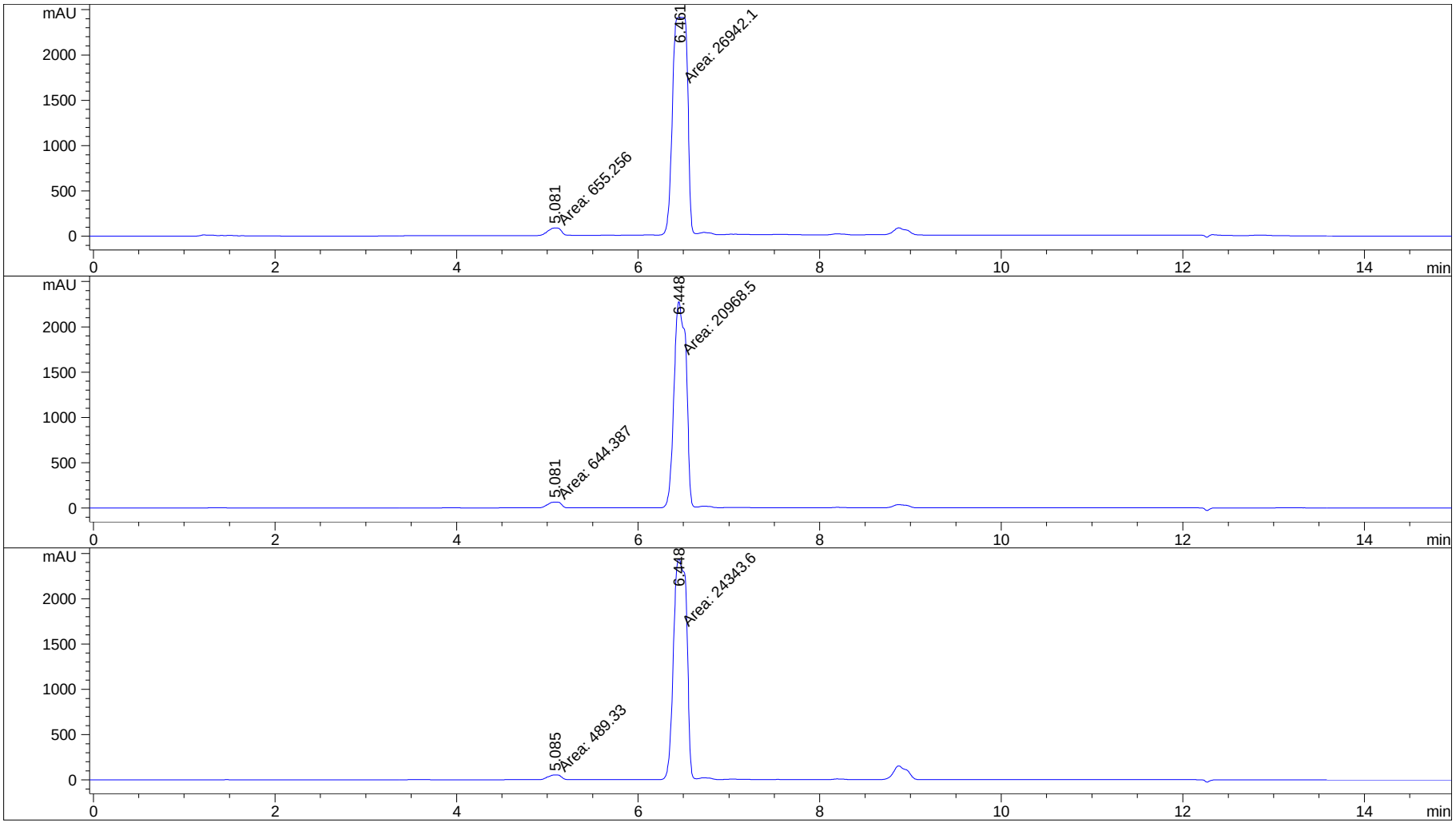
mAU
2000
1500
1000
500
0
6.461
Area: 26942.1
5.081
Area: 655.256
0
2
4
6
8
10
12
14
min
mAU
2000
1500
1000
500
0
6.448
Area: 20968.5
5.081
Area: 644.387
0
2
4
6
8
10
12
14
min
mAU
2000
1500
1000
500
0
6.448
Area: 24343.6
5.085
Area: 489.33
0
2
4
6
8
10
12
14
min

6d

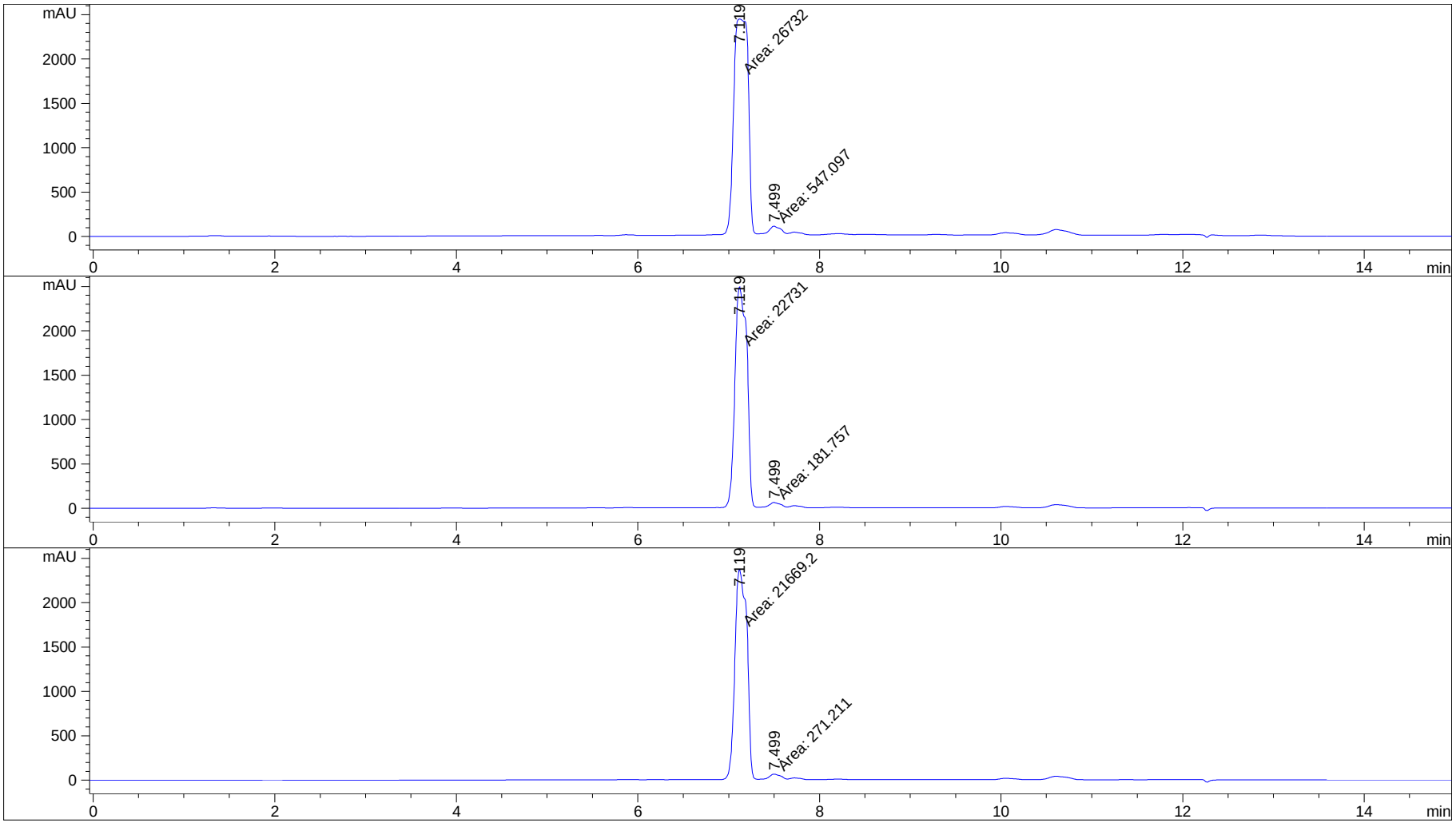
mAU
2000
1500
1000
500
0
7.119
Area: 26732
7.499
Area: 547.097
0
2
4
6
8
10
12
14
min
mAU
2000
1500
1000
500
0
7.119
Area: 22731
7.499
Area: 181.757
0
2
4
6
8
10
12
14
min
mAU
2000
1500
1000
500
0
7.119
Area: 21669.2
7.499
Area: 271.211
0
2
4
6
8
10
12
14
min

6e

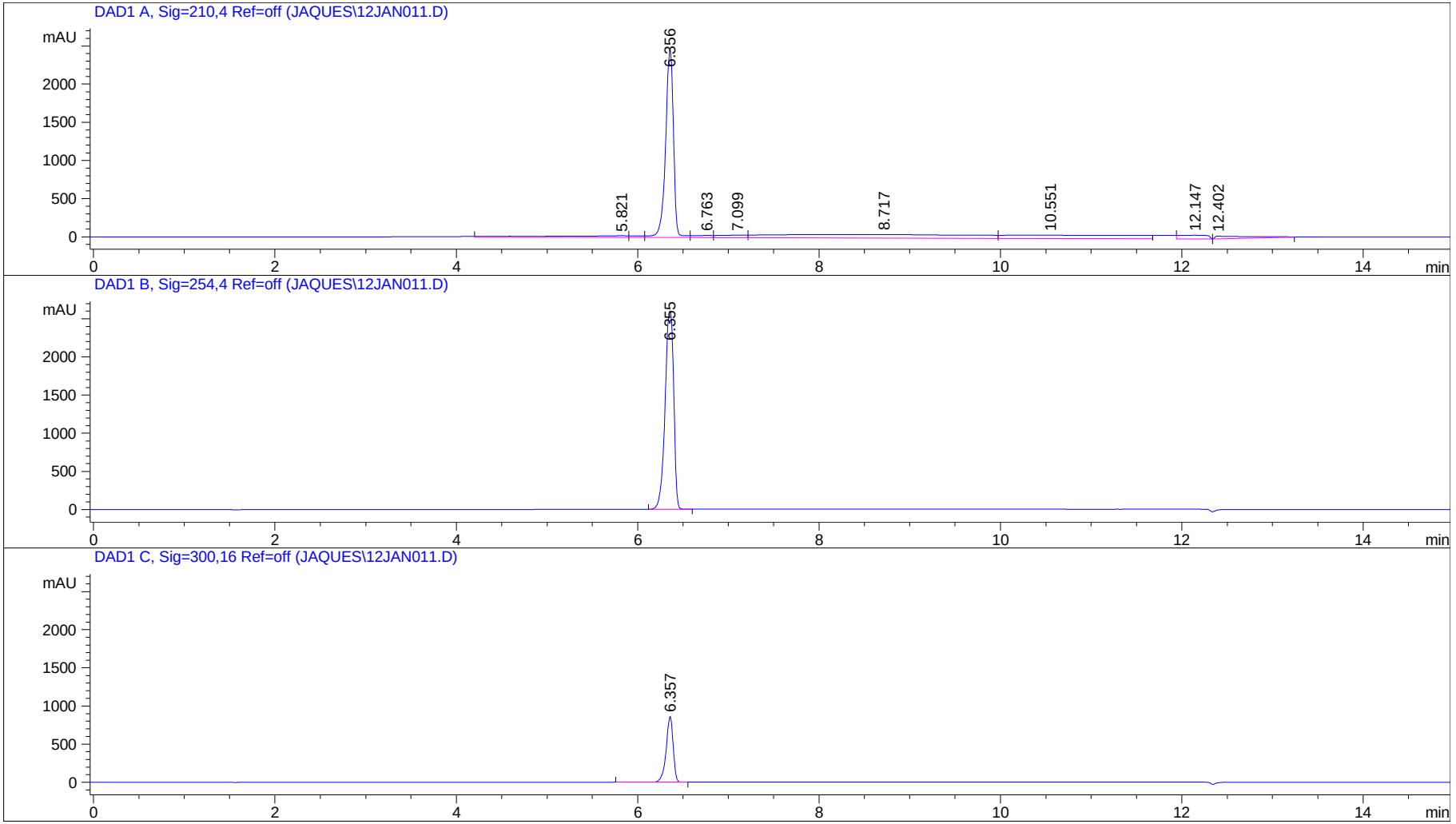
DAD1 A, Sig=210,4 Ref=off (JAQUES\12JAN011.D)
mAU
6.356
5.821
6.763
7.099
8.717
10.551
12.147
12.402
min
DAD1 B, Sig=254,4 Ref=off (JAQUES\12JAN011.D)
mAU
6.355
min
DAD1 C, Sig=300,16 Ref=off (JAQUES\12JAN011.D)
mAU
6.357
min

6f

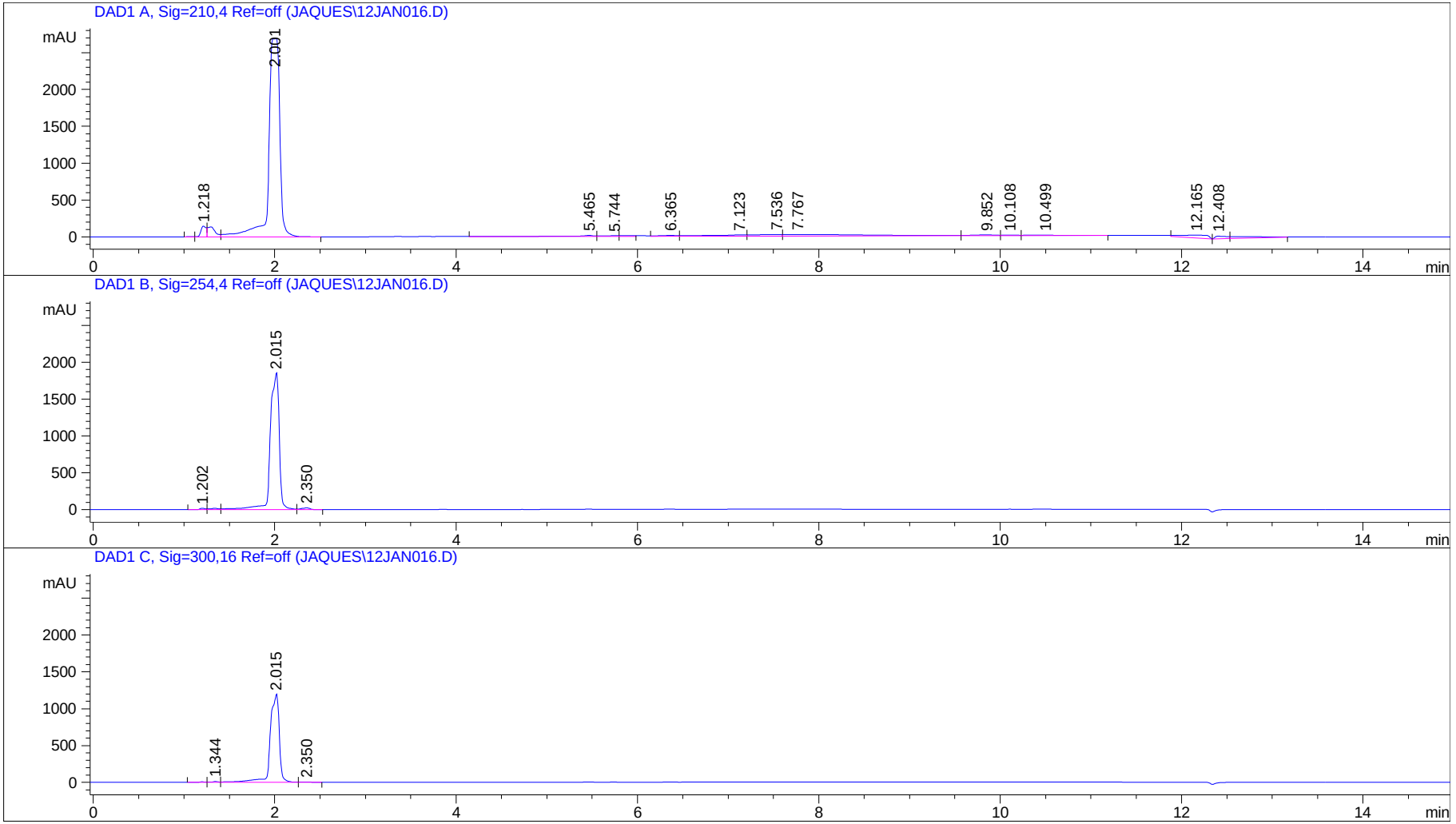
DAD1 A, Sig=210,4 Ref=off (JAQUES\12JAN016.D)
mAU
2.001
1.218
5.465
5.744
6.365
7.123
7.536
7.767
9.852
10.108
10.499
12.165
12.408
min
DAD1 B, Sig=254,4 Ref=off (JAQUES\12JAN016.D)
2.015
1.202
2.350
DAD1 C, Sig=300,16 Ref=off (JAQUES\12JAN016.D)
2.015
1.344
2.350

6g

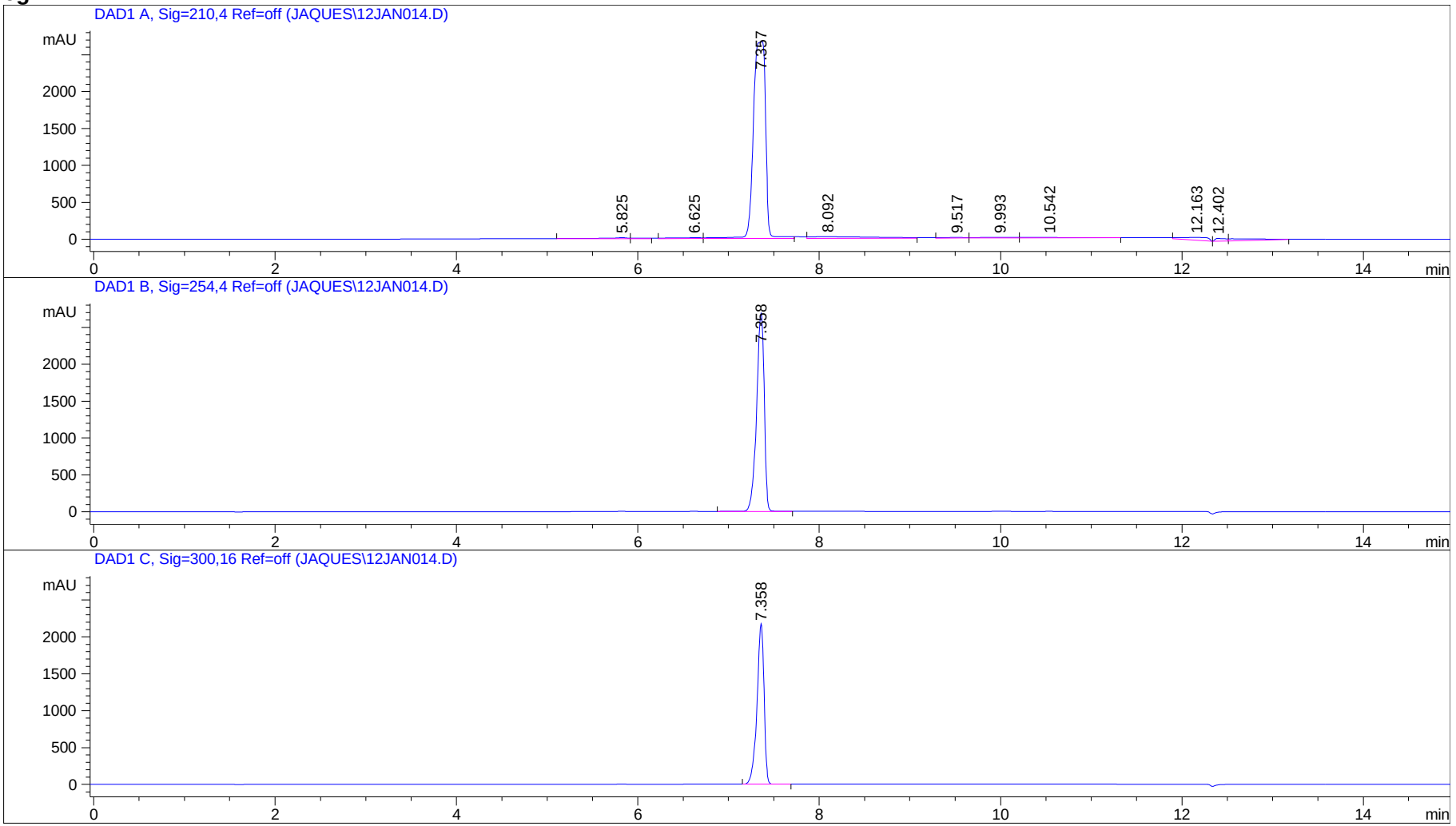
DAD1 A, Sig=210,4 Ref=off (JAQUES\12JAN014.D)
mAU
2000
1500
1000
500
0
7.357
5.825
6.625
8.092
9.517
9.993
10.542
12.163
12.402
0
2
4
6
8
10
12
14
min
DAD1 B, Sig=254,4 Ref=off (JAQUES\12JAN014.D)
mAU
2000
1500
1000
500
0
7.358
0
2
4
6
8
10
12
14
min
DAD1 C, Sig=300,16 Ref=off (JAQUES\12JAN014.D)
mAU
2000
1500
1000
500
0
7.358
0
2
4
6
8
10
12
14
min

8a

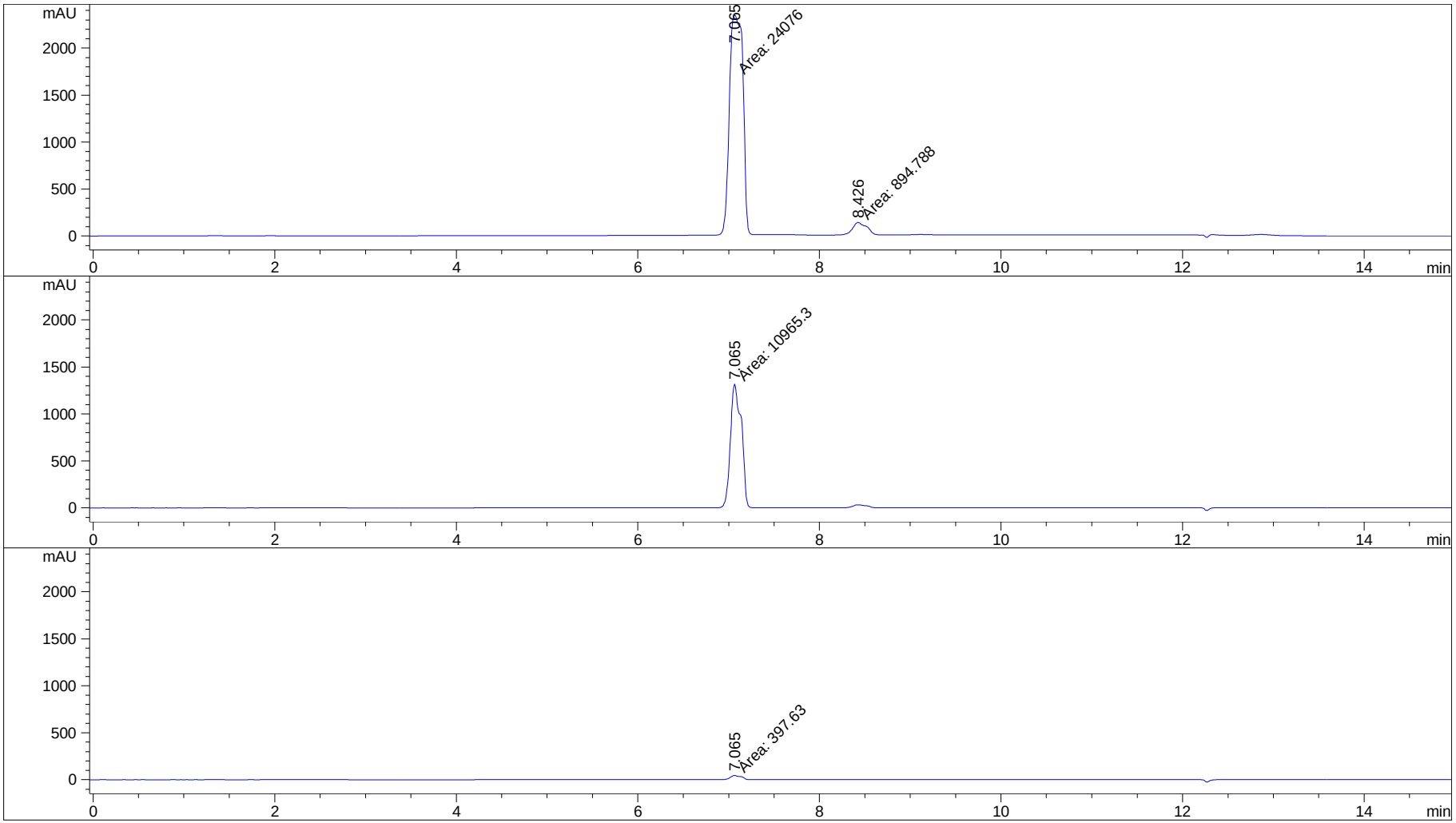
mAU
2000
1500
1000
500
0
7.065
Area: 24076
8.426
Area: 894.788
0
2
4
6
8
10
12
14
min
mAU
2000
1500
1000
500
0
7.065
Area: 10965.3
0
2
4
6
8
10
12
14
min
mAU
2000
1500
1000
500
0
7.065
Area: 397.63
0
2
4
6
8
10
12
14
min

8b

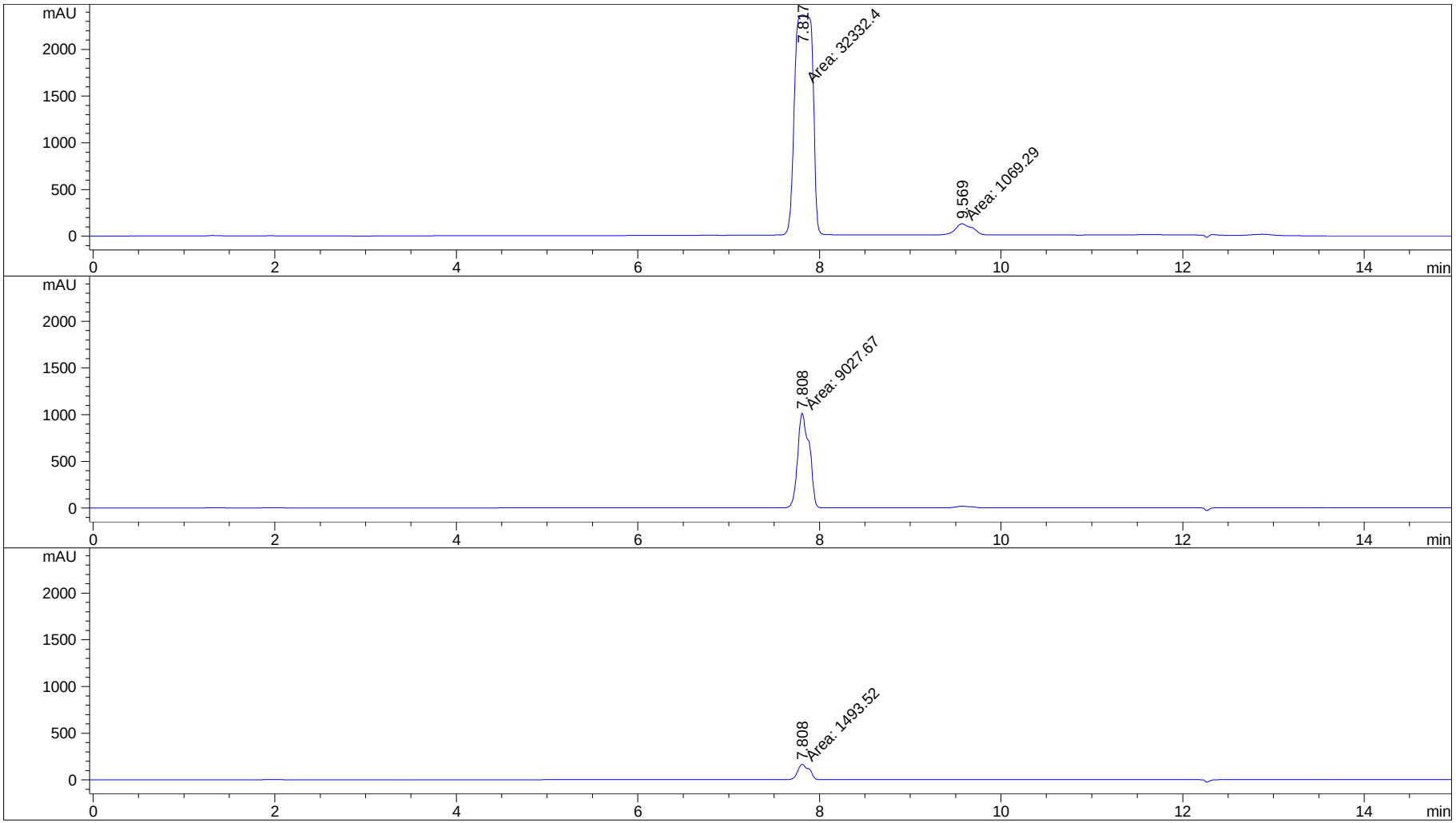
mAU
2000
1500
1000
500
0
7.817
Area: 32332.4
9.569
Area: 1069.29
0
2
4
6
8
10
12
14
min
mAU
2000
1500
1000
500
0
7.808
Area: 9027.67
0
2
4
6
8
10
12
14
min
mAU
2000
1500
1000
500
0
7.808
Area: 1493.52
0
2
4
6
8
10
12
14
min

8c

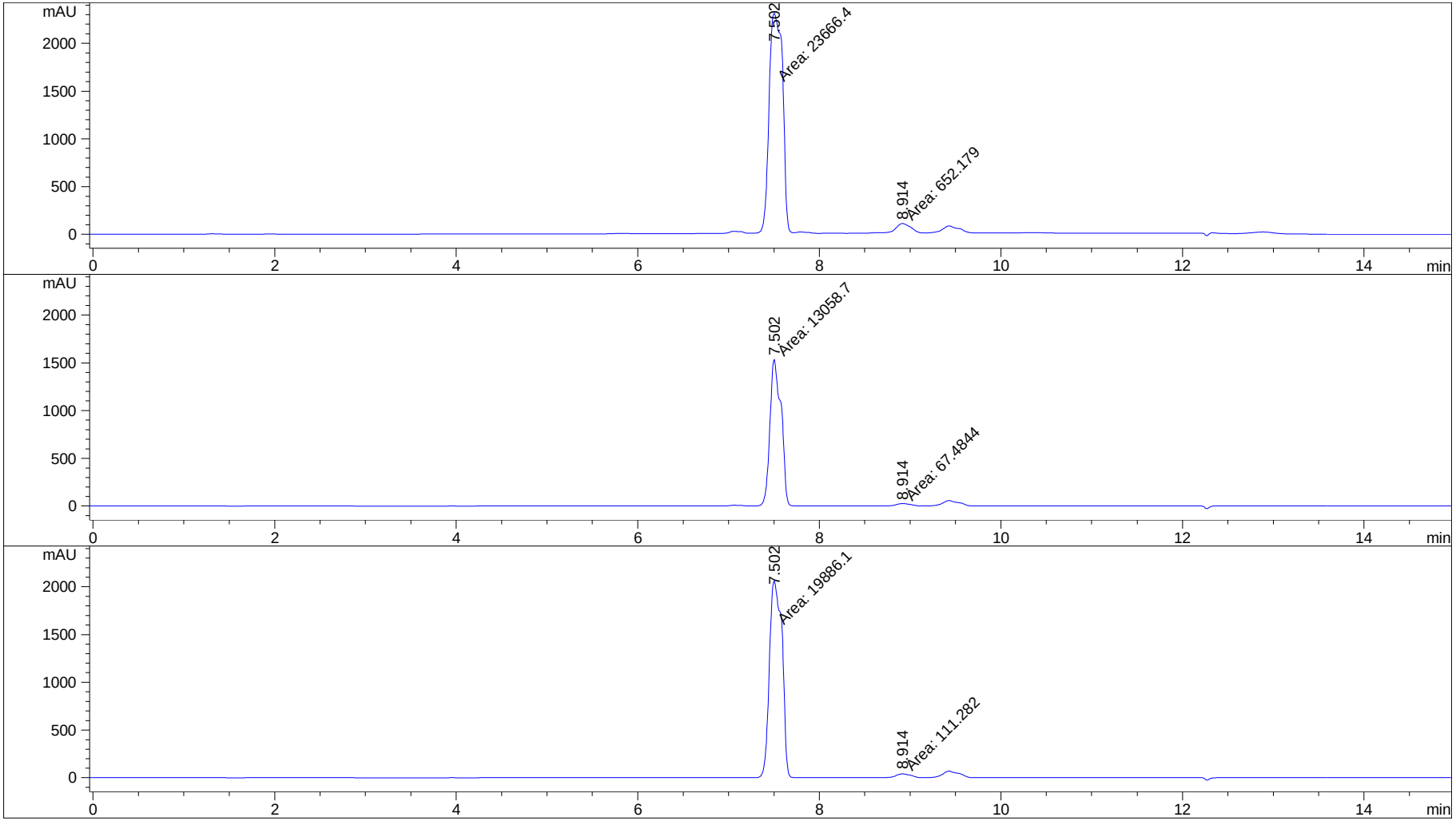
mAU
2000
1500
1000
500
0
7.502
Area: 23666.4
8.914
Area: 652.179
0
2
4
6
8
10
12
14
min
mAU
2000
1500
1000
500
0
7.502
Area: 13058.7
8.914
Area: 67.4844
0
2
4
6
8
10
12
14
min
mAU
2000
1500
1000
500
0
7.502
Area: 19886.1
8.914
Area: 111.282
0
2
4
6
8
10
12
14
min

8d

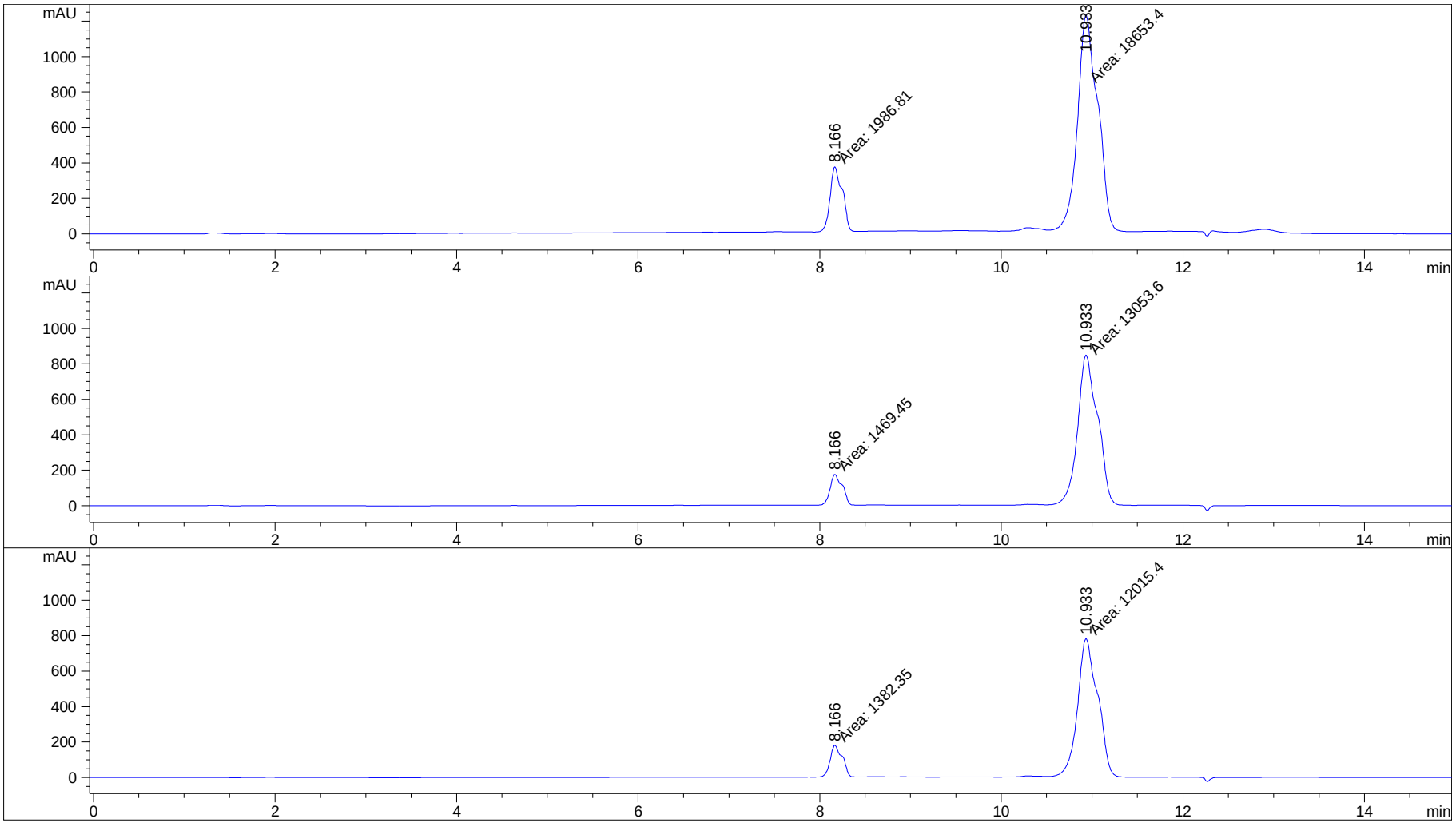
mAU
1000
800
600
400
200
0
8.166
Area: 1986.81
10.933
Area: 18653.4
0
2
4
6
8
10
12
14
min
mAU
1000
800
600
400
200
0
8.166
Area: 1469.45
10.933
Area: 13053.6
0
2
4
6
8
10
12
14
min
mAU
1000
800
600
400
200
0
8.166
Area: 1382.35
10.933
Area: 12015.4
0
2
4
6
8
10
12
14
min

CHAPTER 6
DISCUSSION & CONCLUSIONS

AD and PD are well known neurodegenerative diseases characterised by the progressive loss of neurons from selective brain regions. Oxidative stress is one of many factors thought to play an important role in this neurodegeneration. In PD oxidative stress may be caused by an overproduction of H_2O_2 as a result of an increase in dopamine metabolism by MAO-B. This enzyme isoform therefore plays a dual role in the pathophysiology of PD as it is the main enzyme implicated in the metabolism of dopamine as well as being involved in the formation of free radicals and other neurotoxic species. Increased MAO-B levels have also been observed in plaque-associated astrocytes in the brains of AD patients. NOS is another enzyme thought to be involved in neurodegeneration, as an overproduction of NO may cause injury to the mitochondrial electron transport chain, resulting in damage and eventual death of neurons.

In the current study three series of compounds were synthesised, namely: pteridine-2,4-diones, benzofuranes and indoles. The pteridine-2,4-diones were investigated as multi-target directed ligands by determining their MAO-B and NOS inhibitory activities. They were found to be potent MAO-B inhibitors, but did not show any promise as NOS inhibitors. The benzofuranes and indoles were investigated as MAO-A/B inhibitors with isoform specificity.

The pteridine-2,4-diones proved to be promising as scaffolds for the development of potent reversible MAO-B inhibitors and compounds **9d** and **10d** presented with MAO-B IC_{50} values of 0.602 and 0.314 µM respectively. Interestingly, both **9d** and **10d** are structurally closely related to CSC and those derivatives containing a 3-chloro-styryl functional group at C6 were found to be the most potent MAO-B inhibitors, confirming the important role of 3-chloro substitution in binding to the MAO-B active site. The best-ranked docking solutions for **9b**-**d** and **10b**, **d** showed that they span both the entrance and substate cavities of the MAO-B enzyme and that their binding orientation is similar to that of the caffeine analogues. The pteridine-2,4-dione derivatives are only slightly less

potent than their corresponding caffeine analogues in inhibiting MAO-B and therefore they might thus offer attractive alternatives for future development and optimisation. The weak NOS inhibition profile of the pteridine-2,4-diones can probably be attributed to the styryl phenyl sterically hindering binding of these compounds to the NOS active site, thereby nullifying the structural relation of these compounds to BH_4.

The benzofuranes were indicated to be potent MAO-B inhibitors with compound **8d** exhibiting a K_i value of 0.19 µM. They are however less selective than the indole derivatives. For example, compound **8d** had a selectivity index of 5 compared to a value of 99 for the indole compound **6g**. It is therefore postulated that the benzofuranes show promise for the development of potent, relatively non-selective MAO inhibitors.

The compound series which was found to be the most potent and selective MAO-B inhibitors in the whole study, was that of the indoles. Compound **6g** had a K_i value of 0.03 µM and a selectivity index of 99, making it the most promising compound in the current study. All, except three indole compounds, were selective towards the MAO-B isoform. The indole nucleus is therefore very promising as a scaffold for the design of potent, MAO-B selective inhibitors and should be investigated thoroughly in future studies.

An interesting observation is that chlorine substitution at C3 of the aromatic side chain ring of the benzofuranes and indoles enhanced both MAO-A and -B inhibition potencies. The addition of an additional chlorine substituent to the phenyl ring at C4 further enhanced the binding affinity of the indoles to the MAO-B active site. Compound **6g** (K_i = 0.03 µM) proved to be more potent in inhibiting MAO-B than its corresponding caffeine analogue (K_i = 0.04) (Van den Berg ***et al.***, 2007:3692). This enhancement in MAO-B potency as a result of chlorine substitution may be attributed to the corresponding increase in lipophilicity. This in turn may result in an enhancement of nonspecific lipophilic interactions between the inhibitors and the MAO-B active site. It is therefore concluded that halogen substitution of the aromatic side chain ring at C3 enhances the binding affinity of the benzofuranes and indoles to both the MAO-A and -B active sites and that dual halogen substitution at C3 and C4 enhances the MAO-B inhibition potency of the indoles.

Compounds **6g** and **8b** were characterised as reversible MAO-B inhibitors, as no time-dependent reduction in the rate of MAO-B catalysed oxidation of kynuramine was observed. The mode of inhibition produced by **6g** was further shown to be competitive since the linear Lineweaver-Burk plots intersected on the y-axis. Compound **6g** was thus shown to be a competitive reversible inhibitor, which has the following advantages:

- Recovery from inhibition doesn't require the synthesis of new enzyme.
- Possible loss of selectivity is eliminated.
- Inhibition is affected by changes in substrate concentration, keeping dopamine levels within a normal range.

Molecular modelling studies showed that both **6g** and **8b** had similar binding modes to that of the caffeines, with the relatively polar indole or benzofuran nucleus situated in the substrate cavity and the C5 side chain extending towards the entrance cavity of MAO-B.

Since MAO-B inhibition results in a decrease in oxidative stress by reducing the production of H_2O_2, the compounds from this study that were shown to be MAO-B inhibitors may indirectly be neuroprotective. However, this notion can only be confirmed by performing a proper neuroprotection assay with these compounds. There is also the possibility that they might be neurorescuers as was shown in an earlier study with (*R*)-deprenyl (Salo *et al.*, 1992:394). Both of these hypotheses could be thoroughly investigated in future studies.

During the performance of the oxyhaemoglobin assay the NOS inhibition profile of certain pteridine-2,4-dione compounds could not be determined, due to the fact that they absorbed UV light in the assay detection range (390-430 nm). This limitation may be circumvented in future studies by applying an HPLC assay method for NOS inhibition determination. Limitations in the solubility of these compounds may also be addressed in future by synthesising the appropriate salts thereof. The benzofuran derivatives were postulated to be unstable in the potassium phosphate buffer used for the enzymatic reactions of the MAO-A/B kynuramine assay. Our laboratory will investigate this observation in future studies.

The conclusion drawn from this study is that, although multi-target directed ligands are a promising strategy for neurodegenerative disease treatment, designing drugs that act at multiple targets remains a challenge.

References

SALO, P.T. & TATTON, W.G. 1992. Deprenyl reduces the death of motoneurons caused by axotomy. *Journal of neuroscience research.*, 31(2):394-400.

VAN DEN BERG, D., ZOELLNER, K.R., OGUNROMBI, M.O., MALAN, S.F., TERRE'BLANCHE, G., CASTAGNOLI, N., Jr., BERGH, J.J. & PETZER, J.P. 2007. Inhibition of monoamine oxidase B by selected benzimidazole and caffeine analogues. *Bioorganic & medicinal chemistry*, 15(11):3692-3702.

ANNEXURE A

AUTHOR INSTRUCTIONS – BIOORGANIC & MEDICINAL CHEMISTRY

A.1 Manuscript preparation

A.1.1 ***General requirements:*** The corresponding author's full mailing address, including mail codes, phone number, fax number, and e-mail address should be included. Authors are asked to provide four keywords, which will be used for indexing purposes. The manuscript should be compiled in the following order: Graphical Abstract, Title, Authors, Affiliations, Abstract, Keywords, Introduction, Results, Discussion, Conclusion, Experimental, References and Notes, Tables, Legends, Figures, and Schemes.

A.1.2 ***Graphical abstracts:*** Authors must supply a graphical abstract at the time the paper is first submitted. The abstract should summarise the contents of the paper in a concise, pictorial form designed to capture the attention of a wide readership and for compilation of databases. Carefully drawn chemical structures that serve to illustrate the theme of the paper are desired. Authors may also provide appropriate text, not exceeding 30 words. The content of the graphical abstract will be typeset and should be kept within an area of 5 cm by 17 cm. Authors must supply the graphic separately as an electronic file. For examples of graphical abstracts, please consult a recent issue of the journal or visit the journal home page on ScienceDirect at http://www.sciencedirect.com/science/journal/09680896 and click 'Sample Issue Online'.

A.1.3 ***Title:*** The title should be brief, specific, and rich in informative words; it should not contain any literature references or compound numbers.

A.1.4 ***Authors and affiliations:*** Where possible, supply given names, middle initials, and family names for complete identification. Use superscript lowercase letters to indicate different addresses, which should be as detailed as possible and must include the country name. The corresponding author should be indicated with an asterisk, and contact details (fax, e-mail) should be placed in a footnote. Information relating to other authors

(e.g., present addresses) should be placed in footnotes indicated by the appropriate symbols (see below).

A.1.5 ***Abstracts:*** Authors must include a short abstract of approximately four to six lines that states briefly the purpose of the research, the principal results, and major conclusion(s). References and compound numbers should not be mentioned in the abstract unless full details are given.

A.1.6 ***Text*** should be subdivided in the simplest possible way consistent with clarity. Headings and subheadings should reflect the relative importance of the sections, and all headings should be numbered. In the introductory section of the manuscript, the author should strive to define the significance of the work and the justification for its publication. Any background discussion should be brief and restricted to pertinent material. Ensure that all tables, figures, and schemes are cited in the text in numerical order. The preferred position for chemical structures should be indicated. Trade names should have an initial capital letter. All measurements and data should be given in SI units where possible, or in other internationally accepted units. Abbreviations should be used consistently throughout the text, and all non-standard abbreviations should be defined on first usage. Authors are requested to draw attention to hazardous materials or procedures by adding the word CAUTION followed by a brief descriptive phrase and literature references if appropriate.

A.1.7 ***Reviews:*** When submitting a review article, authors should include biographical information for each author as well as a black-and-white photograph. Each biography should be one paragraph (approximately 150-200 words) and should include date and place of birth, universities attended, degrees obtained, principal professional posts held, present title, a line or two about the major research interests, and anything else professionally relevant that is of special interest.

A.1.8 ***Experimental section:*** Authors should be as concise as possible in experimental descriptions. The Experimental section must contain all the information necessary to guarantee reproducibility. An introductory paragraph containing information concerning solvents, sources of less common starting materials, special equipment, etc.,

should be provided. The procedures should be written in the past tense and include the weight, mmol, volume, etc., in parentheses after the names of the substances or solvents. General reaction conditions should be given only once. The title of an experiment should include the chemical name and compound number of the product prepared; subsequently, this compound should be identified by its number. Details of the workup procedure must be included. Physical and spectroscopic data, including NMR, high-resolution mass analysis, and elemental analysis, can be included in the experimental section or presented in tables.

A.1.9 ***Acknowledgments:*** An acknowledgment section may be included. It should be placed after the manuscript text and before the references.

A.1.10 ***Abbreviations:*** Standard ACS abbreviations should be used throughout the manuscript and are employed without periods. The preferred forms for some of the more commonly used abbreviations are mp, bp, °C, K, min, h, mL, μL, g, mg, μg, cm, mm, nm, mol, mmol, μmol, M, mM, μM, ppm, HPLC, TLC, GC, ^{1}H NMR, GC-MS, HRMS, FABHRMS, UV, IR, EPR, ESR, DNase, ED_{50}, ID_{50}, IC_{50}, LD_{50}, im, ip, iv, mRNA, RNase, rRNA, tRNA, cpm, Ci, dpm, V_{max}, K_m, k, $t_{1/2}$. All non-standard abbreviations should be defined following the first use of the abbreviation. For a detailed listing of standard abbreviations, see The ACS Style Guide; American Chemical Society: Washington, DC, 1997.

A.1.11 ***References and notes:*** In the text, references should be indicated by superscript Arabic numerals which run consecutively through the paper and appear after any punctuation. Please ensure that all references are cited in the text and vice versa. The reference list should preferably contain only literature references, although other information (e.g., experimental details) can be placed in this section. Preferably, each reference should contain only one literature citation. Authors are expected to check the original source reference for accuracy. Journal titles should be abbreviated according to American Chemical Society guidelines (The ACS Style Guide; Dodd, J. S., Ed.: American Chemical Society: Washington DC, 1997). A list of currently accepted journal

abbreviations may be found the journal home page at www.elsevier.com/locate/bmc. Formatting for common references is shown below.

Scientific articles:

1. Barton, D. H. R.; Yadav-Bhatnagar, N.; Finet, J.-P.; Khamsi, J. *Tetrahedron Lett.* **1987,** *28,* 3111.

Books:

2. Doe, J. S.; Smith, J. In *Medicinal Chemistry*; Roe, P., Ed.; Pergamon Press: Oxford, 1990; Vol. 1, pp 301-383.

Patent/Chem. abstract:

3. Lyle, F. R. U.S. Patent 6,973,257, 1995; *Chem. Abstr.* **1995,** *123,* 2870.

Meeting abstract:

4. Prasad, A.; Jackson, P. *Abstracts of Papers,* Part 2, 212th National Meeting of the American Chemical Society, Orlando, FL, Aug 25-29, 1996; American Chemical Society: Washington, DC, 1996; PMSE 189.

A.1.12 ***Footnotes:*** Footnotes should appear at the bottom of the appropriate page and be indicated by the following symbols: asterisk, dagger, double dagger, section sign, paragraph, parallels.

A.1.13 ***Tables:*** All tables should be cited in the text, and numbered in order of appearance with Arabic numerals. All table columns should have a brief explanatory heading and, where appropriate, units of measurement. Vertical lines should not be used. Footnotes to tables should be typed below the table and should be referred to by superscript letters. Each table should have a descriptive heading, which, together with the individual column headings, should make the table, as nearly as possible, self-explanatory. In setting up tabulations, authors are requested to keep in mind the column widths (8.4 cm and 17.7 cm), and to make the table conform to the limitations of these dimensions.

A.1.14 ***Legends:*** Legends for figures and schemes should be grouped together separately.

A.1.15 ***Artwork:*** Figures, schemes, and equations must be cited in the text and numbered in order of appearance with Arabic numerals. Other graphics, such as structures, do not need to be numbered, but please indicate in the text where these are to appear. All graphics (including chemical structures) must be provided at the actual size that they are to appear (single-column width is 8.4 cm; double-column width is 17.7 cm). Please arrange schematics so that they fill the column space (either single or double), so as not to leave a lot of unused white space. Please ensure that all illustrations within a paper are consistent in type, quality, and size. Legends should not be included as part of the graphic; instead all legends should be supplied at the end of the text.

To help authors provide actual size graphics, it is suggested that the following settings be used with CSC ChemDraw and ISIS Draw: font 10 pt Helvetica, chain angle 120°, bond spacing 18% of length, fixed length 10.08 pt (0.354 cm), bold width 1.4 pt (0.049 cm), line width 0.42 pt (0.015 cm), margin width 1.12 pt (0.040 cm), and hash spacing 1.75 pt (0.062 cm). Compound numbers should be in boldface. In order to accurately design schematics to print out at the proper width, the original drawing cannot exceed a column width of 8.4 cm (for single column) and 17.7 cm (for double column). Layout design is facilitated if authors submit their original artwork in the actual size to be published. Please save graphics as an Encapsulated PostScript file (EPS) or a Tagged Image File Format (TIFF), as well as the program the graphic was originally drawn in. For more details on the preparation and submission of artwork, please visit http://www.elsevier.com/artworkinstructions.

A.1.16 ***Colour:*** Colour figures should be supplied in electronic format as JPEG files (minimum 300 dots per inch).

- *In print:* Colour figures may be printed in the journal at no charge to the author, provided that the editor considers the colour necessary to convey scientific information.
- *On the Web:* Any figure can appear free of charge in colour in the Web version of your article (e.g., on ScienceDirect), regardless of whether or not this is reproduced in colour in the printed version. Please note that if you do not opt for colour in print, you should submit relevant figures in both colour (for the Web) and black and white (for print).

A.2 Journal conventions

A.2.1 ***Nomenclature:*** It is the responsibility of the authors to provide correct nomenclature. Chemical names for drugs are preferred. If these are not practical, generic names, names approved by the U.S. Adopted Names Council, or those approved by the World Health Organization may be used. If a generic name is used, its chemical name or structure should be provided at the point of first citation. Authors will find the following as useful reference books for recommended nomenclature.

IUPAC Nomenclature of Organic Chemistry; Rigaudy, J.; Klesney, S. P., Eds; Pergamon: Oxford, 1979.

Enzyme Nomenclature; Webb, E. C., Ed.; Academic Press; Orlando, 1992.

Biochemical Nomenclature and Related Documents; The Biochemistry Society; London, 1978.

The ACS Style Guide; Dodd, J. S., Ed.; American Chemical Society: Washington, DC, 1997.

A.2.2 ***X-ray crystallographic data:*** Prior to submission of the manuscript, the author should deposit crystallographic data for organic and metal organic structures with the Cambridge Crystallographic Data Centre. The data, without structure factors, should be sent by e-mail to deposit@ccdc.cam.ac.uk, as an ASCII file, preferably in CIF format. Hard copy data should be sent to CCDC, 12 Union Road, Cambridge CB2 1EZ. A checklist of data items for deposition can be obtained from the CCDC Home Page on the World Wide Web (http://www.ccdc.cam.ac.uk) or by e-mail to: fileserv@ccdc.cam.ac.uk, with the one-line message, send me checklist. The data will be acknowledged, within three working days, with one CCDC deposition number per structure deposited. These numbers should be included with the following standard text in the manuscript: Crystallographic data (excluding structure factors) for the structures in this paper have been deposited with the Cambridge Crystallographic Data Centre as supplementary publication nos. CCDC.....Copies of the data can be obtained, free of charge, on application to CCDC, 12 Union Road, Cambridge CB2 1EZ, UK, (fax: +44-(0)1223-336033 or e-mail: deposit@ccdc.cam.ac.uk). Deposited data may be accessed by the

journal and checked as part of the refereeing process. If data are revised prior to publication, a replacement file should be sent to CCDC.

Characterization of new compounds: All new compounds should be fully characterized with relevant spectroscopic data. Microanalyses should be included whenever possible. Under appropriate circumstances, high-resolution mass spectra may serve in lieu of microanalysis, if accompanied by suitable NMR criteria for sample homogeneity. CHARACTERIZATION OF ALL NEW COMPOUNDS HAS TO BE SPECIFIED (GIVEN) IN A COMPOUND CHARACTERIZATION CHECKLIST.

A.2.3 ***Characterisation of new compounds:*** All new compounds should be fully characterized with relevant spectroscopic data. Microanalyses should be included whenever possible. Under appropriate circumstances, high-resolution mass spectra may serve in lieu of microanalysis, if accompanied by suitable NMR criteria for sample homogeneity.

A.2.4 ***Biological data:*** Biological test methods must be referenced or described in sufficient detail to permit the experiments to be repeated by others. Standard compounds and established drugs/agents should be tested in the same system for comparison. Statistical limits (statistical significance) for the biological data are usually required. If statistical limits cannot be provided, the number of determinations and an indication of the variability and reliability of the results should be given. References to statistical methods of calculation should be included. Doses and concentrations should be expressed in molar quantities when comparisons of potencies are made with compounds having substantial differences in molecular weights. For inactive agents, the highest concentration or dose level tested should be indicated. Detailed descriptions of biological methods should be placed in the Experimental section.

A.2.5 ***Structural data:*** Atomic coordinates for structures of biological macromolecules determined by X-ray, NMR, or other methods should be deposited with the RCSB Protein Data Bank (PDB). It is the responsibility of the author to obtain a file name for the macromolecule; the file name must be referenced in the manuscript. Deposition (deposit.pdb.org) and release information are available at

http://deposit.pdb.org/depoinfo/depofaq.html. Manuscripts will be sent out for review only after receiving a written statement from the author that the coordinates will be deposited. If a manuscript is accepted for publication and the PDB file name has not yet been obtained, it must be added in the proof prior to publication. Upon written request by the author the PDB will refer requests for coordinates to the originating author, but one year after publication, they will be made generally available upon request. Please address all inquiries about depositing to the PDB.

A.2.6 ***GenBank/DNA sequence linking:*** Authors wishing to enable other scientists to use the accession numbers cited in their papers via links to these sources, should type this information in the following manner:

For each and every accession number cited in an article, authors should type the accession number in bold, underlined text. Letters in the accession number should always be capitalized (see example below.) This combination of letters and format will enable the typesetter to recognize the relevant texts as accession numbers and add the required link to GenBank $ sequences.

Example: GenBank accession nos. **AI631510** , **AI631511** , **AI632198** , and **BF223228**), a B-cell tumour from a chronic lymphatic leukaemia (GenBank accession no. **BE675048**), and a T-cell lymphoma (GenBank accession no. **AA361117**).

Authors are encouraged to check accession numbers used very carefully. An error in a letter or number can result in a dead link.

In the final version of the *printed article,* the accession number text will not appear bold or underlined. In the final version of the *electronic* copy, the accession number text will be linked to the appropriate source in the NCBI databases, enabling readers to go directly to that source from the article.

A.2.7 ***Software:*** Software used as part of computer-aided drug/agent design (e.g., molecular modelling, QSAR, conformational analysis, molecular dynamics) should be readily available from accepted sources and the authors may specify where the software can be obtained. Assurance of the quality of the parameters employed for the relevant potential functions should be detailed in the manuscript.

A.2.8 ***Supplementary material:*** Elsevier accepts electronic supplementary material to support and enhance your scientific research. Supplementary files offer the author additional possibilities to publish supporting applications, movies, animation sequences, high-resolution images, background datasets, sound clips, and more. Supplementary files supplied will be published online alongside the electronic version of your article in Elsevier web products, including ScienceDirect: www.sciencedirect.com. To ensure that your submitted material is directly usable, please provide data in one of our recommended file formats. Supplementary data must be saved in files separate from those for the manuscript and figures, and all file names must be supplied. Supplementary files should either be referred to from within the text of your manuscript in the same way as for figures or tables, or their presence be indicated by adding a paragraph entitled Supplementary data 'at the end of the manuscript, detailing which data are supplied. In addition, authors should also provide a concise and descriptive caption for each file. When supplying supplementary data, authors must state whether the data files are either (i) for online publication or (ii) to be used as an aid for the refereeing of the paper only. All supplementary data will be subject to peer review. For more detailed instructions, please visit http://www.elsevier.com/artworkinstructions.

ANNEXURE B

AUTHOR INSTRUCTIONS – EUROPEAN JOURNAL OF MEDICINAL CHEMISTRY

B.1 Authorship

The text should be arranged in the following order: Introduction, Chemistry, Pharmacology, Results, Discussion, Conclusion and Experimental protocols. Each section should be clearly marked with a separate, numbered heading and may be numbered down to the fourth order.

Analytical data should be included for examination by the editor and referees. However, these data will not be printed if they agree within within 0.4 % with calculated values, but may be noted as follows: 'Anal. C14H15NO3 (C, H, N, O)', with the mentioning under Experimental protocols: 'Analyses indicated by the symbols of the elements or functions were within – 0.4 % of the theoretical values'.

B.2 Copyright

Upon acceptance of an article, authors will be asked to complete a 'Journal Publishing Agreement' (for more information on this and copyright see http://www.elsevier.com/copyright). Acceptance of the agreement will ensure the widest possible dissemination of information. An e-mail will be sent to the corresponding author confirming receipt of the manuscript together with a 'Journal Publishing Agreement' form or a link to the online version of this agreement.

Subscribers may reproduce tables of contents or prepare lists of articles including abstracts for internal circulation within their institutions. Permission of the Publisher is required for resale or distribution outside the institution and for all other derivative works, including compilations and translations (please consult http://www.elsevier.com/permissions). If excerpts from other copyrighted works are included, the author(s) must obtain written permission from the copyright owners and

credit the source(s) in the article. Elsevier has pre-printed forms for use by authors in these cases: please consult http://www.elsevier.com/permissions.

B.3 Retained author rights

As an author you (or your employer or institution) retains certain rights; for details you are referred to: http://www.elsevier.com/authorsrights.

B.4 Role of the funding source

You are requested to identify who provided financial support for the conduct of the research and/or preparation of the article and to briefly describe the role of the sponsor(s), if any, in study design; in the collection, analysis and interpretation of data; in the writing of the report; and in the decision to submit the paper for publication. If the funding source(s) had no such involvement then this should be stated. Please see http://www.elsevier.com/funding.

B.5 Funding body agreements and policies

Elsevier has established agreements and developed policies to allow authors whose articles appear in journals published by Elsevier, to comply with potential manuscript archiving requirements as specified as conditions of their grant awards. To learn more about existing agreements and policies please visit http://www.elsevier.com/fundingbodies.

B.6 Language and language services

Please write your text in good English (American or British usage is accepted, but not a mixture of these). Authors who require information about language editing and copyediting services pre- and post-submission please visit http://www.elsevier.com/languageediting or our customer support site at http://epsupport.elsevier.com for more information.

B.7 Submission

Submission to this journal proceeds totally online and you will be guided stepwise through the creation and uploading of your files. The system automatically converts source files to a single PDF file of the article, which is used in the peer-review process. Please note that even though manuscript source files are converted to PDF files at

submission for the review process, these source files are needed for further processing after acceptance. All correspondence, including notification of the Editor's decision and requests for revision, takes place by e-mail removing the need for a paper trail.

B.8 Referees

Please submit, with the manuscript, the names, addresses and e-mail addresses of 3 potential referees. Note that the editor retains the sole right to decide whether or not the suggested reviewers are used.

B.9 Preparation

B.9.1 *Use of word-processing software*

It is important that the file be saved in the native format of the word processor used. The text should be in single-column format. Keep the layout of the text as simple as possible. Most formatting codes will be removed and replaced on processing the article. In particular, do not use the word processor's options to justify text or to hyphenate words. However, do use bold face, italics, subscripts, superscripts etc. Do not embed "graphically designed" equations or tables, but prepare these using the word processor's facility. When preparing tables, if you are using a table grid, use only one grid for each individual table and not a grid for each row. If no grid is used, use tabs, not spaces, to align columns. The electronic text should be prepared in a way very similar to that of conventional manuscripts (see also the Guide to Publishing with Elsevier: http://www.elsevier.com/guidepublication). Do not import the figures into the text file but, instead, indicate their approximate locations directly in the electronic text and on the manuscript. See also the section on Electronic illustrations.
To avoid unnecessary errors you are strongly advised to use the "spell-check" and "grammar-check" functions of your word processor.

B.9.2 *Essential title page information*

• **Title.** Concise and informative. Titles are often used in information-retrieval systems. Avoid abbreviations and formulae where possible.

• **Author names and affiliations.** Where the family name may be ambiguous (e.g., a double name), please indicate this clearly. Present the authors ' affiliation addresses

(where the actual work was done) below the names. Indicate all affiliations with a lower-case superscript letter immediately after the author's name and in front of the appropriate address. Provide the full postal address of each affiliation, including the country name, and, if available, the e-mail address of each author.

• **Corresponding author.** Clearly indicate who will handle correspondence at all stages of refereeing and publication, also post-publication. **Ensure that telephone and fax numbers (with country and area code) are provided in addition to the e-mail address and the complete postal address.**

• **Present/permanent address.** If an author has moved since the work described in the article was done, or was visiting at the time, a "Present address" (or "Permanent address") may be indicated as a footnote to that author's name. The address at which the author actually did the work must be retained as the main, affiliation address. Superscript Arabic numerals are used for such footnotes.

B.9.3 *Graphical abstract*

A Graphical abstract is mandatory for this journal. It should summarize the contents of the paper in a concise, pictorial form designed to capture the attention of a wide readership online. Authors must provide images that clearly represent the work described in the paper. Graphical abstracts should be submitted as a separate file in the online submission system. Maximum image size: 400 × 600 pixels (h × w, recommended size 200 × 500 pixels). Preferred file types: TIFF, EPS, PDF or MS Office files. See http://www.elsevier.com/graphicalabstracts for examples.

B.9.4 *Keywords*

Immediately after the abstract, provide a maximum of 6 keywords, using American spelling and avoiding general and plural terms and multiple concepts (avoid, for example, "and", "of"). Be sparing with abbreviations: only abbreviations firmly established in the field may be eligible. These keywords will be used for indexing purposes.

B.9.5 *Abbreviations*

Define abbreviations that are not standard in this field in a footnote to be placed on the first page of the article. Such abbreviations that are unavoidable in the abstract must be

defined at their first mention there, as well as in the footnote. Ensure consistency of abbreviations throughout the article.

B.9.6 *Acknowledgements*

Collate acknowledgements in a separate section at the end of the article before the references and do not, therefore, include them on the title page, as a footnote to the title or otherwise. List here those individuals who provided help during the research (e.g., providing language help, writing assistance or proof reading the article, etc.).

B.9.7 *Nomenclature*

The author is responsible for providing the correct nomenclature which must be consistent and unambiguous. The use of chemical names for drugs is preferred.

B.9.8 *Accession Numbers*

DNA sequences and GenBank Accesion numbers: Many Elsevier journals cite "gene accession numbers" in their running text and footnotes. Gene accession numbers refer to genes or DNA sequences about which further information can be found in the database at the National Centre for Biotechnical Information (NCBI) at the National Library of Medicine. Elsevier authors wishing to enable other scientists to use the accession numbers cited in their papers via links to these sources, should type this information in the following manner: For each and every accession number cited in an article, authors should type the accession number in bold, underlined text. Letters in the accession number should always be capitalised (see Example 1 below). This combination of letters and format will enable Elsevier$ typesetters to recognize the relevant texts as accession numbers and add the required link to GenBank$ sequences.

Example 1: "GenBank accession nos. AI631510, AI631511, AI632198, and BF223228, a B-cell tumour from a chronic lymphatic leukaemia (GenBank accession no. BE675048), and a T-cell lymphoma (GenBank accession no. AA361117)". Authors are encouraged to check accession numbers used very carefully. An error in a letter or number can result in a dead link. In the final version of the printed article, the accession number text will not appear bold or underlined (see Example 2 below). Example 2: "GenBank accession nos. AI631510, AI631511, AI632198, and BF223228, a

B-cell tumour from a chronic lymphatic leukaemia (GenBank accession no. BE675048), and a T-cell lymphoma (GenBank accession no. AA361117)".
In the final version of the electronic copy, the accession number text will be linked to the appropriate source in the NCBI databases enabling readers to go directly to that source from the article.

B.9.9 *Math formulae*

Present simple formulae in the line of normal text where possible and use the solidus (/) instead of a horizontal line for small fractional terms, e.g., X/Y. In principle, variables are to be presented in italics. Powers of e are often more conveniently denoted by exp. Number consecutively any equations that have to be displayed separately from the text (if referred to explicitly in the text).

B.9.10 *Footnotes*

Footnotes should be used sparingly. Number them consecutively throughout the article, using superscript Arabic numbers. Many word processors build footnotes into the text, and this feature may be used. Should this not be the case, indicate the position of footnotes in the text and present the footnotes themselves separately at the end of the article. Do not include footnotes in the Reference list.

Table footnotes

Indicate each footnote in a table with a superscript lowercase letter.

B.9.11 *Artwork*

Electronic artwork

General points

- Make sure you use uniform lettering and sizing of your original artwork.
- Save text in illustrations as "graphics" or enclose the font.
- Only use the following fonts in your illustrations: Arial, Courier, Times, Symbol.
- Number the illustrations according to their sequence in the text.
- Use a logical naming convention for your artwork files.

- Provide captions to illustrations separately.
- Produce images near to the desired size of the printed version.
- Submit each figure as a separate file.

A detailed guide on electronic artwork is available on our website: http://www.elsevier.com/artworkinstructions

You are urged to visit this site; some excerpts from the detailed information are given here.

Formats

Regardless of the application used, when your electronic artwork is finalised, please "save as" or convert the images to one of the following formats (note the resolution requirements for line drawings, halftones, and line/halftone combinations given below): EPS: Vector drawings. Embed the font or save the text as "graphics". TIFF: colour or greyscale photographs (halftones): always use a minimum of 300 dpi. TIFF: Bitmapped line drawings: use a minimum of 1000 dpi. TIFF: Combinations bitmapped line/half-tone (colour or greyscale): a minimum of 500 dpi is required.

DOC, XLS or PPT: If your electronic artwork is created in any of these Microsoft Office applications please supply "as is".

Please do not:

- Supply embedded graphics in your word processor (spreadsheet, presentation) document;
- Supply files that are optimised for screen use (like GIF, BMP, PICT, WPG); the resolution is too low;
- Supply files that are too low in resolution;
- Submit graphics that are disproportionately large for the content.

Colour artwork

Please make sure that artwork files are in an acceptable format (TIFF, EPS or MS Office files) and with the correct resolution. If, together with your accepted article, you submit

usable colour figures then Elsevier will ensure, at no additional charge, that these figures will appear in colour on the Web (e.g., ScienceDirect and other sites) regardless of whether or not these illustrations are reproduced in colour in the printed version. **For colour reproduction in print, you will receive information regarding the costs from Elsevier after receipt of your accepted article.** Please indicate your preference for colour in print or on the Web only. For further information on the preparation of electronic artwork, please see http://www.elsevier.com/artworkinstructions.

Please note: Because of technical complications which can arise by converting colour figures to "grey scale" (for the printed version should you not opt for colour in print) please submit in addition usable black and white versions of all the colour illustrations.

Figure captions

Ensure that each illustration has a caption. Supply captions separately, not attached to the figure. A caption should comprise a brief title (**not** on the figure itself) and a description of the illustration. Keep text in the illustrations themselves to a minimum but explain all symbols and abbreviations used.

Text graphics

Present incidental graphics not suitable for mention as figures, plates or schemes at the end of the article and number them "Graphic 1", etc. Their precise position in the text can then be indicated. See further under Electronic artwork. If you are working with LaTeX and have such features embedded in the text, these can be left, but such embedding should not be done specifically for publishing purposes. Further, high-resolution graphics files must be provided separately.

B.9.12 *Tables*

Number tables consecutively in accordance with their appearance in the text. Place footnotes to tables below the table body and indicate them with superscript lowercase letters. Avoid vertical rules. Be sparing in the use of tables and ensure that the data presented in tables do not duplicate results described elsewhere in the article.

B.9.13 *References*

Citation in text

Please ensure that every reference cited in the text is also present in the reference list (and vice versa). Any references cited in the abstract must be given in full. Unpublished results and personal communications are not recommended in the reference list, but may be mentioned in the text. If these references are included in the reference list they should follow the standard reference style of the journal and should include a substitution of the publication date with either "Unpublished results" or "Personal communication" Citation of a reference as "in press" implies that the item has been accepted for publication.

Web references

As a minimum, the full URL should be given and the date when the reference was last accessed. Any further information, if known (DOI, author names, dates, reference to a source publication, etc.), should also be given. Web references can be listed separately (e.g., after the reference list) under a different heading if desired, or can be included in the reference list.

References in a special issue

Please ensure that the words 'this issue 'are added to any references in the list (and any citations in the text) to other articles in the same Special Issue.

Reference style

Text: Indicate references by number(s) in square brackets in line with the text. The actual authors can be referred to, but the reference number(s) must always be given. Example: "..... as demonstrated [3,6]. Barnaby and Jones [8] obtained a different result ...."

List: Number the references (numbers in square brackets) in the list in the order in which they appear in the text.

Examples:

Reference to a journal publication:

[1] J. van der Geer, J.A.J. Hanraads, R.A. Lupton, The art of writing a scientific article, J. Sci. Commun. 163 (2000) 51-59.

Reference to a book:

[2] W. Strunk Jr., E.B. White, The Elements of Style, third ed., Macmillan, New York, 1979.

Reference to a chapter in an edited book:

[3] G.R. Mettam, L.B. Adams, How to prepare an electronic version of your article, in: B.S. Jones, R.Z. Smith (Eds.), Introduction to the Electronic Age, E-Publishing Inc., New York, 1999, pp. 281-304.

B.9.14 *Video data*

Elsevier accepts video material and animation sequences to support and enhance your scientific research. Authors who have video or animation files that they wish to submit with their article are strongly encouraged to include these within the body of the article. This can be done in the same way as a figure or table by referring to the video or animation content and noting in the body text where it should be placed. All submitted files should be properly labelled so that they directly relate to the video file's content. In order to ensure that your video or animation material is directly usable, please provide the files in one of our recommended file formats with a maximum size of 30 MB and running time of 5 minutes. Video and animation files supplied will be published online in the electronic version of your article in Elsevier Web products, including ScienceDirect: http://www.sciencedirect.com. Please supply 'stills' with your files: you can choose any frame from the video or animation or make a separate image. These will be used instead of standard icons and will personalize the link to your video data. For more detailed instructions please visit our video instruction pages at http://www.elsevier.com/artworkinstructions. Note: since video and animation cannot be embedded in the print version of the journal, please provide text for both the electronic and the print version for the portions of the article that refer to this content.

B.9.15 *Supplementary data*

Elsevier accepts electronic supplementary material to support and enhance your scientific research. Supplementary files offer the author additional possibilities to publish supporting applications, high-resolution images, background datasets, sound clips and more. Supplementary files supplied will be published online alongside the electronic

version of your article in Elsevier Web products, including ScienceDirect: http://www.sciencedirect.com. In order to ensure that your submitted material is directly usable, please provide the data in one of our recommended file formats. Authors should submit the material in electronic format together with the article and supply a concise and descriptive caption for each file. For more detailed instructions please visit our artwork instruction pages at http://www.elsevier.com/artworkinstructions.

B.9.16 *Submission checklist*

It is hoped that this list will be useful during the final checking of an article prior to sending it to the journal's Editor for review. Please consult this Guide for Authors for further details of any item.

Ensure that the following items are present:

One Author designated as corresponding Author:

- E-mail address
- Full postal address
- Telephone and fax numbers

All necessary files have been uploaded

- Keywords
- All figure captions
- All tables (including title, description, footnotes)

Further considerations:

- Manuscript has been "spellchecked" and "grammar-checked"
- References are in the correct format for this journal
- All references mentioned in the Reference list are cited in the text, and vice versa
- Permission has been obtained for use of copyrighted material from other sources (including the Web)

- Colour figures are clearly marked as being intended for colour reproduction on the Web (free of charge) and in print or to be reproduced in colour on the Web (free of charge) and in black-and-white in print
- If only colour on the Web is required, black and white versions of the figures are also supplied for printing purposes

For any further information please visit our customer support site at http://epsupport.elsevier.com.

LETTERS OF PERMISSION

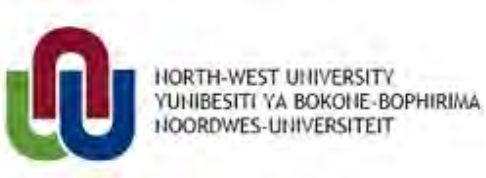

TO WHOM IT MAY CONCERN

Department of Pharmaceutical Chemistry
Tel.: +27 18 299 2206
Fax: +27 18 299 4243
e-mail: Jacques.Petzer@nwu.ac.za
8th April 2010

Dear Sir / Madam

CO-AUTHORSHIP ON RESEARCH PAPERS

The undersigned, as co-authors of the research articles listed below, hereby give permission to Mr. Louis H.A. Prins to submit the papers as part of the degree Ph.D. in Pharmaceutical Chemistry at the North-West University, Potchefstroom Campus.

I. Synthesis and In Vitro Evaluation of Pteridine Analogues as Monoamine Oxidase B and Nitric Oxide Synthase Inhibitors.

II. Inhibition of Monoamine Oxidase by Indole and Benzofuran Derivatives.

Yours sincerely,

_____ _____

J. P. Petzer S. F. Malan

Permission from Elsevier, as per the website:

http://authors.elsevier.com/definitions.html?journal_name=Remote%20Sensing%20of%20Environment&lang=English&dc=OCTDEF

Personal Use

Use by an author in the author's classroom teaching (including distribution of copies, paper or electronic), distribution of copies to research colleagues for their personal use, use in a subsequent compilation of the author's works, inclusion in a thesis or dissertation, preparation of other derivative works such as extending the article to book-length form, or otherwise using or re-using portions or excerpts in other works (with full acknowledgment of the original publication of the article).